UNIVERSIDADE FEDERAL DE GOIÁS
INSTITUTO DE MATEMÁTICA E ESTATÍSTICA

ANA MARIA ALVES DA SILVA

Limit Cycles in Planar Piecewise Smooth Systems having Non-regular Switches, Time Scales or Rotated Properties

Goiânia
2022

UNIVERSIDADE FEDERAL DE GOIÁS
INSTITUTO DE MATEMÁTICA E ESTATÍSTICA

TERMO DE CIÊNCIA E DE AUTORIZAÇÃO (TECA) PARA DISPONIBILIZAR VERSÕES ELETRÔNICAS DE TESES E DISSERTAÇÕES NA BIBLIOTECA DIGITAL DA UFG

Na qualidade de titular dos direitos de autor, autorizo a Universidade Federal de Goiás (UFG) a disponibilizar, gratuitamente, por meio da Biblioteca Digital de Teses e Dissertações (BDTD/UFG), regulamentada pela Resolução CEPEC nº 832/2007, sem ressarcimento dos direitos autorais, de acordo com a Lei 9.610/98, o documento conforme permissões assinaladas abaixo, para fins de leitura, impressão e/ou download, a título de divulgação da produção científica brasileira, a partir desta data.

O conteúdo das Teses e Dissertações disponibilizado na BDTD/UFG é de responsabilidade exclusiva do autor. Ao encaminhar o produto final, o autor(a) e o(a) orientador(a) firmam o compromisso de que o trabalho não contém nenhuma violação de quaisquer direitos autorais ou outro direito de terceiros.

1. Identificação do material bibliográfico

[ ] Dissertação [X] Tese [ ] Outro*:_____________

*No caso de mestrado/doutorado profissional, indique o formato do Trabalho de Conclusão de Curso, permitido no documento de área, correspondente ao programa de pós-graduação, orientado pela legislação vigente da CAPES.

Exemplos: Estudo de caso ou Revisão sistemática ou outros formatos.

2. Nome completo do autor

Ana Maria Alves da Silva

3. Título do trabalho

Limit cycles in planar piecewise smooth systems having non-regularswitches, time scales or rotated properties

4. Informações de acesso ao documento (este campo deve ser preenchido pelo orientador)

Concorda com a liberação total do documento [X] SIM [ ] NÃO[1]

[1] Neste caso o documento será embargado por até um ano a partir da data de defesa. Após esse período, a possível disponibilização ocorrerá apenas mediante:
a) consulta ao(à) autor(a) e ao(à) orientador(a);
b) novo Termo de Ciência e de Autorização (TECA) assinado e inserido no arquivo da tese ou dissertação.
O documento não será disponibilizado durante o período de embargo.
Casos de embargo:
- Solicitação de registro de patente;
- Submissão de artigo em revista científica;
- Publicação como capítulo de livro;
- Publicação da dissertação/tese em livro.

Obs. Este termo deverá ser assinado no SEI pelo orientador e pelo autor.

Documento assinado eletronicamente por **ANA MARIA ALVES DA SILVA**, **Discente**, em 03/10/2022, às 08:18, conforme horário oficial de Brasília, com fundamento no § 3º do art. 4º do Decreto nº 10.543, de 13 de novembro de 2020.

Documento assinado eletronicamente por **Rodrigo Donizete Euzébio**, **Professor do Magistério Superior**, em 13/10/2022, às 13:42, conforme horário oficial de Brasília, com fundamento no § 3º do art. 4º do Decreto nº 10.543, de 13 de novembro de 2020.

A autenticidade deste documento pode ser conferida no site https://sei.ufg.br/sei/controlador_externo.php?acao=documento_conferir&id_orgao_acesso_externo=0, informando o código verificador **3233627** e o código CRC **69C4A888**.

Ana Maria Alves da Silva

Limit Cycles in Planar Piecewise Smooth Systems having Non-regular Switches, Time Scales or Rotated Properties

Thesis presented to the Postgraduate Program in Mathematics of the Instituto de Matemática e Estatística of the Universidade Federal de Goiás, as partial requirement for obtaining the title of PhD in Mathematics.

Concentration Area: Dynamical Systems.

Advisor: Prof. Dr. Rodrigo Donizete Euzébio

Goiânia
2022

Ficha de identificação da obra elaborada pelo autor, através do
Programa de Geração Automática do Sistema de Bibliotecas da UFG.

Silva, Ana Maria Alves da
Limit Cycles in Planar Piecewise Smooth Systems having Non regular Switches, Time Scales or Rotated Properties [manuscrito] / Ana Maria Alves da Silva. - 2022.
108 f.: il.

Orientador: Prof. Dr. Rodrigo Donizete Euzébio.
Tese (Doutorado) - Universidade Federal de Goiás, Instituto de Matemática e Estatística (IME), Programa de Pós-Graduação em Matemática, Goiânia, 2022.
Bibliografia.

1. Piecewise Smooth Vector Fields. 2. Periodic Trajectories. 3. Fast-Slow Systems. 4. Piecewise Rotated Vector Fields. 5. Bifurcation Theory. I. Euzébio, Rodrigo Donizete, orient. II. Título.

CDU 517.938

UFG

UNIVERSIDADE FEDERAL DE GOIÁS

INSTITUTO DE MATEMÁTICA E ESTATÍSTICA

ATA DE DEFESA DE TESE

Ata nº **05** da sessão de Defesa de Tese de **Ana Maria Alves da Silva,** que confere o título de Doutora em Matemática, **na área de concentração de Sistemas Dinâmicos.**

Ao trigésimo dia do mês de setembro do ano de dois mil e vinte e dois, a partir das dez horas, via Web videoconferência, realizou-se a sessão pública de Defesa de Tese intitulada **"Limit cycles in planar piecewise smooth systems having non-regular switches, time scales or rotated properties."** Os trabalhos foram instalados pelo Orientador e Presidente da banca, Professor Doutor **Rodrigo Donizete Euzébio - IME/UFG** com a participação dos demais membros da Banca Examinadora: Professora Doutora **Kamila da Silva Andrade - IME/UFG** membro titular interno, Professor Doutor **Ricardo Miranda Martins - IMECC/UNICAMP** membro titular externo, Professora Doutora **Regilene Delazari dos Santos Oliveira - ICMC/USP** membro titular externa e Professora Doutora **Luci Any Francisco Roberto - IBILCE/UNESP,** membro titular externa. Durante a arguição os membros da banca **não fizeram** sugestão de alteração do título do trabalho. A Banca Examinadora reuniu-se em sessão secreta a fim de concluir o julgamento da Tese, tendo sido a candidata **aprovada** pelos seus membros. Proclamados os resultados pelo Professor Doutor **Rodrigo Donizete Euzébio - IME/UFG**, Presidente da Banca Examinadora, foram encerrados os trabalhos e, para constar, lavrou-se a presente ata que é assinada pelos Membros da Banca Examinadora, ao trigésimo dia do mês de setembro do ano de dois mil e vinte e dois.

TÍTULO SUGERIDO PELA BANCA

Limit cycles in planar piecewise smooth systems having non-regular switches, time scales or rotated properties

sei! assinatura eletrônica

Documento assinado eletronicamente por **Kamila Da Silva Andrade**, **Professor do Magistério Superior**, em 01/11/2022, às 13:36, conforme horário oficial de Brasília, com fundamento no § 3º do art. 4º do Decreto nº 10.543, de 13 de novembro de 2020.

sei! assinatura eletrônica

Documento assinado eletronicamente por **Luci Any Francisco Roberto**, **Usuário Externo**, em 01/11/2022, às 13:47, conforme horário oficial de Brasília, com fundamento no § 3º do art. 4º do Decreto nº 10.543, de 13 de novembro de 2020.

sei! assinatura eletrônica

Documento assinado eletronicamente por **Rodrigo Donizete Euzébio**, **Professor do Magistério Superior**, em 01/11/2022, às 14:18, conforme horário oficial de Brasília, com fundamento no § 3º do art. 4º do Decreto nº 10.543, de 13 de novembro de 2020.

Documento assinado eletronicamente por **Regilene Delazari dos Santos Oliveira**, **Usuário Externo**, em 01/11/2022, às 19:38, conforme horário oficial de Brasília, com fundamento no § 3º do art. 4º do Decreto nº 10.543, de 13 de novembro de 2020.

Documento assinado eletronicamente por **Ricardo Miranda Martins**, **Usuário Externo**, em 01/11/2022, às 20:43, conforme horário oficial de Brasília, com fundamento no § 3º do art. 4º do Decreto nº 10.543, de 13 de novembro de 2020.

A autenticidade deste documento pode ser conferida no site https://sei.ufg.br/sei/controlador_externo.php?acao=documento_conferir&id_orgao_acesso_externo=0, informando o código verificador **3304819** e o código CRC **524F73D8**.

Referência: Processo nº 23070.049760/2022-19 SEI nº 3304819

Ana Maria Alves da Silva

Possui Mestrado em Matemática pela Universidade Federal de Goiás (2018), no qual trabalhou no projeto de pesquisa intitulado "Aspectos topológicos e ergódicos de sistemas dinâmicos suaves por partes". Exerceu, na qualidade de aluno(a) de graduação, a função de MONITOR de um aluno com deficiência visual, do Instituto de Matemática e Estatística da Universidade Federal de Goiás. Ainda na graduação, foi bolsista do Programa Institucional de Bolsa de Iniciação Científica - CNPQ no projeto intitulado "EDO'S e Geometria". Tem experiência na área de Geometria e Topologia, com ênfase em Sistemas Dinâmicos, mediante bolsa de pesquisa do CNPq, atuando principalmente nos seguintes temas: sistemas lineares suaves por partes e ciclos limites.

To my great godmother Vanda (In memoriam), my dear grandmother Verônica (In memoriam) and my beloved aunt Zulma (In memoriam), with all my love and affection. I wish I could hug you one last time.

Acknowledgment

To my husband, Lucas Eduardo for all comprehension, for being by my side inall situations, and for always believing in me. You are one of the most power that I could have.You always hold me. Like you did the first time we kissed, a long time ago, when therewas nothing but our love. Some infinities are bigger than other infinities and our love isthe biggest of them.

To my mommy, Elaine, for being my first example of dedication and for always encouraging me to study and learn. A mother's love is the fuel that enables an ordinary human being to do something extraordinary and I was powered by that fuel. To my grand-mom, Marlene, for being one of the most inspiring person that I have the luck to know. You are my light on the dark nights. To my younger sister, Ana Flávia, to whom I have always tried to be an example in pursuing my dreams to inspire her to also pursue her dreams. To my godparents, Marlene and Heleno, for being always present in my life and for the financial support in the months without a research grant. To my daddy, Eurípedes, for always doing the best he could under the conditions he had. All of you are essential to my life and make my life worth living.

To my advisor, Rodrigo, for the learning, teachings, guidance, and patience that made this work possible. You are the best professor that I could have. Thank you for everything.

To FAPEG and CAPES for the financial support that made this work happens.

"Nobody said it was easy
No one ever said it would be this hard"

Coldplay,
The Scientist.

Resumo

Silva, Ana Maria Alves da. **Limit Cycles in Planar Piecewise Smooth Systems having Non-regular Switches, Time Scales or Rotated Properties**. Goiânia, 2022. 108p. Tese de Doutorado Relatório de Graduação. Instituto de Matemática e Estatística, Universidade Federal de Goiás.

Nesta tese, estudamos trajetórias periódicas em sistemas lineares planares suaves por partes com uma variedade de descontinuidade não-regular. Fornecemos cotas superiores para ciclos limites para uma classe do modelo considerado, a cota é de um ou dois ciclos dependendo das condições consideradas. Estabelecemos a estabilidade e hiperbolicidade desses ciclos limites fornecemos exemplos que atingem a cota de um e dois ciclos limite para as classes consideradas. Realizamos uma análise global de um modelo representativo através da teoria da bifurcação para analisar o nascimento de ciclos limites, trajetórias periódicas deslizantes e tangenciais. Fornecemos alguns resultados abordando a coexistência de trajetórias periódicas. Estudamos sistemas Fast-Slow com a variedade de descontinuidade não-regular com uma nova abordagem. Este estudo permite provar que uma trajetória periódica de deslize específica é na verdade uma trajetória periódica homoclínica que surge a partir da bifurcação de ciclos limites deslizantes que não são topologicamente equivalentes. Propomos a teoria de campos de vetores rodados por partes com o objetivo de entender como as trajetórias de duas famílias de campos de vetores rodados se comportam quando um mesmo parâmetro é variado. Neste contexto, provamos o teorema de não interseção para os campos considerados.

Palavras–chave

Campos de Vetores Suves por Partes, Trajetórias Periódicas, Sistemas Rápido-lento, Campos de Vetores Rodados por Partes, Teoria de Bifurcação

Abstract

Silva, Ana Maria Alves da. **Limit Cycles in Planar Piecewise Smooth Systems having Non-regular Switches, Time Scales or Rotated Properties**. Goiânia, 2022. 108p. PhD. Thesis Instituto de Matemática e Estatística, Universidade Federal de Goiás.

In this thesis, periodic trajectories in planar discontinuous piecewise linear systems with a nonregular switching line are studied. We provide sharp upper bounds of one or two limit cycles for certain classes of the model considered. We also establish the stability and hyperbolicity of these limit cycles. In addition, we provide examples reaching one and two limit cycles for these classes. We perform the global analysis of a representative model through bifurcation theory to analyze the birth of limit cycles, sliding periodic trajectories, and tangential ones. We also provide some results addressing the coexistence of periodic trajectories. We studied Fast-Slow systems with nonregular switching line with a new approach. This study allows proving that a specific sliding periodic trajectory is in fact a homoclinic trajectory. This homoclinic trajectory arises from a bifurcation of sliding limit cycles that are not topologically equivalents. We propose the theory of piecewise rotated vector fields with the goal of understanding how the trajectories of two families of rotated vector fields behave as the same parameter is varied. In this context, we prove the non-intersection theorem for closed periodic trajectories for piecewise rotated vector fields.

Keywords

Piecewise Smooth Vector Fields, Periodic Trajectories, Fast-Slow Systems, Piecewise Rotated Vector Fields, Bifurcation Theory

Contents

Introduction

The beginning of the studies on Dynamical Systems was due to the theory of Differential and Integral Calculus developed by Newton and Leibniz. Differential and Integral Calculus aims to solve questions motivated by many applications on physical and geometrical real problems. It allows relating the position and velocity of moving objects with mathematical expressions known as differential equations. With time, Differential Equations became a new mathematical area in mathematics and one of the most important areas due to the effective methods of scientific research. Many mathematicians, such as Euler, Lagrange, Laplace, and Poincaré among others notably contributed and expanded this area with calculus of variations, celestial mechanics, and fluid dynamics. In some of these areas, many complicated phenomena can be modeled by differential equations.

Dynamical Systems are systems characterized by states that change with time. They emerged from science to model and make prevision (for instance, in physics, biology mechanics, financial, and engineering) and are usually described by ordinary differential equations in finite or infinite dimensions and sometimes by partial differential equations in infinite dimension. The goal of Dynamical Systems is to explain the asymptotic and qualitative behavior of a system by flow of a differential equation. Formally, it is an action of a 1-parameter group of maps into a set to perform a qualitative analysis instead of a quantitative one.

There are many dynamical systems explored and studied by mathematicians. Some of these dynamical systems are inspired by real life problems, others have applications in physics, engineering, biology, robotics, statistics, etc. In this thesis, we are interested in studying those who are non-smooth (discontinuous). Discontinuities occur, for example, when neurons or electronic switches are activated. In other words, discontinuities happen when processes enact a change of regime or rule. These changes in rules are an inspiration for building dynamical models, however, there is a violation in a central requirement of Differential and Integral Calculus.

Aleksel Fedorovidh Filippov was one of the most important researchers in an attempt of formalizing the mathematical theory for non-smooth dynamical systems. The theory developed by him is one of the most used to study these systems and is known as Filippov's theory. Another knowing theory is due to Barbashin, Caratheodory, and Utikin. In this thesis, we are using the Filippov's Convention. We explain it in more details in Chapter 1. Also in Chapter 1 we briefly present all the preliminary concepts and results used in this thesis.

In Chapter 2 periodic trajectories of dynamical systems presenting discontinuities are studied. The considered model consists of two distinct linear differential systems which are defined on disjoint regions of the plane, the separation line being a union of two half straight lines contained on the coordinate axes. The obtained differential system is therefore non-smooth and so we apply Filippov's theory to study the transitions from one dynamical system to another. The combination of the two linear plus the Filippov's system acting on the separation line generates a nonlinear regime observed by the presence of limit cycles, sliding, and tangential periodic trajectories as well as the coexistence of such objects. In Theorems 25 and 26 we, respectively, provide sharp upper bounds of one or two limit cycles for certain classes of the considered model. We also establish the stability and hyperbolicity of these limit cycles. Moreover, we provide examples of reaching theses sharp upper bounds of one or two limit cycles.

In Chapter 3 we present a particular example of two distinct linear differential systems which are defined on disjoint regions of the plane, the separation line being the union of two half straight lines contained on the coordinate axes. The main result of this chapter, Theorem 29, presents a description of one-parameter family of piecewise vector fields. As we shall see the examples of systems reaching the bounds in Theorems 25 and 26 can be captured by that referred one-parameter family. The result exhibit some very interesting bifurcation phenomena as the bifurcation of a sliding periodic trajectory into a limit cycle and a *boundary equilibrium bifurcation* - BEB. A BEB occurs when an equilibrium or pseudo-equilibrium point moves under some parameter variation and collides with the switching manifold Σ. We also perform a global analysis of a representative model through bifurcation theory to analyze the birth of limit cycles, sliding periodic trajectories, and tangential ones.

The main techniques employed to obtain the results of Chapters 2 and 3 are first integrals, Poincaré half return maps, and elements of bifurcation theory. The main difference between our work and the work of several researchers in this line of study is that in addition to providing the upper bounds using first integrals, we study the displacement function as well as the conic equations associated with the problem and were able to say exactly the point that corresponds to limit cycle, information about hyperbolicity and stability. In this way, we provide a novel and useful incrementation to other results on the maximum number of possible limit cycles for the case that we studied.

In Chapter 4 we consider the same system present in Chapters 2 and 3 and we use Fenichel theory to better understand the dynamics of a point belonging to a nonregular region of the separation line. This approach allowed us to prove Theorem 36 which shows that the sliding periodic trajectory studied in Chapter 3 is, in fact, a homoclinic trajectory. Also, we establish and prove a result, Theorem 34 about the dynamic at the origin point for the discontinuous fast-slow generated by applied one blow-up of each vector field of $Z = (X, Y)$.

In Chapter 5 we propose the theory of Rotated Piecewise Smooth Vector Fields and we provide some results analogous to the results of classical smooth rotated vector fields. The goals of this chapter concern the comprehension of how the trajectories of two families of rotated vector fields behave as the same parameter is varied. The extension of the results from the classical theory of dynamical systems to the discontinuous framework is not clear since the last one involves the existence of tangency points, sliding and escaping points besides the fact that the vector fields can be rotated in different ways even in the case they depend on the same parameter which is the case considered in this chapter. The first goal of the chapter is to present some general results on rotated vector fields. First, we state sufficient conditions for which the regularization of rotated piecewise smooth vector fields is still rotated, see Theorem 42. After, we study how the rotation of a family of rotated vector fields affects the contact of fold points with a co-dimension one manifold, see Theorem 44. We also study the robustness of certain closed trajectories when the small parameter defining the rotation of the vector fields varies, see Theorem 45. Moreover, we establish some results similar to classical ones, such as the Classical non-intersection Theorem. In this way, we state Theorems 46, 47 and 48. As far we know, this is the first time that such a framework is considered in the literature.

Lastly, we introduce some sections on Appendix A whose purpose is to present and propose some problems and questions to be explored in the future. Those questions emerged during the studies and research developed in the Chapters presented in this thesis.

CHAPTER 1

Preliminaries

This chapter is divided into four sections. Each section is important to a good reading of this thesis because the theory introduced is used in the following chapters. In Section 1.1, Piecewise Smooth Vector Fields and Filippov Convection are introduced. In Section 1.2, smooth rotated vector fields are presented. In Section 1.3, we present regularization process. In Section 1.4, slow-fast systems and Classical Singular Perturbation theory are presented.

1.1 Piecewise Smooth Vector Fields and Filippov's Convention

In Piecewise Smooth Vector Fields there is a positive co-dimension manifold that divides the space into regions where vector fields are defined. Although in many works this division generated two regions, see [30, 46, 51, 52], we also can find works with more than two regions, see [48]. In this thesis, the focus is to study the case of two regions. We notice that this positive co-dimension manifold could be non-smooth as we can find in [2] and also is studied in Chapters 2, 3, and 4.

This division generates an interaction between smooth vector fields and the discontinuity set. A consequence of those interactions is the dynamic which presents some aspects non-existent in the smooth case like sliding and escaping regions. Roughly speaking, the sliding region can be defined as discontinuity's subset where each vector field of each region has a direction pointed for this subset in the sense of trajectories are moving for this subset while in the escaping region both vector fields have opposite directions in the sense of trajectories are moving away of the subset. Also, the notion of trajectories needs to be studied carefully. One of the most important convection used in piecewise smooth vector fields is due to Filippov [28] but there are others conventions like Barbashin, Caratheodory, and Utikin, see [22]. Due to the nondeterminism, probabilistic approaches can also take place, see for instance [64]. The choice to work with Filippov's convention is due to several applications on real problems in physics, control systems, electrical engineering, and problems involving impact, friction, among others, see [3, 18, 22, 40, 43, 50, 65, 66]. In this section, some basic results and definitions of Piecewise Smooth Vector Fields are introduced. We begin defining the discontinuity set as follows.

Let $\mathcal{V} = \mathbb{R}^2$ be an open set of $\mathbb{R}^n$ and let be Σ a manifold of co-dimension one of $\mathbb{R}^n$ given by $\Sigma = f^{-1}(0)$, where $f : \mathcal{V} \to \mathbb{R}$ is C^1 function and 0 is a regular value of f, i.e., $\nabla f(p) \neq 0$ for all $p \in f^{-1}(0)$. We call Σ the **discontinuity set (or switching manifold)**, that is the separating boundary of the regions $\Sigma^+ = \{p \in \mathcal{V}; f(p) \geq 0\}$ and $\Sigma^- = \{p \in \mathcal{V}; f(p) \geq 0\}$. We remark that f can be any function, if is necessary f will be specified.

Designate by $\mathcal{X}$ the space of C^r-vector fields defined on $\mathbb{R}^2$, endowed with the C^r-topology, with $r \geq 1$. Call Ω^r the space of vector fields $Z : U \subseteq \mathbb{R}^2 \to \mathbb{R}^2$, with U being an open subset of $\mathbb{R}^2$, such that

$$Z(x,y) = \begin{cases} X(x,y), \text{ if } (x,y) \in \Sigma^+; \\ Y(x,y), \text{ if } (x,y) \in \Sigma^-, \end{cases} \tag{1-1}$$

where $X = (X_1, X_2)$, $Y = (Y_1, Y_2) \in \mathcal{X}$. Notice that an analogous definition can be done for Z being a vector field on $\mathbb{R}^n$ but since in this thesis the focus is two dimensional space we directly defined for vector fields on $\mathbb{R}^2$. We can represent the piecewise smooth vector field Z by using the notation $Z = (X, Y, f)$.

Definition 1 *Consider the Lie derivatives,* $Xf(p) = \langle \nabla f(p), X(p) \rangle$ *and* $X^i f(p) =$

$\langle \nabla X^{i-1} f(p), X(p) \rangle$, $i \geq 2$, *where* $\langle , \rangle$ *is the usual inner product in* $\mathbb{R}^n$. *If* $\langle \nabla f(p), X(p) \rangle \neq 0$ *classify the points on* Σ *according to one of the following types:*

1. ***sewing (or crossing) region*** *is the set* $\Sigma^c = \{p \in \Sigma;\ (Xf(p))(Yf(p)) > 0\}$; *see Figure 1.1.*
2. ***escaping region*** *is the set* $\Sigma^e = \{p \in \Sigma;\ (Xf(p)) > 0$ *and* $(Yf(p)) < 0\}$; *see Figure 1.2.*
3. ***sliding region*** *is the set* $\Sigma^s = \{p \in \Sigma;\ (Xf(p)) < 0$ *and* $(Yf(p)) > 0\}$; *see Figure 1.2.*

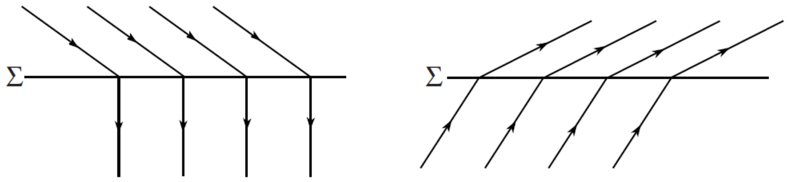

Figure 1.1: *Sewing Region according Filippov's Convention.*

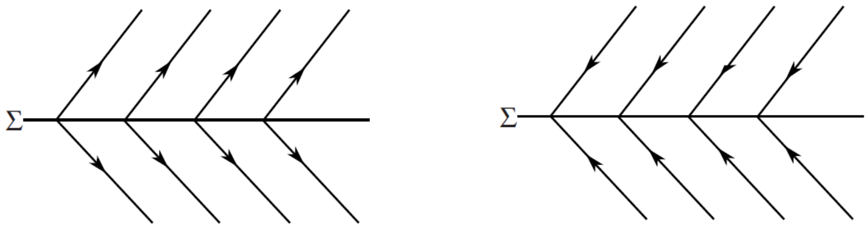

Figure 1.2: *On let: escaping region. On right: sliding region.*

When $p \in \Sigma^e \cup \Sigma^s$ following Filippov's convention presented in [28], we can define the *sliding vector field* associated to $Z \in \Omega^r$ it is defined as follows.

Definition 2 *Let be* p *in* Σ^s *then* $Z^s(p)$ *denotes the vector which is given by the convex combination of* X *and* Y. $Z^s(p)$ *can be denoted as:*

$$Z^s(p) = \lambda X(p) + (1 - \lambda) Y(p). \tag{1-2}$$

By assumption that $Z^s(p)$ is tangent to Σ at p, we obtain:

$$\begin{aligned}\langle \nabla f(p), Z^s(p)\rangle = 0 \quad &\Rightarrow \quad \langle \nabla f(p), \lambda X(p) + (1-\lambda)Y(p)\rangle = 0\\ &\Rightarrow \quad (\lambda X(p) + (1-\lambda)Y(p))\, f(p) = 0\\ &\Rightarrow \quad \lambda(X(p)f(p) - Y(p)f(p)) + Y(p)f(p) = 0\\ &\Rightarrow \quad \lambda = \frac{Y(p)f(p)}{X(p)f(p) - Y(p)f(p)}. \qquad (1\text{-}3)\end{aligned}$$

Finally, replacing equation (1-3) on equation (1-2) we obtain the expression of the sliding vector field as:

$$Z^s(p) = \frac{(Yf(p))X(p) - (Xf(p))Y(p)}{Yf(p) - Xf(p)}.$$

The Figure 1.3 show geometrically the sliding vector field.

Notice the escaping region Σ^e is the sliding region for the vector field $-Z$. Therefore, the vector field for the escaping region can be defined as $-(-Z)^s$. For both cases, the notation Z^s will be used.

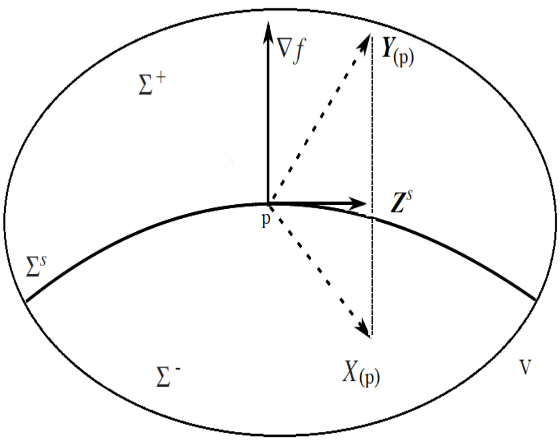

Figure 1.3: *Sliding vector field*

Definition 3 *We say that $q \in \Sigma$ is a Σ-regular if:*

(i) $(Xf(q))(Yf(q)) > 0$ *or*

(ii) $(Xf(q))(Yf(q)) < 0$ *and* $Z^s(q) \neq 0$*, i.e.,* $q \in \Sigma^s \cup \Sigma^e$ *and it is a regular point of* Z^s*.*

The points of Σ which are not Σ-regular are called Σ-*singular*. We distinguish two subsets in the set of Σ-*singular*, namely, Σ^t and Σ^p. Any point $q \in \Sigma^p$ is called a *pseudo equilibrium* of Z and it is characterized by $Z^s(q) = 0$. Any point $q \in \Sigma^t$ is called a *tangential singularity* or a *tangency point* of Z and it is characterized by $(Xf(q))(Yf(q)) = 0$ (q is a tangent contact point between the trajectories of X and/or Y with Σ at point q).

For $W \in \mathcal{X}$ we say that k is the *contact order* of the trajectory Γ_W passing through point p with $p \in \Sigma$ if $W^r(f(p)) = 0$, for all $r = 0,\ 1,\ \dots\ k-1$ e $W^k(f(p)) \neq 0$. If $W = X$ (respect. Y) we say that $p \in \Sigma$ is an *invisible* tangency if the contact order of Γ_X (respect. Γ_Y) passing through p is even and $X^k(f(p)) < 0$ (respect. $Y^k(f(p)) > 0$). On the other hand, we say that $p \in \Sigma$ is a *visible* tangency if the contact order of Γ_X (respect. Γ_Y) passing through p is odd or if it is even and $X^k(f(p)) > 0$ (respect. $Y^k(f(p)) < 0$). A tangential singularity $p \in \Sigma^t$ is *singular* if p is an invisible tangency for both X and Y. On the other hand, $p \in \Sigma^t$ is *regular* if it is not singular.

We say that p is a *critical element* of the vector field X (respect. Y) if p is an equilibrium point of X (respect. Y) or a pseudo equilibrium of X (respect. Y) or a tangency point of X (respect. Y). Let p be an equilibrium point of X (respect. Y). We say that p is *real* if $p \in \Sigma^+$ (respect. if $p \in \Sigma^-$) otherwise we say that p is *virtual*.

Normally, Σ is defined $\Sigma = f^{-1}(0)$ as defined before. However, Σ can be defined as the union of $f_i^{-1},\ \dots\ n$ with f_i^{-1} being at least a C^1 function and 0 being a regular value for each i. In this case, could exist points of Σ that those points are not regular. In this situations, we say that p is a $\Sigma-$non-regular point if Σ is non-regular at p. Thus, it is not possible to use Lie derivatives to classify such points. Nevertheless, we say it is (i) of crossing type if trajectories cross it from one side of Σ to another; (ii) of sliding or escaping type if they are the boundary of sliding and escaping regions of Σ^s or Σ^e, respectively, (iii) of regular tangential type if either X or Y have a tangential contact to it or (iv) of singular tangential type if no trajectories can reach it but itself.

Consider $W \in \mathcal{X}$ and denote its solution of the differential equation by $\phi_W(t, p)$, that is,

$$\begin{cases} \frac{d}{dt}\phi_W(t,p) = W(\phi_W(t,p)), \\ \phi_W(0,p) = p, \end{cases}$$

where $t \in I = I(p,W) \subset \mathbb{R}$ is an interval depending on $p \in I$ and W. The next two definitions state the concepts of the local and global trajectory of the non-smooth systems and they are slight modifications of those presented in [28]. The following can be found in [33] except by bullet (vi) that we have added due to the possibility of a non-regular shape of Σ.

Definition 4 *The* ***local trajectory*** $\phi_Z(t,p)$ *of a piecewise smooth vector field given by* (1-1) *is defined as follows:*

(i) For $p \in \Sigma^+ \setminus \Sigma^-$ and $q \in \Sigma^- \setminus \Sigma^+$ the trajectory is given by $\phi_Z(t,p) = \phi_X(t,p)$ and $\phi_Z(t,q) = \phi_Y(t,q)$, respectively, where $t \in I$.

(ii) For $p \in \Sigma^c$ such that $Xf(p) > 0$ and $Yf(p) > 0$, and taking the origin of the time at p, the trajectory is defined as $\phi_Z(t,p) = \phi_X(t,p)$ for $t \in I \cap \{t \geq 0\}$ and $\phi_Z(t,p) = \phi_Y(t,p)$ for $t \in I \cap \{t \leq 0\}$. For the case $Xf(p) < 0$ and $Yf(p) < 0$ the definition is the same reversing the time.

(iii) Taking the origin of the time at p, for $p \in \Sigma^e$ the trajectory is defined as $\phi_Z(t,p) = \phi_{Z^s}(t,p)$ for $t \in I \cap \{t \leq 0\}$ and it is either $\phi_Z(t,p) = \phi_X(t,p)$or $\phi_Y(t,p)$ or $\phi_Z(t,p) = \phi_{Z^s}(t,p)$ for $t \in I \cap \{t \geq 0\}$. For the case $p \in \Sigma^s$ the definition is the same but reversing time.

(iv) For $p \in Sigma$ a regular tangency point and taking the origin of the time at p, the trajectory is defined as $\phi_Z(t,p) = \phi_1(t,p)$ for $t \in I \cap \{t \leq 0\}$ and $\phi_Z(t,p) = \phi_2(t,p)$ for $t \in I \cap \{t \geq 0\}$, where each ϕ_1 and ϕ_2 is either ϕ_X or ϕ_Y or ϕ_{Z^S}.

(v) For p a singular tangency point we have $\phi_Z(t,p) = p$, $\forall t \in I$.

(vi) For p being a non-regular point of Σ, the trajectory is defined according to (ii), (iii), (iv) or (v) if p is a $\Sigma-$non-regular points of crossing, escaping/sliding, regular tangential or singular tangential type, respectively.

The following definition is presented in [4].

Definition 5 *A* ***global trajectory (orbit)*** $\Gamma_Z(t,p_0)$ *of* $Z \in \Omega^r$ *passing through* p_0 *is the union:*

$$\Gamma_Z(t,p_0) = \bigcup_{i\in\mathbb{Z}} \{\sigma(t,p_i);\ t_i \le t \le t_{i+1}\},$$

of preserving-orientation local trajectories $\sigma(t,p_i)$ *satisfying* $\sigma(t_{i+1},p_i) = \sigma(t_{i+1},p_{i+1}) = p_{i+1}$ *and* $t_i \to \pm\infty$ *as* $i \to \pm\infty$. *A global trajectory is* ***positive*** *(respectively,* ***negative****) if* $i \in \mathbb{N}$ *(respectively,* $-i \in \mathbb{N}$ *) and* $t_0 = 0$.

Definition 6 *Let* $\Gamma_Z(t,q)$ *be a global trajectory of system* (1-1). *We say that* Γ_Z *is periodic if* Γ_Z *is periodic in the variable* t, *i.e., if there exist* $T_n > 0$ *such that* $\Gamma_Z(t+T_n,q) = \Gamma_Z(t,q)$ *for all* t.

The next definition introduces the different types of periodic trajectories that we consider in this thesis, see Figure 1.4.

Definition 7 *Consider the piecewise smooth vector field* (1-1). *A closed global trajectory* Δ *of* Z *is a*

(i) ***crossing periodic trajectory*** *if it is isolated and does not contains points or segments in* $\Sigma^s \cup \Sigma^e$,

(ii) ***sliding periodic trajectory*** *if it is isolated and contain points or segments in* $\Sigma^s \cup \Sigma^e$,

(iii) ***tangential periodic trajectory*** *if it is isolated and contain points in* Σ^t,

(iv) ***internally center type periodic trajectory*** *if it is tangent to* Σ, *there is an arbitrary small inner neighborhood of* Δ *filled with periodic trajectories and for all arbitrary outer neighborhood of* Δ, *it is isolated.*

Notice that a closed global trajectory is isolated if in a small neighborhood $\mathcal{N}$ of Δ there is any other closed global trajectory Δ_1 of Z.

Remark 8 *Due to the similarity between the concepts of limit cycle for smooth dynamical systems theory and of crossing periodic trajectory, from now on we also call the last one as limit cycle. We emphasize, nonetheless, that it refers to an object in the non-smooth context and not a classical limit cycle.*

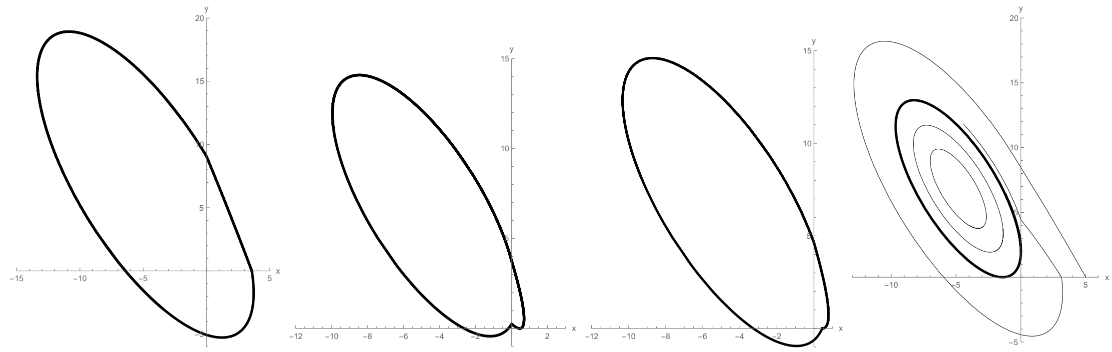

Figure 1.4: *Periodic trajectories, from left to right: crossing, sliding, tangential and internally center type.*

Concerning to bullet (iv), we also remark that in the literature an internally center type periodic trajectory does not need to be tangent a specific region but we will still use this nomenclature in this thesis for simplicity. We also notice that, because we are dealing with discontinuities, two types of internally center types periodic trajectories take place. On one hand, we have those whose outer small neighborhoods attract or repel trajectories asymptotically without reaching the periodic trajectory. On the other hand, it can be reached in finite time through trajectories sliding on Σ, which is the generic case. In this thesis, we do not explicitly distinguish these two situations.

An important tool to study hyperbolicity and stability of periodic trajectories is the displacement function, we define it in what follows. Consider $P_0 = (x_0, y_0)$ an initial condition. Denote the solutions associated with the vector fields X and Y in (1-1), respectively, by the maps $(t_0, P_0) \mapsto (x_1(t_0, P_0), x_2(t_0, P_0))$ and $(t_0, P_0) \mapsto (y_1(t_0, P_0), y_2(t_0, P_0))$. Let $P = (r, 0) \in \Sigma$ be a point such that $P \notin \Sigma^{e,s}$, and let $t^+ > 0$ be the smallest time such that $X(t^+, P) \cap \Sigma \neq \emptyset$. The first half return map associated with the vector field X in (1-1) is giving implicitly by the transition function $\rho_1(P) = x_1(t^+, P)$. Similarly, the first half return map associated with the vector field Y in (1-1) is giving by $\rho_2(P) = y_1(-t^-, P)$. Therefore, the **first return map** associated with system (1-1) is

$$\rho : \Omega \subset \Sigma \longrightarrow \Sigma, \; \rho(P) = (\rho_1 \circ \rho_2^{-1})(P),$$

where Σ is a suitable set formed by crossing points of Σ. Of course, if P^* is such that

$\rho(P^*) = P^*$, then the trajectory passing through P^* is periodic which is isolated (that is, a limit cycle) provided that $|\rho'(P)| \neq 1$.

Equivalently, one can also define the **displacement function** given by $P \mapsto d(P) = \rho(P) - P$, that is, periodic trajectories correspond to zeroes of such a map. Moreover, if $d(P^*) = 0$ satisfies $d'(P^*) \neq 0$, then the limit cycle passing through P^* is hyperbolic. In this case, if $d(P^*) > 0$ (respect. $d(P^*) < 0$) the limit cycle unstable (respect. stable). We notice that a limit cycle Γ can be neither stable nor unstable, in this case, we say that Γ is a semi-stable limit cycle. That happens if Γ is the $\alpha-$limit set for all trajectories contained on one side of Γ and close to it but the $\omega-$limit set for all trajectories that are close to Γ on the opposite side.

The next two definitions are extracted from [5] and they present the concept of closed poly-trajectory. Closed poly-trajectories are important objects studied in Chapter 5 which we discuss piecewise rotated vector fields.

Definition 9 *Consider $Z \in \Omega^r$. We say that the curve Γ is a* ***closed poly-trajectory*** *of Z if the following conditions are satisfied:*

(i) either Γ contains arcs of at least two of the vector fields $X_{|\Sigma^+}$, $Y_{|\Sigma^-}$ or Z^s or it is composed by a simple arc of Z^s;

(ii) the transition between the arcs of X an Y happens only in sewing points (and vice versa);

(iii) the transition between the arcs of X or Y and the arcs of Z^s happening in $\Sigma-$fold points or regular points in the escape or sliding arc, respecting the orientation. Besides that, if $\Gamma \neq \Sigma$ then there is at least one visible $\Sigma-$fold point on each connected component of $\Gamma \cap \Sigma$.

Definition 10 *Consider $Z \in \Omega^r$. We say that the curve Γ is a* ***closed poly-trajectory*** *of:*

(i) ***kind 1*** *if Γ meets Σ only in sewing points, i.e., only in Σ^c;*

(ii) ***kind 2*** *if $\Gamma = \Sigma$;*

(iii) ***kind 3*** *if Γ contains at least one visible $\Sigma-$fold point of Z.*

Moreover, we say that Γ *is hyperbolic if it is satisfied:*

(i) Γ *is of the kind 1 and* $\rho^{'}(p) \neq 01$, *where* ρ *is the first return map defined on a segment* T *with* $p \in T \pitchfork \Gamma$. *Besides, if* $\rho^{'}(p) < 1$ *(respect.* $\rho^{'}(p) > 1$*) then* Γ *is* ***stable*** *(respect.* ***unstable****).*

(ii) Γ *is of kind 2.*

(iii) Γ *is of kind 3,* $\overline{\Sigma^{e}} \cap \overline{\Sigma^{s}} \cap \Gamma = \varnothing$ *and either* $\Gamma \cap \Sigma \subseteq \Sigma^{c} \cup \Sigma^{e} \cup \Sigma^{p}$ *or* $\Gamma \cap \Sigma \subseteq \Sigma^{c} \cup \Sigma^{s} \cup \Sigma^{p}$.

Remark 11 *We notice that a closed poly-trajectory of kind 1 is a crossing periodic trajectory as defined in Definition 7. In the same way, a closed poly-trajectory of kind 3 is a particular case of sliding periodic trajectory as defined in Definition 7. We do this differentiation because it will be important in the proofs of results in Chapter 5.*

In what follows we introduce the notion of topological equivalence in Ω^{r}. This concept is necessary to prove some results in Chapter 3. We say that two piecewise smooth vector fields $Z = (X^{+}, X^{-}, f)$ and $\overline{Z} = (\overline{X}^{+}, \overline{X}^{-}, \overline{f})$ are $\Sigma-$ topologically equivalent if there exist an orientation-preserving homeomorphism h that sends $f^{-1}(0)$ to $\overline{f}^{-1}(0)$, the trajectories of X^{+} (respect. X^{-}) restricted to Σ^{+} (respect. Σ^{-}) to the trajectories of $\overline{X}^{+}$ (respect. $\overline{X}^{-}$) restricted to Σ^{+} (respect.Σ^{-}) preserving orientation, critical elements (equilibrium point, tangency point...) of Z to critical elements of $\overline{Z}$ and sliding (respect. escaping) regions of Z to sliding (respect. escaping) regions of $\overline{Z}$.

The notion of equivalence considered above is a strong one but it suits the problem addressed on Chapter 3.

1.2 Smooth Rotated Vector Fields

The classical theory of rotated vector fields started with Duff [23]. He developed this theory motivated by finding the solution for the general problem of limit cycles in the plane formulated by Poincaré [60]. Duff showed that a rotated vector field expands or contracts monotonically with a parameter until it intersects a critical point on the

Poincaré sphere. He also showed that the only possible type of bifurcation that occurs in one parameter family of limit cycles generated by a family of rotated vector fields is a saddle-node bifurcation at a semistable limit cycle of that family. Chen [14, 15, 16] and Perko [58, 59] extend this theory. Perko presented conditions for families of rotated vector fields having applications in the study of the precession of saddle separatrices under a rotation of the vector field. He also studied the existence and global behavior of limit cycles for certain classes of quadratic systems. Han [34] provided a general definition for rotated vector fields and established certain new theorems for the global behavior of limit cycles for a family of rotated vector fields which generalize, improve or correct some results in [14, 15, 16, 23, 58, 59].

In this section we briefly summarize the classical theory of rotated vector fields to familiarize the reader with some concepts that will be used in Chapter 5. First, we define a family of rotated vector fields as follows:

Definition 12 *We say that $X = (P(x,y,\mu), Q(x,y,\mu))$, with $X \in C^1(\mathbb{R}^2 \times \mathbb{R})$ define an one-parameter family of rotated vector fields if the equilibrium points of X are isolated and in all regular points of X we have:*

$$\det X = \begin{vmatrix} P & Q \\ P_\mu & Q_\mu \end{vmatrix} \neq 0. \tag{1-4}$$

If $\det X > 0$ (respec. $\det X < 0$) we say that the vector fields X is positively oriented (respec. negatively oriented).

We notice that if X does not have equilibrium points but in all regular points the condition (1-4) is satisfied, X is also one-parameter family of rotated vector fields.

Two of the most important results and properties of the rotated vector field are given in the Non-intersection Theorem and the Expansion and Contraction Theorem. The Non-intersection Theorem 13 establishes that limit cycles of different parameter values of an one-parameter family of rotated vector fields does not intersect each other. Theorem 14 provides properties about stable and unstable limit cycles. The Expansion and Contraction

Theorem 15 is an immediate consequence of Theorems 13 and 14 and it provides the behavior of stable and unstable limit cycles. We have summarized them as follows and we notice that their proofs can be found, for instance, in [56].

Theorem 13 (Non-Intersection Theorem) *Let be X an one-parameter family of rotated vector fields. Suppose that there are values $\mu = \mu_0$ and $\mu = \mu_1$, with $\mu_0 \neq \mu_1$, for which the systems associated to X and X admits limit cycles Γ_{μ_0} and Γ_{μ_1}, respectively. Then, Γ_{μ_0} does not intersect Γ_{μ_1}.*

Theorem 14 *Let X be an one-parameter family of rotated vector fields. Then, there exists an outer neighborhood U of any externally stable limit cycle Γ_{μ_0} of $f(X,\mu)$ such that through every point of U there passes a cycle Γ_μ of X where $\mu < \mu_0$ if Γ_{μ_0} is positively oriented and $\mu > \mu_0$ if Γ_{μ_0} is negatively oriented. Corresponding statements hold regarding unstable limit cycles and inner neighborhoods.*

Theorem 15 (Expansion and Contraction Theorem) *Let X be an one-parameter family of rotated vector fields. Stable and unstable limit cycles of X expand or contract monotonically as the parameter μ varies in a fixed sense and the motion covers an annular neighborhood of the initial position.*

1.3 Sotomayor-Teixeira Regularization

In this section we present some results and examples addressing approximations of piecewise smooth vector fields. We start introducing a central tool used in Chapter 5, the so-called Sotomayor-Teixeira regularization, see [63]. The regularization process of a piecewise smooth vector field consists in approximate a piecewise vector field by a C^r one-parameter family of vector fields. Shortly, given a piecewise smooth vector field $Z = (X,Y)$ the regularization processes consist in considering an X and Y in a suitable way, to recover information on the dynamical behavior of Z. Accordingly, let $\varphi : \mathbb{R} \longrightarrow \mathbb{R}$ be a C^r-function satisfying that $\varphi(x) = -1$ for $x \leq 1$, $\varphi(x) = 1$ for $x \geq 1$ and $\varphi'(x) > 0$

for $x \in (-1,1)$. As defined, φ is usually called a *transition function*. The φ-*regularization* of Z is the two-parameter family Z_μ^δ given by

$$Z_\mu^\delta(x,y) = \frac{X+Y}{2} + \varphi_\delta(f(x,y))\left(\frac{X-Y}{2}\right)$$

where $\varphi_\delta(x) = \varphi(x/\delta)$ and h is such that $\Sigma = h^{-1}(0)$. Clearly Z_μ^δ coincides with X and Y according to $|h(x,y)| \geq \delta$.

We cite two important results that will support in the prove of some results of Chapter 5. These results can be found, respectively, in [62] and [5].

Proposition 16 *(see [62]) Let Γ_0 be a closed hyperbolic poly-trajectory of* (1-1)*. Then, given a transition function φ there is a neighborhood V of Γ_0 and $\varepsilon_0 > 0$ such that for $0 < \varepsilon \leq \varepsilon_0$, Z^ε has only one hyperbolic periodic trajectory in V.*

Theorem 17 *(see [5]) Let Γ_0 be a closed hyperbolic poly-trajectory of* (1-1)*. Then, for any $\varepsilon > 0$ the regularized vector field Z^ε has only one hyperbolic limit cycle Γ_ε such that $\Gamma_\varepsilon \to \Gamma_0$ when $\varepsilon \to 0$.*

1.4 Slow-Fast Systems

In this section, we briefly summarize the Classical Singular Perturbation theory developed by Fenichel [27]. Which provides many asymptotic techniques. This section will be a very useful tool in Chapter 4.

Let $\mathcal{W} \subset \mathbb{R}^{n+1}$ be an open set whose elements are represented by (x,y). Let $f : \mathcal{W} \times [0,1] \to \mathbb{R}^m$ and $g : \mathcal{W} \times [0,1] \to \mathbb{R}^n$ be vector fields of class C^r, with $r \leq 1$. Given $0 < \varepsilon \ll 1$ consider the following system of differential equations

$$\begin{cases} \dot{x} &= f(x,y,\varepsilon), \\ \dot{y} &= \varepsilon g(x,y,\varepsilon), \end{cases}$$

where $\dot{\Box} = \dfrac{d\Box}{d\tau}$, $x = x(\tau)$ and $y(\tau)$. Applying at system (1-5) a time rescaling given by $\tau = \varepsilon t$ we obtain the following new system

$$\begin{cases} \varepsilon x' & = f(x, y, \varepsilon), \\ y' & = g(x, y, \varepsilon), \end{cases}$$

where $\Box' = \dfrac{d\Box}{dt}$, $x = x(t)$ and $y(t)$.

Notice that since $0 < \varepsilon \ll 1$, (1-5) and (1-5) have exactly the same phase portrait except for the trajectories speed. The trajectories speed is faster for (1-5) than for (1-5). Therefore the following definition makes sense.

Definition 18 *We say that equations* (1-5) *and* (1-5) *defines a* ***slow-fast system*** *where* (1-5) *is the* ***fast system*** *and* (1-5) *is the* ***slow system****.*

We can refer to τ as the **fast time scale** or only fast time and to t as the **slow time scale** or only slow time. The parameter ε is called the **time-scale parameter**. In several situations, we can have that f and g are independent of ε.

One of the reasons why slow-fast systems are studied is that they regularly appear in mathematical models in many areas of science. Another reason is that they present a very complex structure due to the parameter ε.

The first natural attempt to study a fast-slow system is to consider the case when $\varepsilon = 0$. We have the following definitions:

Definition 19 *Consider the equation* (1-5).

(i) The differential-algebraic equation obtained from (1-5) *by setting* $\varepsilon = 0$ *is called* ***slow subsystem*** *or* ***reduced problem*** *and it is given by equations:*

$$\begin{cases} 0 = & f(x, y, 0), \\ y' = & g(x, y, 0). \end{cases}$$

The flow generated by (1-5) *is called the* ***slow flow****.*

(ii) The parameterized system of differential equations obtained from equation (1-5) *by setting* $\varepsilon = 0$ *is called* ***fast subsystem*** *or* ***layer problem*** *and it is given by equations:*

$$\begin{cases} \dot{x} = & f(x,y,0), \\ \dot{y} = & 0. \end{cases}$$

The flow generated by (1-5) *is called the* ***fast flow***.

(iii) The cases $\varepsilon = 0$ *are called* ***singular limit***.

The natural strategy to study a fast-slow system is to decompose the solution curves of a fast-slow systems into singular limit segments. The idea is that depending on the region in phase space, we should use either the layer or the reduced problems. The trajectory described by the algebraic equation $f(x,y,0) = 0$ should be approximately by the solutions of the slow problem. Sufficiently far away from $\{f(x,y,0) = 0\}$, we expect the slow motion of the variables y to be irrelevant and hope to approximate trajectories by the fast flow. So, the following definition establishes the critical manifold for fast-slow systems.

Definition 20 *The set*

$$C_0 = \{(x,y) \in \mathbb{R}^m \times \mathbb{R}^n : f(x,y,0) = 0\} \tag{1-5}$$

is called the ***critical set***. *If* C_0 *is a submanifold of* $\mathbb{R}^m \times \mathbb{R}^n$ *then we say that* C_0 *is a* ***critical manifold***.

A relation between the equilibrium points of the fast flow and the critical manifold C_0 is given by the following proposition.

Proposition 21 *There is an one-to-one correspondence between the equilibrium points of the fast flow and the points of the critical manifold* C_0.

The main idea of Classical Singular Perturbation theory developed by Fenichel consists into combining the dynamics of the layer and reduced problems to recover the dynamics of the slow-fast system 18 with $\varepsilon > 0$ small enough. We enunciate the Fenichel theorem in what follows, this version can be found in [44].

Theorem 22 (Fenichel) *Suppose $S = S_0$ is a compact normally hyperbolic submanifold (possibly with boundary) of the critical manifold C_0 of (1-5) and that $f, g \in C^r (r < \infty)$. Then, for $\varepsilon > 0$ sufficiently small, the following hold:*

(i) There exists a locally invariant manifold S_ε diffeomorphic to S_0. Local invariance means that trajectories can enter or leave S_ε only through its boundaries.

(ii) S_ε has Hausdorff distance of order $O(\varepsilon)$ (as $\varepsilon \to 0$) from S_0.

(iii) The flow on S_ε converges to the slow flow as $\varepsilon \to 0$.

(iv) S_ε is C^r-smooth.

(v) S_ε is normally hyperbolic and has the same stability properties with respect to the fast variables as S_0 (attracting, repelling, or of saddle type).

(vi) S_ε is usually not unique. In regions that remain at a fixed distance from ∂S_ε, all manifolds satisfying items (i) to (v) lie at a Hausdorff distance $O(e^{\frac{-K}{\varepsilon}})$ from each other for some $K > 0$, $K = O(1)$.

Note that all asymptotic notation refers to $\varepsilon \to 0$. The same conclusions as for S_0 hold locally for its stable and unstable manifolds.

CHAPTER 2

Periodic Trajectories in Planar Discontinuous Piecewise Linear Systems with only Centers and a Nonregular Switching Line

A widely studied object in dynamical systems is the limit cycles which are the central problem of the famous Hilbert's 16^{th} problem. Nevertheless, a crucial problem in dynamics refers to studying the existence, number, and distribution of limit cycles, and in particular the birth and robustness of such objects. We recall that a limit cycle is a periodic trajectory of a differential system that is isolated in the set of all periodic trajectories of the system. In the piecewise smooth context, the Hilbert question becomes even more complicated because beyond limit cycles there exist other types of distinguished periodic trajectories like the sliding ones, related to the so-called sliding motion. In this chapter, we address the above questions and study several types of periodic trajectories.

The simplest type of piecewise smooth vector field consists of a continuous piecewise linear system separated with a straight line and it is known that such systems have at most one limit cycle, see [30, 46, 51, 52]. On the other hand, if the piecewise smooth linear system is discontinuous and separated with a straight line there exist no result providing an upper bound for the number of limit cycles, although several papers indicated that such an upper bound maybe three, see [2, 6, 31, 35, 38, 47, 61].

In [42], the authors studied the maximum number of crossing limit cycles of piecewise snooth linear systems formed by centers separated by a conic. A particular kind of piecewise smooth linear system is considered by Llibre and Teixeira [48]. In that paper, authors prove that, when both linear systems are of center type, the continuous or discontinuous non-smooth linear system has no limit cycles. It is also proved that a continuous piecewise smooth linear system separated with two parallel straight lines formed by three linear centers has no limit cycles. However, by considering two straight lines but discontinuous systems, it is proved that the system has at most one limit cycle and there are systems in this class having a limit cycle. Therefore the results in [48] suggest the switching manifold plays an important role in the existence of limit cycles.

In this chapter, the considered switching manifold is non-regular at a point that we assume to be the origin. Other papers considering a non-regular switching manifold can be found in the literature. For instance, Llibre and Zhang [49] prove that non-smooth linear systems formed by three linear centers and separated by the set $\Sigma = \{(x,\, y) : y = 0$ or $x = 0$ and $y \geq 0\}$ can have at most three limit cycles. The same bound is obtained in [70] by fixing the former set Σ and considering saddles and centers but five limit cycles are obtained in such context for a focus-focus type system. When the separation line is formed by two semi-straight lines that coincide at the origin forming an angle θ, where $\theta \in (0, \pi)$, Cardin and Torregrosa [10] proved that the system with a perturbation of the linear center has five limit cycles. With the same separation line but fixing $\theta = \frac{\pi}{2}$, Huan and Yang [39] provided an example of a focus-focus type system with five limit cycles as well. We remark that the authors in [39] also proved that it is enough to study the case when the angle is $\theta = \frac{\pi}{2}$ by showing that there is an invertible linear transformation transforming the system with $\theta \in (0, \pi)$ in the system with $\theta = \frac{\pi}{2}$. This is the reason why we set the discontinuity as we describe at the beginning of this chapter.

Starting by fixing a particular discontinuity set that will be used over this chapter. We set $\Sigma = \Sigma_1 \cup \Sigma_2$ where $\Sigma_1 = \{f_1^{-1}(0); x \geq 0\}$ and $\Sigma_2 = \{f_2^{-1}(0); y \geq 0\}$ being $f_1(x,y) = y$ and $f_2(x,y) = x$. Furthermore, we define the sets $\Sigma^+ = Q_1 \cup \Sigma$ and $\Sigma^- = Q_2 \cup Q_3 \cup Q_4 \cup \Sigma$, where $Q_n,\ n = 1, 2, 3, 4$, is the $n-$th quadrant of the plane $\mathbb{R}^2$.

Let $Z = (X,Y)$ be a piecewise vector field as defined in equation (1-1). In this chapter we assume that X and Y are linear vector fields given by

$$\begin{aligned} X(x,y) &= (\alpha x + \beta y + \gamma,\ ax + by + c) \text{ and} \\ Y(x,y) &= \left(\widetilde{\alpha} x + \widetilde{\beta} y + \widetilde{\gamma},\ \widetilde{a} x + \widetilde{b} y + \widetilde{c}\right), \end{aligned} \tag{2-1}$$

where $\alpha b - a\beta$, and $\widetilde{\alpha}\widetilde{b} - \widetilde{a}\widetilde{\beta}$ are positive values, $\alpha = -b$, and $\widetilde{\alpha} = -\widetilde{b}$, these conditions are set to both X and Y possesses a single equilibrium point of center type. We stress that neither X nor Y can have limit cycles since they are linear but every trajectory is closed and have the same period except by the equilibrium points.

In this chapter, we perform a global analysis of the piecewise smooth vector field (2-1) focusing on its periodic trajectories, more specifically, the upper bound, stability and hyperbolicity of its limit cycles. Under some hypotheses, we prove that system (2-1) has at most one or two hyperbolic limit cycles and we provide explicit systems for which these upper bound are reached.

The novelty of our approach consists, differently from the methodology adopted in the works mentioned above, in employing qualitative techniques to quantitative ones to guarantee that the kind of periodic trajectories we obtain are well oriented, isolated, and feasible. The geometric approach consists of the use of the Hamiltonian structure of the considered system to detect potential periodic trajectories. Once detected these *candidates* periodic trajectories, we switch our approach to an analytical one in order to verify they are indeed fixed points of the associated first return map. Having obtained the Poincaré map, we are able to establish the stability and hyperbolicity of the obtained limit cycles.

2.1 Statement of the Main Results of the Chapter

In this section, we state the main results of the chapter. The following lemma simplifies the calculations and can be found in [48].

Lemma 23 *System (2-1) can be written as* $Z = (X,Y)$ *with*

$$\begin{aligned} X(x,y) &= \left(-bx - \frac{4b^2+w^2}{4a}y + d,\; ax+by+c\right), \\ Y(x,y) &= \left(-Bx - \frac{4B^2+W^2}{4A}y + D,\; Ax+By+C\right), \end{aligned} \tag{2-2}$$

and $a,\ A,\ b,\ B,\ w,\ W > 0$.

Proof: The proof of Lemma 23 is quite simple so we outline it in what follows. Consider the piecewise vector field given in (2-1) where X and Y are replaced by $\widetilde{X}$ and $\widetilde{Y}$, respectively, to avoid confusion on the notation. By hypotheses $\widetilde{X}$ is linear and it has an isolated equilibrium point of center type. The conditions for the existence of a center are straightforward and given by $\alpha + b = 0$ and $4a\beta + (\alpha - b)^2 < 0$ so $\alpha = -b$. Moreover, by introducing the new parameter $w > 0$ satisfying $-w^2 = 4a\beta + (\alpha - b)^2 < 0$ we obtain $\beta = -\frac{4b^2+w^2}{4a}$ with $a > 0$. By replacing the obtained conditions for $\widetilde{X}$ in the system (2-1) we obtain X of the system (2-2). Similarly, we obtain Y from $\widetilde{Y}$, so the result is proven. $\square$

Remark 24 *We briefly explain the meaning of the conditions* $a,\ A,\ b,\ B,\ w,\ W > 0$. *Conditions* $a > 0$ *and* $A > 0$ *guarantee the escaping and sliding regions are bounded, this is explained in more detail in Lemma 27. Conditions* $w > 0$ *and* $W > 0$ *guarantee the equilibrium points of* X *and* Y *are indeed of center type. Finally, conditions* $b > 0$ *and* $B > 0$ *guarantee that both centers rotate counter-clockwise. The analogous results can be obtained by assuming* $b < 0$ *and* $B < 0$*, in this case, we only have a switch on the orientation of the trajectories.*

From now on in this chapter we consider the following parameters $\delta = 4b^2 + w^2$, $\Delta = 4B^2 + W^2$, $K = \frac{4(ad\Delta - AD\delta)}{A\delta - a\sqrt{\delta}\sqrt{\Delta}}$, $Q = \frac{4(ad\Delta - AD\delta)}{A\sqrt{\delta}\sqrt{\Delta} - a\Delta}$,
$M = A\sqrt{\Delta}\left[\frac{16(AD\delta - ad\Delta)^2}{\delta\left(A\sqrt{\delta} - a\sqrt{\Delta}\right)^2} + 4D(K+D)\right]^{1/2}$, and $N = a\sqrt{\delta}\left[\frac{16(AD\delta - ad\Delta)^2}{\Delta\left(A\sqrt{\delta} - a\sqrt{\Delta}\right)^2} + 4d(Q+d)\right]^{1/2}$.

Theorem 25 *Consider system (2-2) and assume that* $c = \frac{2a|d|}{\sqrt{\delta}}$ *and* $C = \frac{2A|D|}{\sqrt{\Delta}}$. *The following statements hold.*

(i) *If* $ad\Delta - AD\delta > 0$ *and* $A\sqrt{\delta} - a\sqrt{\Delta} > 0$, *then system* (2-2) *has at most one limit cycle* $\widetilde{\Gamma}$ *satisfying*

$$\widetilde{\Gamma}\cap\Sigma_1 = (r,0) = \left(\frac{4(ad\Delta - AD\delta)}{\sqrt{\delta}\sqrt{\Delta}\left(A\sqrt{\delta}-a\sqrt{\Delta}\right)},0\right) \text{ and } \widetilde{\Gamma}\cap\Sigma_2 = \left(0,\frac{8aA\left(D-\frac{d\sqrt{\Delta}}{\sqrt{\delta}}\right)}{a\Delta - A\sqrt{\delta}\sqrt{\Delta}}\right),$$

where $r > \max\left\{-\frac{c}{a}, -\frac{2C}{A}, -\frac{c}{a} + \frac{\sqrt{\delta(\delta c^2 - 4a^2d^2)}}{a\delta}\right\}$.

(ii) *The hyperbolicity of* $\widetilde{\Gamma}$ *is classified as follows.*

- $\widetilde{\Gamma}$ *is a hyperbolic stable limit cycle if* $-A^2(K+2D)M^{-1} > a^2(2d+Q)N^{-1}$,
- $\widetilde{\Gamma}$ *is a hyperbolic unstable limit cycle if* $-A^2(K+2D)M^{-1} < a^2(2d+Q)N^{-1}$ *and*
- $\widetilde{\Gamma}$ *is a non-hyperbolic limit cycle if* $-A^2(K+2D)M^{-1} = a^2(2d+Q)N^{-1}$.

(iii) *There are values of parameters for which system* (2-2) *has exactly one hyperbolic limit cycle.*

As can be observed in Theorem 25, the limit cycles that we detect in this chapter have two intersections with Σ, one of them in Σ_1 and the other one in Σ_2. Notice that due to Remark 24 those limit cycles must surround escaping and sliding regions if they exist at all.

Theorem 26 *Consider system* (2-2) *and assume that it satisfies either* $c = \frac{2a|d|}{\sqrt{\delta}}$ *or* $C = \frac{2A|D|}{\sqrt{\Delta}}$. *Then, system* (2-2) *has at most two limit cycles. Moreover, there are values of parameters for which there exist one or two hyperbolic limit cycles.*

2.2 Proof of the Main Results

This section is divided in three subsections. In the first one, we prove some preliminary results that are useful in the proof of Theorems 25 and 26. The other ones consist in the proofs of Theorems 25 and 26. One of the preliminary results concerns the displacement function and integrability associated with the vector fields of the system (2-2). We start proving Lemma 27 which characterizes the tangency points. We first notice that for the system (2-2) we get $\Sigma^t = \{T_1, T_2, T_3, T_4\}$, with

$$T_1 = \left(-\frac{c}{a},0\right), \quad T_2 = \left(-\frac{C}{A},0\right), \quad T_3 = \left(0,\frac{4ad}{\delta}\right) \quad \text{and} \quad T_4 = \left(0,\frac{4AD}{\Delta}\right), \tag{2-3}$$

where T_1 and T_3 are tangency points of the vector field X while T_2 and T_4 are tangency points of the vector field Y.

Lemma 27 *The following statements hold for system* (2-2)*:*

(i) the segments $\overline{T_1T_3} \subset \Sigma_1$ *and* $\overline{T_2T_4} \subset \Sigma_2$ *are formed by escaping or sliding points.*

(ii) The tangency points T_1 *and* T_3 *are visible if* $-\frac{ad}{b} < c < -\frac{4adb}{\delta}$ *and invisible if* $-\frac{4adb}{\delta} < c < -\frac{ad}{b}$.

(iii) The tangency points T_2 *and* T_4 *are visible if* $-\frac{4ADB}{\Delta} < C < -\frac{AD}{B}$ *and invisible if* $-\frac{AD}{B} < C < -\frac{4ADB}{\Delta}$.

Proof: In order to prove statement (a), consider the segment $\overline{T_1T_3}$ and notice the product of the Lie derivatives is a quadratic function on x given by $aAx^2 + aCx + Acx + Cc$ with discriminant $(Ac - aC)^2$, so $aAx^2 + aCx + Acx + Cc$ is negative for $x \in \Sigma_1$ between T_1 and T_3. The conclusion for the segment $\overline{T_2T_4}$ is analogous. The proof of statements (b) and (c) are straightforward. □

As a consequence of the previous Lemma, we have the region outside the bounded interval defined by the tangency points formed by crossing points. This lemma is important because it ensures how to take crossing points at Σ to obtain crossing limit cycles.

A central fact used in this chapter is that the vector fields X and Y of the system $Z = (X,Y)$ defined in (2-2) have first integrals

$$\begin{aligned} H_1(x,y) &= 4(ax+by)^2 + 8a(cx-dy) + y^2w^2 \text{ and} \\ H_2(x,y) &= 4(Ax+By)^2 + 8A(Cx-Dy) + y^2W^2, \end{aligned} \tag{2-4}$$

respectively, since

$$\begin{aligned} \frac{\partial H_1}{\partial x}\left(-bx - \frac{4b^2+w^2}{4a}y + d\right) + \frac{\partial H_1}{\partial y}(ax+by+c) &= 0 \text{ and} \\ \frac{\partial H_2}{\partial x}\left(-Bx - \frac{4B^2+W^2}{4A}y + D\right) + \frac{\partial H_2}{\partial y}(Ax+By+C) &= 0. \end{aligned}$$

These first integrals will be used to establish the upper bound for the number of periodic trajectories.

Next, we define the *displacement function* associated with the system (2-2), which allows us to determine the hyperbolicity of the limit cycles given by Theorems 25 and 26, as well as the stability of the limit cycles present in examples we provide throughout the chapter. Indeed let $P=(r,\ 0)\in\Sigma_1$ be an arbitrary point in Σ_1. The goal is to obtain conditions on r, in terms of the parameters of system $Z=(X,Y)$ defined in (2-2), such that the trajectory through P is periodic.

The first step in that direction is to determine the values of r for which trajectories of X and Y passing through $(r,0)$ meet Σ_2 in two points that can be coincident or not. In such case, we associate to each r the distance between those points. Of course, if the intersection points coincide, the distance is zero and we obtain a periodic trajectory. In other words, zeroes of such a correspondence between $r\in\Sigma_1$ and the referred distance will provide the limit cycles we are looking for. That correspondence is what we call the displacement function in this chapter.

The second step is to guarantee the displacement function is well defined. As commented before we are interested in limit cycles crossing Σ_1 and Σ_2 at most one point each. Therefore $P=(r,0)$ should be a point external to the sliding (or escaping) segment on Σ_1, that is, it must be located the tangency point in $\Sigma_1=\{(x,y);x\geq 0,y=0\}$ with has the biggest distance from origin point. The following result defines the displacement function.

Lemma 28 *Consider $P=(r,\ 0)\in\Sigma_1$ and let $Z=(X,Y)$ be a non-smooth vector field as defined in (2-2). Call $\varphi_X(P)$ and $\varphi_Y(P)$ the trajectories of X and Y starting at P, respectively. The following statements hold:*

(i) if $r>\max\{-\frac{c}{a},-\frac{C}{A}\}$ then P is a crossing point and, for some positive time, $\varphi_X(P)$ intersects the $y-$axis at two points $(0,y^+_{1,2})$ given by

$$y^+_{1,2}=2\frac{\left(\left[a\left(4ab^2r^2+4ad^2+ar^2w^2+8b^2cr+2crw^2\right)\right]^{1/2}\pm 2ad\right)}{\delta}.$$

Moreover,

(i.1) if $\delta c^2 - 4a^2d^2 \leq 0$*, then the intersections occur for all* $r > \max\{-\frac{c}{a}, -\frac{C}{A}\}$*;*

(i.2) if $\delta c^2 - 4a^2d^2 > 0$*, then the intersections occur for all* $r > \max\{-\frac{c}{a}, -\frac{C}{A}\}$ *where* $r \notin [r_-, r_+]$*, being*

$$r_\pm = -\frac{c}{a} \pm \frac{\sqrt{\delta(\delta c^2 - 4a^2d^2)}}{a\delta}.$$

(ii) If $r > \max\{-\frac{c}{a}, -\frac{2C}{A}\}$ *then* P *is a crossing point and, for some negative time,* $\varphi_Y(P)$ *intersects* Σ_2 *at a single point* $(0, y_2^-)$ *with*

$$y_2^+ = 2\frac{\left[A\left(4AB^2r^2 + 4AD^2 + Ar^2W^2 + 8B^2r + 2CrW^2\right)\right]^{1/2} \pm 2AD}{\Delta}.$$

(iii) If $y_2^+ > 0$*, then a displacement function* $d : I_r \longrightarrow \mathbb{R}$ *associated to system (2-2) is given by*

$$\begin{aligned} d(r) \quad &= 2\left(\frac{\left[a\left(4ab^2r^2+4ad^2+ar^2w^2+8b^2cr+2crw^2\right)\right]^{1/2}+2ad}{\delta}\right. \\ &\left. - \frac{\left[A\left(4AB^2r^2+4AD^2+Ar^2W^2+8B^2Cr+2CrW^2\right)\right]^{1/2}+2AD}{\Delta}\right), \end{aligned} \tag{2-5}$$

where I_r *is the open interval* $\left(\max\left\{-\frac{c}{a}, -\frac{2C}{A}, r_+\right\}, \infty\right)$*.*

Before we start the proof we notice that in order to define the displacement function at least one of the intersection points $(0, y_{1,2}^+)$ must occur in Σ_2, the weaker condition being $y_1^+ < 0$ and $y_2^+ > 0$. The condition $y_2^+ > 0$ is sufficient to reach the maximal cyclicity, but we remark that other configurations of the limit cycle may be obtained by replacing y_2^+ with y_1^+ in the previous result.

Proof: We start proving item (i). Consider $P = (r, 0) \in \Sigma_1$ and let n_1 be the level of H_1 associated to $\varphi_X(P)$ which writes $n_1(P) = 4a^2r^2 + 8acr$. By the expressions of the tangency points provided in (2-3), clearly, P is a crossing point and every tangency point is located on the left of P in Σ_1. From the expression of H_1, the trajectory $\varphi_X(P)$ intersects the $y-$axis if, and only if, y is a zero of $h_1(y)$ where $h_1(y)$ is given by

$$h_1(y) = (w^2+4b^2)y^2 - 8ady - 8acr - 4a^2r^2.$$

Notice that $h_1(y) = H_1(0,y) - n_1(P)$. Denote by y_1^+ and y_2^+ the zeroes of h_1 which writes as

$$y_{1,2}^+ = \pm 2\frac{\left(\left[a\left(4ab^2r^2+4ad^2+ar^2w^2+8b^2cr+2crw^2\right)\right]^{1/2} \pm 2ad\right)}{\delta}.$$

Clearly $y_{1,2}^+$ depend on the discriminant of h_1 which writes $disc_{h_1} = 16a(4ad^2+8b^2cr+2cw^2r+(4ab^2+aw^2)r^2)$. Notice that $disc_{h_1}$ is positive for every $r > \max\{-\frac{c}{a}, -\frac{C}{A}\}$ if $\delta c^2 - 4a^2d^2 < 0$, where $disc_{h_1}$ is the discriminant of h_1 respect to r. If $\delta c^2 - 4a^2d^2 = 0$ then the only zero of $disc_{h_1}$ is $r = -\frac{c}{a}$ which is a contradiction with the hypotheses. Thus we have the statement $(a.1)$ of item (i). A similar analysis leads to statements $(i.2)$. To prove item (ii) we now consider n_2 the level of H_2 associated with $\varphi_Y(P)$ which writes $n_2(P) = 4A^2r^2 + 8ACr$. Again P is a crossing point because $r > \max\{-\frac{c}{a}, -\frac{2C}{A}\}$ so, in particular, $r > \max\{-\frac{c}{a}, -\frac{C}{A}\}$. In this case, we claim that the trajectory $\varphi_Y(P)$ always intersects the $y-$axis in two points y_1^- and y_2^- being $y_1^- < 0 < y_2^-$ where

$$y_{1,2}^- = \pm 2\frac{\left(\left[A\left(4AB^2r^2+4AD^2+Ar^2W^2+8B^2r+2CrW^2\right)\right]^{1/2} \pm 2AD\right)}{\Delta}.$$

Indeed, the claim is proved by noticing that the trajectory $\varphi_Y(P)$ associated to level $n_2(P)$ of H_2 intersects the $x-$axis at the points P and $\left(\frac{-2C-Ar}{A}, 0\right)$. Since the trajectory of P by $\varphi_Y(P)$ is closed (in particular, an ellipse), a sufficient condition to obtain $y_{1,2}^-$ with $y_1^- < 0 < y_2^-$ is to set $\frac{-2C-Ar}{A} < 0$. But this condition is fulfilled when $r > -\frac{2C}{A}$ and from hypotheses the proof its done.

In order to finish the proof now we prove item (iii). When $y_2^+ > 0$ the expression (2-5) is well defined provided that r is a crossing point and the trajectories $\varphi_X(P)$ and $\varphi_Y(P)$ intercept Σ_2 ta crossing point, that is, provided that $r > \max\left\{-\frac{c}{a}, -\frac{2C}{A}, r_+\right\}$ so this concludes the proof. $\square$

2.2.1 Proof of Theorem 25

To prove Theorem 25 we have four cases to analyze depending on the signals of d and D. We start considering the case $d,\ D>0$, that is, assuming $c=\frac{2ad}{\sqrt{\delta}}$ and $C=\frac{2AD}{\sqrt{\Delta}}$. To prove item i), notice that the expressions of the first integrals (2-4) assuming c and C as above are

$$\begin{aligned} H_{c1}(x,y) &= 8a\left(\frac{x(2ad)}{\sqrt{\delta}}-dy\right)+4(ax+by)^2+w^2y^2,\\ H_{c2}(x,y) &= 8A\left(\frac{x(2AD)}{\sqrt{\Delta}}-Dy\right)+4(Ax+By)^2+W^2y^2. \end{aligned}$$

Clearly if system (2-2) has a candidate trajectory to be a limit cycle intersecting Σ at two points $(\bar{x},0)\in\Sigma_1$ and $(0,\bar{y})\in\Sigma_2$ with $\bar{x},\bar{y}>0$, then they satisfy

$$\begin{aligned} H_{c1}(\bar{x},0)-H_{c1}(0,\bar{y}) &= 0,\\ H_{c2}(0,\bar{y})-H_{c2}(\bar{x},0) &= 0. \end{aligned}$$

Thus we obtain

$$\begin{cases} \frac{16a^2d\bar{x}}{\sqrt{\delta}}+4a^2\bar{x}^2+8ad\bar{y}-4b^2\bar{y}^2-w^2\bar{y}^2=0,\\ \\ -\frac{16A^2D\bar{x}}{\sqrt{\Delta}}-4A^2\bar{x}^2-8AD\bar{y}+4B^2\bar{y}^2+W^2\bar{y}^2=0. \end{cases} \tag{2-6}$$

From Bézout's Theorem (see, for instance, [54]), the polynomial system (2-6) has at most 4 isolated real solutions $(\bar{x}_i,\bar{y}_i)$, $i=1,2,3,4$, so system (2-2) has at most 4 limit cycles. On the other hand, the trivial solution $(0,0)$ of (2-6) does not correspond to limit cycles, therefore system (2-6) can have at most 3 solutions. We shall prove that, under the hypotheses of Theorem 25, there exists at most one real isolated solution so the system (2-2) has at most one limit cycle.

Note that the equations of system (2-6) correspond to conics. Moreover, because $\bar{x},\bar{y}>0$, we are interested in the intersections of two conics occurring at the first quadrant. As long as they are isolated, we shall obtain a limit cycle. Accordingly, it is not difficult to see that both equations in (2-6) correspond to a pair of concurrent straight lines r_1, r_2 and s_2, s_2 where

$$r_1 : \overline{x} = -\frac{\sqrt{\delta}}{2a}\overline{y}, \quad r_2 : \overline{x} = \frac{\delta}{2a}\overline{y} - \frac{4d}{\sqrt{\delta}}$$

and

$$s_1 : \overline{x} = -\frac{\sqrt{\Delta}}{2A}\overline{y}, \quad s_2 : \overline{x} = \frac{\Delta}{2A}\overline{y} - \frac{4D}{\sqrt{\Delta}},$$

see Figure 2.1. The intersection between $r_{1,2}$ and $s_{1,2}$ occurs at the following points

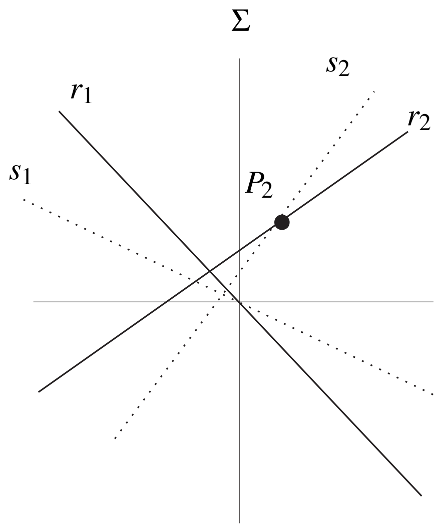

Figure 2.1: *The intersections between r_1, r_2, s_1, and s_2. P_2 is the point that is a candidate to be limit cycle.*

$$\begin{aligned}
P_1 &= (0,0), \\
P_2 &= \left(\frac{4\,(ad\Delta - AD\delta)}{\sqrt{\delta}\sqrt{\Delta}\left(A\sqrt{\delta} - a\sqrt{\Delta}\right)}, \frac{8aA\left(D - \frac{d\sqrt{\Delta}}{\sqrt{\delta}}\right)}{a\Delta - A\sqrt{\delta}\sqrt{\Delta}} \right), \\
P_3 &= \frac{1}{a\sqrt{\delta}\sqrt{\Delta} + A\delta}\left(-4ad\sqrt{\Delta}, 8aAd\right) \text{ and} \\
P_4 &= \frac{1}{\sqrt{\Delta}\left(a\sqrt{\Delta} + A\sqrt{\delta}\right)}\left(-4AD\sqrt{\delta}, 8aAD\right).
\end{aligned}$$

Notice that P_1, P_3, and P_4 do not correspond to zeroes of equations (2-6) because they do not belong to the first quadrant and we obtain at most one zero if the coordinates of P_2 are both positive. That is the case if the conditions $ad\Delta - AD\delta > 0$ and $A\sqrt{\delta} - a\sqrt{\Delta} > 0$ are fulfilled. Therefore, we obtain at most one limit cycle of $\widetilde{\Gamma}$.

We also notice that, since $\widetilde{\Gamma}$ corresponds to the solution $P_2 = (\bar{x}, \bar{y})$ of the equations (2-6) and by construction we have $(\bar{x}, 0) \in \Sigma_1$ and $(0, \bar{y}) \in \Sigma_2$, then it satisfies $r = \bar{x}$ and $s = \bar{y}$. In particular, there exist at most one limit cycle $\widetilde{\Gamma}$ satisfying the above conditions and such that $r > \max\{-\frac{c}{a}, -\frac{2C}{A}, -\frac{c}{a} + \frac{\sqrt{\delta(\delta c^2 - 4a^2d^2)}}{a\delta}\}$, thus item i) is proved.

To prove item ii) assume that system (2-6) has a limit cycle $\widetilde{\Gamma}$ according to item i). Since $r = \bar{x} = \frac{4(ad\Delta - AD\delta)}{\sqrt{\delta\Delta}\left(A\sqrt{\delta} - a\sqrt{\Delta}\right)}$ and $r > \max\{-\frac{c}{a}, -\frac{2C}{A}, r_{\pm} = -\frac{c}{a} + \frac{\sqrt{\delta(\delta c^2 - 4a^2d^2)}}{a\delta}\}$, then from Lemma 28 there exist a displacement function associated to system (2-6), that is, associated to $\widetilde{\Gamma}$. Therefore, using equation (2-5) we obtain

$$d(r) = \frac{2\left(a^2\left(4dr\sqrt{\delta} + \delta r^2 + 4d^2\right)\right)^{1/2} + 4ad}{\delta} - \frac{2\left(A^2\left(4Dr\sqrt{\Delta} + \Delta r^2 + 4D^2\right)\right)^{1/2} + 4AD}{\Delta},$$

where c and C in equation (2-5) have been replaced by the respective values provided in the hypotheses of the theorem setting d, $D > 0$.

It is not difficult to calculate the derivative of $d(r)$ and by replacing the values corresponding to r at the point P_2 above we obtain

$$d_s'(r_{P_2}) \quad = \quad 2\left(-\frac{A^2\,(K + 2D)}{M} + \frac{a^2\,(2d + Q)}{N}\right).$$

Therefore, if $-\frac{A^2(K+2D)}{M} \neq \frac{a^2(2d+Q)}{N}$ then $d_s'(r_{P_2}) \neq 0$ and P_2 corresponds to a hyperbolic limit cycle, being stable if $d_s'(r_{P_2}) < 0$ and unstable if $d_s'(r_{P_2}) > 0$. If $-\frac{A^2(K+2D)}{M} = \frac{a^2(2d+Q)}{N}$ then $\widetilde{\Gamma}$ is clearly non-hyperbolic. The previous arguments apply similarly for the cases where D and d are both negative or have opposite signs.

To complete the proof of Theorem 25 we exhibit an example of a system having one hyperbolic limit cycle so item (iii) is proved. Indeed, consider the piecewise linear vector field (2-2) with $a = 2$, $b = 1$, $c = -4\sqrt{2}$, $d = -4$, $w = 2$, $A = 1$, $B = 2$, $C = -\frac{2}{5}$,

$D = -1$ and $W = 3$. We obtain

$$X(x,y) = \left(-x-y-4, \quad 2x+y-4\sqrt{2}\right) \text{ and}$$
$$Y(x,y) = \left(-2x-\tfrac{25}{4}y-1, \quad x+2y-\tfrac{2}{5}\right), \tag{2-7}$$

which have one equilibrium for each of center type and they are oriented counterclockwise. It is straightforward that the points $T_1 = (\frac{2}{5}, 0)$, $T_2 = (2\sqrt{2}, 0)$ are, respectively, visible and invisible tangency points. The segment $(\frac{2}{5}, 2\sqrt{2}) \in \Sigma_1$ is a sliding region, so we have an internally center type periodic trajectory passing through T_1.

The first integrals of the two linear differential systems (2-7) are, respectively,

$$H_1(x,y) = 4(2x+y)^2 + 16\left(4y-4\sqrt{2}x\right) + 4y^2 \text{ and}$$
$$H_2(x,y) = 4(x+2y)^2 + 8\left(y-\frac{2x}{5}\right) + 9y^2,$$

then system (2-4) for the non-smooth vector field (2-7) becomes

$$-2\bar{x}^2 + 8\sqrt{2}\bar{x} + \bar{y}(\bar{y}+8) = 0 \text{ and}$$
$$-20\bar{x}^2 + 16\bar{x} + 5\bar{y}(25\bar{y}+8) = 0.$$

Taking into account that $\bar{x}$, $\bar{y} > 0$, the suitable solution of the previous system is

$$(\bar{x}, \bar{y}) = \left(\frac{9}{6}115\left(5\sqrt{2}+2\right), \frac{8}{115}\left(24\sqrt{2}+5\right)\right).$$

The solution $(x_1(t), y_1(t))$ of the first linear differential system (2-7) such that $(x_1(0), y_1(0)) = (\bar{x}, 0)$ is

$$x_1(t) = \tfrac{4}{115}\left(\left(-120\sqrt{2}-163\right)\sin(t) + \left(5\sqrt{2}-67\right)\cos(t) + 115\left(1+\sqrt{2}\right)\right) \text{ and}$$
$$y_1(t) = -\tfrac{4}{115}\left(\left(-125\sqrt{2}-96\right)\sin(t) + \left(-115\sqrt{2}-230\right)\cos(t) + 115\sqrt{2}+230\right).$$

and the solution $(x_2(t), y_2(t))$ of the second linear differential system (2-7) such that

$(x_2(0), y_2(0)) = (\bar{x}, 0)$ is

$$x_2(t) = \tfrac{2}{69}\left(\left(-240\sqrt{2}-73\right)\sin\left(\tfrac{3t}{2}\right) - 69\cos\left(\tfrac{3t}{2}\right) + 69\right) \text{ and}$$
$$y_2(t) = -\tfrac{4}{345}\left(\left(-192\sqrt{2}-17\right)\sin\left(\tfrac{3t}{2}\right) - \left(144\sqrt{2}+99\right)\cos\left(\tfrac{3t}{2}\right) + 69\right).$$

Since there is no sliding or escaping region in Σ_2 and $\bar{x} > 2\sqrt{2}$, the trajectories of $(x_1(t),\, y_1(t))$ and $(x_2(t),\, y_2(t))$ for $t \in [-\pi, \pi]$ correspond to a limit cycle Γ_u, see Figure 2.2. The displacement function of system (2-7) is given by

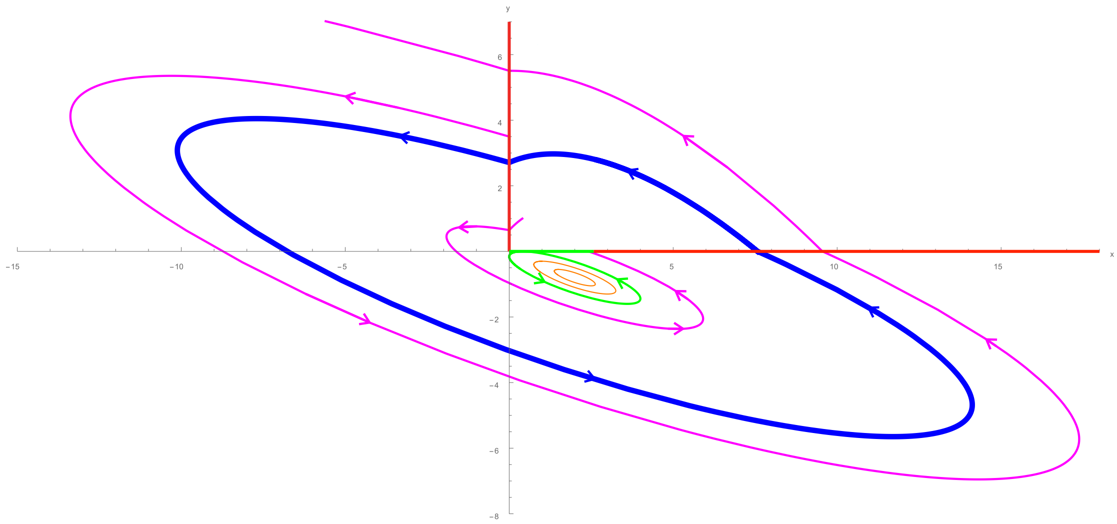

Figure 2.2: *In blue line limit cycle of the system (2-7) with $a = 2$, $b = 1$, $c = -4\sqrt{2}$, $d = -4$, $w = 2$, $A = 1$, $B = 2$, $C = -\frac{2}{5}$, $D = -1$ and $W = 3$. In addition, we notice the green line is an internally center type periodic trajectory.*

$$d(r) = \sqrt{2}\sqrt{\left(r-2\sqrt{2}\right)^2} - \frac{2}{25}\sqrt{(5r-2)^2} - \frac{96}{25},$$

and the zeroes are $p_1 = 0$ and $p_2 = \frac{96}{115}\left(5\sqrt{2}+2\right)$. Notice that $\bar{x} = p_2$, then we can study the hyperbolicity of the limit cycle, in fact we have

$$d'(r) = \frac{\sqrt{2}\left(r-2\sqrt{2}\right)}{\sqrt{\left(r-2\sqrt{2}\right)^2}} - \frac{2(5r-2)}{5\sqrt{(5r-2)^2}} \quad \Longrightarrow \quad d'(\bar{x}) = \sqrt{2} - \frac{2}{5} > 0.$$

Therefore, Γ_u is a hyperbolic unstable limit cycle so Theorem 25 is proved.

2.2.2 Proof of Theorem 26

To prove Theorem 26 we have consider four cases, the case when $d < 0$ or $d > 0$ or $D < 0$ or $D > 0$. We start proving the case $D > 0$, and the other cases are proved similarly. Indeed, since $D > 0$ we obtain $C = \frac{2AD}{\sqrt{\Delta}}$. Replacing this condition into the first integrals (2-4) and proceeding analogously to the proof of Theorem 25 we obtain two conics whose equations are given

$$H_1(\bar{x},\bar{y}) : (2a\bar{x}-2c)^2 - \left(\bar{y}\sqrt{\delta} - \frac{4ad}{\sqrt{\delta}}\right)^2 - \frac{16a^2d^2}{\delta} - 4c^2 = 0,$$
$$H_2(\bar{x},\bar{y}) : \left(\bar{x} + \frac{\bar{y}\sqrt{\Delta}}{2A}\right)\left(\bar{x} - \frac{\bar{y}\Delta - 8AD}{2A\sqrt{\Delta}}\right) = 0.$$

The equation $H_2(\bar{x},\bar{y})$ corresponds to a pair of concurrent straight lines s_1 and s_2 being

$$s_1 : \bar{x} = -\frac{\bar{y}\sqrt{\Delta}}{2A}, \qquad s_2 : \bar{x} = \frac{\bar{y}\Delta - 8AD}{2A\sqrt{\Delta}},$$

and the analysis is the same as done in the proof of Theorem 25. The equation $H_1(\bar{x},\bar{y}) = 0$ corresponds to a hyperbole $\mathcal{H}$. It can be checked that $\mathcal{H}$ crosses the coordinates axes at the points

$$P_0 = (0,0), \quad P_y = \left(0, \frac{8ad}{\delta}\right), \quad P_x = \left(-\frac{2c}{a}, 0\right).$$

The position of $\mathcal{H}$ with respect to the axes depends on the signs of c and d, so we have four cases to be considered. More precisely, the center of $\mathcal{H}$ belongs either to the first quadrant if $c < 0 < d$ or to the second if $c, d > 0$ or to the third if $d < 0 < c$ or to the fourth one if $c, d < 0$, see Figures 2.3, 2.4 and 2.5, respectively.

Now we study the intersection of $\mathcal{H}$, s_1, and s_2. Since we are looking for limit cycles the only interest we have is on the intersections occurring in the first quadrant. Without loss of generality, we shall study the case $c < 0 < d$, the other cases being

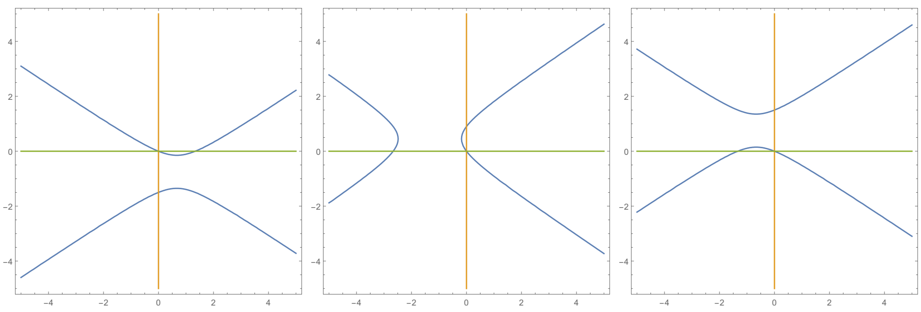

Figure 2.3: *The left and central figures correspond to the possibilities for $\mathcal{H}$ with $c, d > 0$. The right figure corresponds to $\mathcal{H}$ with $c, d < 0$.*

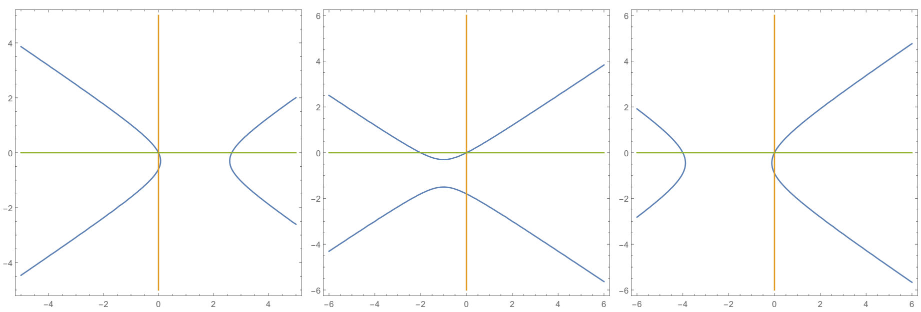

Figure 2.4: *In figure on left we have one possibility for the hyperbole $\mathcal{H}$ with $c, d < 0$ and in figure on center and right we have possibilities for the hyperbole $\mathcal{H}$ with $d < 0 < c$.*

analogous. Indeed $\mathcal{H}$, s_1, and s_2 have four intersections points, namely

$$P_1 = \frac{\left(-2A\left(-2aD\sqrt{\gamma}+C\gamma\right), 4aA\left(2aD-C\sqrt{\gamma}\right)\right)}{T}, \quad P_{2,3} = (X_{2,3}, Y_{2,3}), \quad P_4 = (0,\, 0),$$

where

$$\begin{aligned} X_{2,3} &= \frac{4a^3 d\Delta - 2a^2AD\delta - aAC\delta^{3/2}}{R} \pm \frac{\delta}{R}\left(a^2A\left(4aA\delta D\left(\sqrt{\delta}C - 4Ad\right) + A\delta^2C^2\right)\right)^{1/2} \\ &\quad \pm \frac{\delta}{R}\left(\frac{a^2A\left(4a^2\left(4A\Delta d^2 + A\delta D^2 - 2\Delta\sqrt{\delta}dC\right)\right)}{\delta}\right)^{1/2}, \\ Y_{2,3} &= \frac{-4a^2AD + 8aA^2d - 2aAC\sqrt{\delta}}{T} \pm \frac{1}{2T}\left(a^2A\left(A\left(8aD - 16Ad + 4\sqrt{\delta}C\right)^2\right)\right)^{1/2} \\ &\quad \pm \frac{1}{2T}\left(a^2A\frac{128d\left(a^2\Delta - A^2\delta\right)\left(2Ad - \sqrt{\delta}C\right)}{\delta}\right)^{1/2}. \end{aligned}$$

with $R = a\sqrt{\delta}\left(A^2\delta - a^2\Delta\right)$ and $T = \left(A^2\delta - a^2\Delta\right)$.

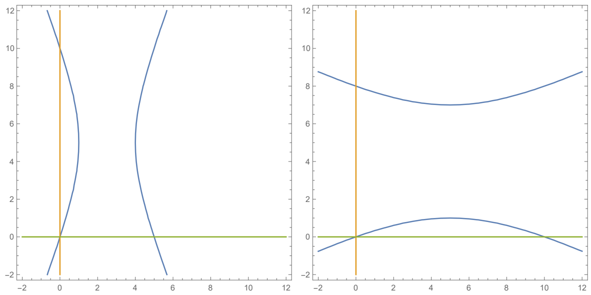

Figure 2.5: *Possibilities for the hyperbole $\mathcal{H}$ with $c < 0 < d$.*

Notice that we cannot determine which of these points belong to the first quadrant, however, we know the position of these conics relative to coordinated axes and one of these points is the origin, so we have at most two intersections between the conics $\mathcal{H}$, s_1, and s_2 occurring at the first quadrant, see Figure 2.6. Therefore we can obtain at most two limit cycles. To complete the proof of Theorem 26 we exhibit examples with

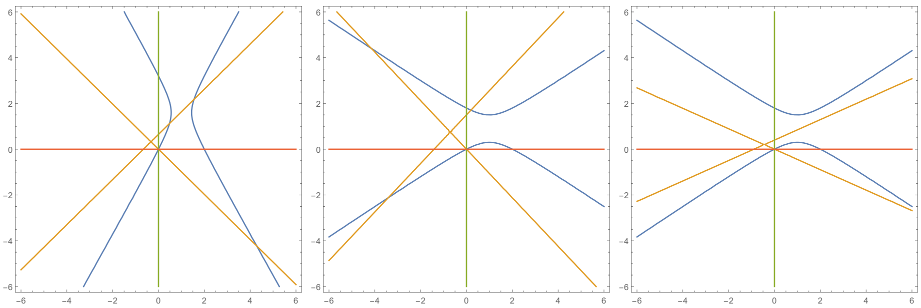

Figure 2.6: *Example with two, one and zero intersection between the conics $\mathcal{H}$, s_1 and s_2 occurring at the first quadrant.*

one and two hyperbolic limit cycles. Indeed, consider the piecewise linear vector field (2-2) with $a = 9$, $b = 4$, $c = -4$, $d = 4$, $w = 2$, $A = 2$, $B = 1$, $C = 2\sqrt{2}$, $D = 2$ and $W = 2$ we get

$$
\begin{aligned}
X(x,y) &= \left(-4x - \frac{17y}{9} + 4, 9x + 4y - 4\right), \\
Y(x,y) &= \left(-x - y + 2, 2x + y + 2\sqrt{2}\right).
\end{aligned}
\tag{2-8}
$$

We show that system (2-8) has one hyperbolic limit cycle. We have two systems with a linear center, indeed the eigenvalues of the matrices of the two linear differential systems (2-8) are both $\pm i$. Besides that, the linear centers are counterclockwise oriented.

It is not difficult to see that $T_1 = \left(\frac{4}{9}, 0\right)$ and $T_4 = (0, 2)$ are a real visible tangency point and $T_3 = \left(0, \frac{36}{17}\right)$ is a real invisible tangency point. Furthermore, the segment $\left(0, \frac{4}{9}\right) \in \Sigma_1$ is a sliding region while the segment $\left(2, \frac{36}{17}\right) \in \Sigma_2$ is an escaping region. The displacement function associated with (2-8) is

$$d(r) = \sqrt{2}\left(\left(r+\sqrt{2}\right)^2\right)^{1/2} - \frac{3}{17}\left(17r(9r-8)+144\right)^{1/2} - \frac{2}{17}.$$

Similarly to the proof of Theorem 25 the zeros of $d(r)$ coincide with the x-coordinate of the points P_i, $i = 1, 2, 3$ provided above. The particular zero of $d(r)$ satisfying the hypotheses of Lemma 28 is

$$X_2 = \frac{4}{47}\left(8\sqrt{2} + \left(2\left(72\sqrt{2}+81\right)\right)^{1/2} + 9\right).$$

One can see that X_2 corresponds to the x-coordinate of the point P_2. Notice also that $X_2 \notin \left(0, \frac{4}{9}\right) \in \Sigma_1$ so the limit cycle passing through X_2 corresponds is a crossing one. Moreover, because

$$d'(X_2) = \frac{47}{17\sqrt{2} + 3\left(256\sqrt{2} - 135\right)^{1/2}}$$

is positive, the limit cycle passing through X_2 is hyperbolic and unstable. The unstable limit cycle is shown in Figure 2.7.

Now, consider the non-smooth linear system (2-2) with $a = 9$, $b = 4$, $c = -4$, $d = 5$, $w = 2$, $A = 2$, $B = 1$, $C = 2\sqrt{2}$, $D = 2$ and $W = 2$. We get

$$\begin{aligned} X(x,y) &= \left(-4x - \frac{17y}{9} + 5,\, 9x + 4y - 4\right), \\ Y(x,y) &= \left(-x - y + 2,\, 2x + y + 2\sqrt{2}\right). \end{aligned} \tag{2-9}$$

We now show that system (2-9) has two limit cycles. Again we obtain two systems with a linear center counterclockwise oriented.

It is straightforward to determine the tangency points and to see that the segments $\left(0, \frac{4}{9}\right) \in \Sigma_1$ and $\left(2, \frac{45}{17}\right) \in \Sigma_2$ are formed by sliding and escaping points, respectively. The displacement function associated with (2-9) is now

$$d(r) = -\sqrt{2}\left(r+\sqrt{2}\right) + \frac{3}{17}\left(17r(9r-8)+225\right)^{1/2} + \frac{11}{17}, \tag{2-10}$$

and the zeros satisfying the hypotheses of Lemma 28 associated with the x-coordinate of P_i, $i = 1,\ 2,\ 3$ are

$$\begin{aligned} X_2 = &\ \tfrac{1}{47}\left(23\sqrt{2} - \left(1656\sqrt{2}-1782\right)^{1/2} + 36\right), \\ X_3 = &\ \tfrac{1}{47}\left(23\sqrt{2} + \left(1656\sqrt{2}-1782\right)^{1/2} + 36\right), \end{aligned} \tag{2-11}$$

where X_2 is associated to P_2 and X_3 is associated to P_3. Notice that $X_2,\ X_3 \notin \left(0, \frac{4}{9}\right) \in \Sigma_1$ so they correspond to limit cycles.

As done previously, it is straightforward to see that $d'(X_2) < 0$ so the limit cycle associated with X_2 is hyperbolic and stable. Also, $d'(X_3) > 0$ so the limit cycle associated with X_3 is hyperbolic and unstable, see Figure 2.8. This concludes the proof.

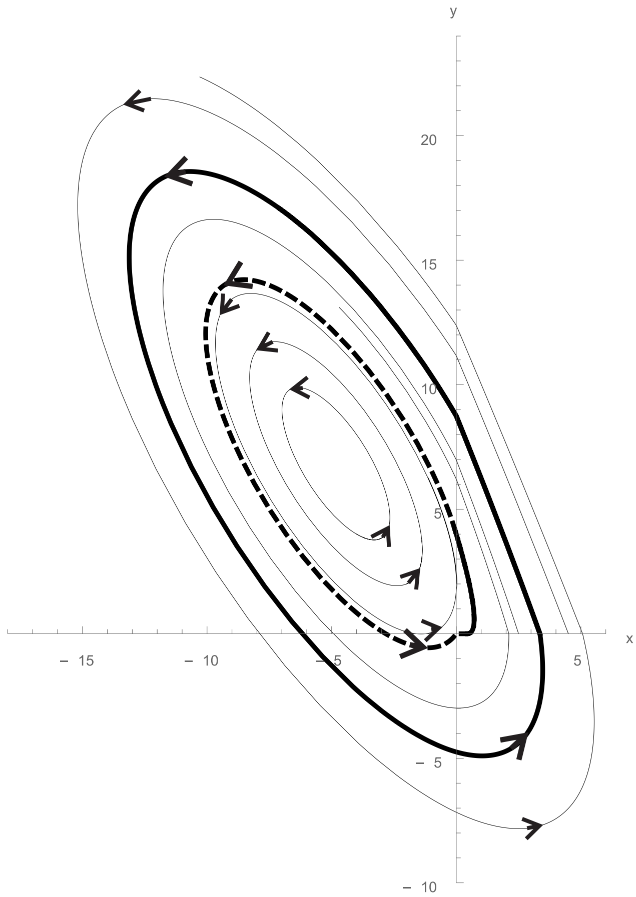

Figure 2.7: *In bold line the limit cycle of system* (2-8) *with* $a = 9$, $b = 4$, $c = -4$, $d = 4$, $w = 2$, $A = 2$, $B = 1$, $C = 2\sqrt{2}$, $D = 2$ *and* $W = 2$. *In addition, the dashed line is a sliding periodic trajectory.*

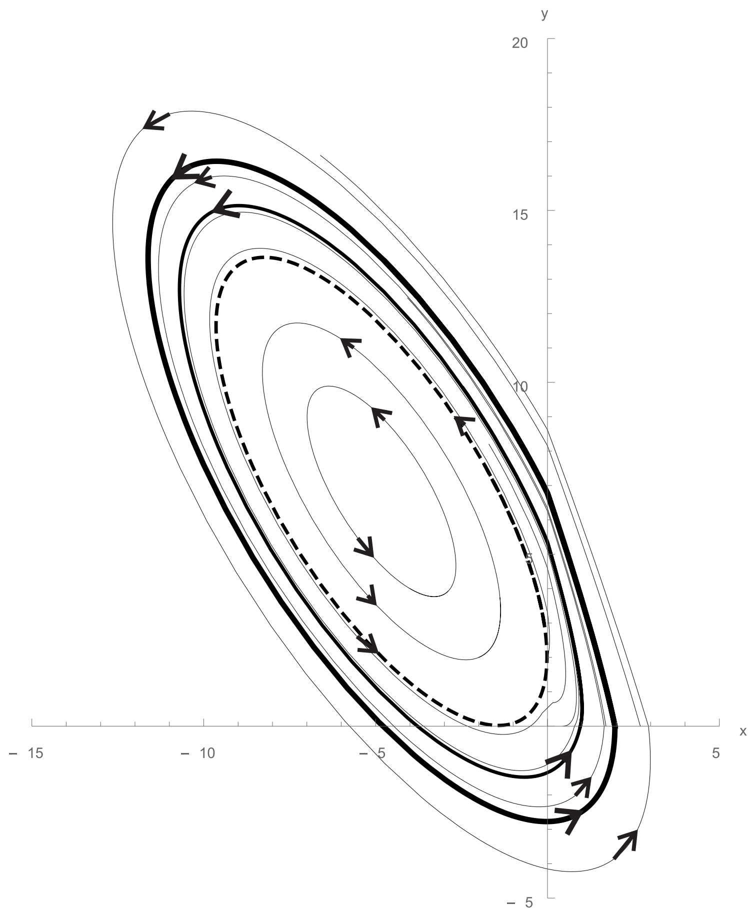

Figure 2.8: *The bold lines are the two limit cycles of system* (2-9) *with* $a = 9$, $b = 4$, $c = -4$, $d = 5$, $w = 2$, $A = 2$, $B = 1$, $C = 2\sqrt{2}$, $D = 2$ *and* $W = 2$. *It presents an unstable limit cycle (external) and a stable limit cycle (internal). In addition, the dashed line is the internally center type periodic trajectory.*

CHAPTER 3

Bifurcation of Periodic Trajectories in Planar Discontinuous Piecewise Linear Systems with only Centers and with a Nonregular Switching Line

In this chapter we perform the global analysis of a representative model through bifurcation theory to analyze the birth of limit cycles, sliding periodic trajectories, and tangential ones. We also provide some results addressing the coexistence of periodic trajectories and a physical interpretation of the model considered in the chapter. The main techniques employed to obtain the results are first integrals, first return maps, and elements of bifurcation theory.

3.1 Statement of the Main Results of the Chapter

In this chapter, we study a particular one-parametric model coming from the system (2-1), for which we analyze the birth of several kinds of periodic trajectories. We also detected some interesting bifurcation phenomena involving equilibrium, tangential and periodic trajectories. We highlight that we have detected every bifurcation value for the mentioned one-parametric model since we are able to prove the topologically conjugation of systems (2-1) for non-bifurcation values. In particular, we study the entire finite portion of the phase portrait of such model, classifying the trajectories for every real value of the parameters defining the model.

We fix a particular discontinuity set that will be used over this chapter. The discontinuity set is the same discontinuity set of chapter 2. We set $\Sigma = \Sigma_1 \cup \Sigma_2$ where $\Sigma_1 = \{f_1^{-1}(0); x \geq 0\}$ and $\Sigma_2 = \{f_2^{-1}(0); y \geq 0\}$ being $f_1(x,y) = y$ and $f_2(x,y) = x$. Furthermore, we define the sets $\Sigma^+ = Q_1 \cup \Sigma$ and $\Sigma^- = Q_2 \cup Q_3 \cup Q_4 \cup \Sigma$, where $Q_n,\ n = 1, 2, 3, 4$, is the $n-$th quadrant of the plane $\mathbb{R}^2$.

The main result of this chapter presents a description of one-parameter family of piecewise vector fields. As we shall see the examples of systems reaching the bounds in Theorems 25 and 26 can be captured by that referred one-parameter family. The results exhibit some very interesting bifurcation phenomena as the bifurcation of a sliding periodic trajectory into a limit cycle and a *boundary equilibrium bifurcation* - BEB. A BEB occurs when an equilibrium or pseudo-equilibrium point moves under some parameter variation and collides with the switching manifold Σ. We start fixing $a = 9$, $b = 4$, $c = -4$, $d = \mu \in \mathbb{R}$, $w = 2$, $A = 2$, $B = 1$, $C = 2\sqrt{2}$, $D = 2$ and $W = 2$, so system (2-2) becomes

$$X_\mu(x,y) = \begin{cases} X(x,y) = \left(-4x - \frac{17}{9}y + \mu, 9x + 4y - 4\right), & (x,y) \in \Sigma^+, \\ Y(x,y) = \left(-x - y + 2, 2x + y + 2\sqrt{2}\right), & (x,y) \in \Sigma^-. \end{cases} \tag{3-1}$$

The following theorem addresses some elements of the phase portrait of X_μ as sliding and escaping regions, tangency points, etc, and also addresses the bifurcation of limit cycles, sliding, tangential and center type periodic trajectories.

Theorem 29 *There exists seventeen distinct phase portraits for the vector field X_μ according to Table 3.1. In particular, eight bifurcations take place corresponding to the following bifurcation values*

(i) at $\mu_1 = -2\sqrt{2}$ a boundary saddle-node bifurcation occurs at the origin with the birth of two coincident pseudo-equilibrium points;

(ii) *at $\mu_2 = 0$ a bifurcation occurs at the origin with the birth of the visible tangency point T_2;*

(iii) *at $\mu_3 = \frac{16}{9}$ a border equilibrium bifurcation occurs at the point $\left(\frac{4}{9}, 0\right) \in \Sigma_1$. At this point a triple collision involving an equilibrium, a pseudo equilibrium and two tangency points takes place;*

(iv) *at $\mu_4 = \frac{17}{9}$ a border equilibrium bifurcation occurs at the point $(0,1) \in \Sigma_2$. At this point a triple collision involving an equilibrium, a pseudo equilibrium and two tangency points takes place;*

(v) *at $\mu_5 = \frac{34}{9}$ a bifurcation occurs at the point $(0,2)$ with the collision of two tangency points; There is a birth of a sliding periodic trajectory Γ_{ρ_1} and an stable center type periodic trajectory Γ_{ts} becomes an unstable center type periodic trajectory Γ_{tu};*

(vi) *at $\mu_6 = 4$ a "corner" bifurcation takes place with the appearance of a sliding periodic trajectory Γ_{ρ_2} passing through the origin;*

(vii) *at $\mu_7 = \frac{4\left(631\sqrt{2}+6408\right)}{6399}$ a bifurcation of a tangential periodic trajectory Γ_{ρ_4} occurs;*

(viii) *at $\mu_8 = 2(\sqrt{2}+9) - \frac{2}{3}\sqrt{47(2\sqrt{2}+9)}$ a semi-stable limit cycle Γ_{su} bifurcates through the collision of two limit cycles.*

Moreover, for every $\mu_i < \overline{\mu}, \widetilde{\mu} < \mu_{i+1}$, $i = 1, \ldots, 7$, $X_{\overline{\mu}}$ and $X_{\widetilde{\mu}}$ are $\Sigma-$topologically equivalent.

3.2 Proof of Theorem 29

To prove Theorem 29 we study each feature of the system (3-1) to fully describe its phase portrait as summarized in Table 3.1. We start studying the equilibria.

Part 1 - Equilibrium points: Notice that the equilibrium point of the vector field Y in (3-1) is $E_2 = \left(-2\left(\sqrt{2}+1\right), 2\left(\sqrt{2}+2\right)\right)$ which belongs to the second quadrant and it is of real type. Also, it does not depend on μ. The equilibrium point of the vector field X in (3-1) is the point $E_1 = \left(\frac{68}{9} - 4\mu, 9\mu - 16\right)$, which depends on μ. In fact, if $\mu < \frac{16}{9}$ the equilibrium point is located on the fourth quadrant and it is virtual. For $\mu = \frac{16}{9}$, E_1 is located at $\left(\frac{4}{9}, 0\right)$, i.e., it moves until colliding to the switching manifold so a boundary

	μ	Σ_1	Σ_2	e^-	e^+	pe^1	pe^2	T_1	T_2	T_4	$P.T.$
1	$\mu < \mu_1$	s	s	1	0	0	0	i	0	v	Γ_{ts}, Γ_u
2	$\mu = \mu_1$	s	s	1	0	1	1	i	0	v	Γ_{ts}, Γ_u
3	$\mu_1 < \mu < \mu_2$	s	s	1	0	1	1	i	0	v	Γ_{ts}, Γ_u
4	$\mu = \mu_2$	s	s	1	0	1	1	i	v	v	Γ_{ts}, Γ_u
5	$\mu_2 < \mu < \mu_3$	s	s	1	0	1	1	i	v	v	Γ_{ts}, Γ_u
6	$\mu = \mu_3$	s	s	1	Σ_1	0	1	∞	v	v	Γ_{ts}, Γ_u
7	$\mu_3 < \mu < \mu_4$	s	s	1	1	0	1	v	v	v	Γ_{ts}, Γ_u
8	$\mu = \mu_4$	s	s	1	Σ_2	0	0	v	v	∞	Γ_{ts}, Γ_u
9	$\mu_4 < \mu < \mu_5$	s	s	1	0	0	0	v	i	v	Γ_{ts}, Γ_u
10	$\mu = \mu_5$	s	0	1	0	0	0	v	i	v	$\Gamma_{tu}, \Gamma_u, \Gamma_{\rho_1}$
11	$\mu_5 < \mu < \mu_6$	s	u	1	0	0	0	v	i	v	$\Gamma_{tu}, \Gamma_u, \Gamma_{\rho_1}$
12	$\mu = \mu_6$	s	u	1	0	0	0	v	i	v	$\Gamma_{tu}, \Gamma_u, \Gamma_{\rho_2}$
13	$\mu_6 < \mu < \mu_7$	s	u	1	0	0	0	v	i	v	$\Gamma_{tu}, \Gamma_u, \Gamma_{\rho_3}$
14	$\mu = \mu_7$	s	u	1	0	0	0	v	i	v	$\Gamma_{tu}, \Gamma_u, \Gamma_{\rho_4}$
15	$\mu_7 < \mu < \mu_8$	s	u	1	0	0	0	v	i	v	$\Gamma_{tu}, \Gamma_u, \Gamma_s$
16	μ=μ_8	s	u	1	0	0	0	v	i	v	Γ_{tu}, Γ_{su}
17	$\mu > \mu_8$	s	u	1	0	0	0	v	i	v	Γ_{tu}

Table 3.1: *Description of the phase portrait of X_μ for all $\mu \in \mathbb{R}$. Here "1" stands by the presence of that object and "0" for the absence of it. Γ_s and Γ_u stand by stable and unstable limit cycles, e_+ and e_- stand by the equilibrium point of X_+ and X_-, respectively. T_i denote the tangency points for $i = 2,\ 3,\ 4$, being "v" and "i" the notation for visible and invisible, respectively; ∞ stands by a tangency vanishing every Lie derivative (degenerate). Also, Γ_{ts} and Γ_{tu} stand by stable or unstable center type periodic trajectory, respectively. Finally, Γ_{su} stands by semi-stable limit cycle and Γ_{ρ_i} stands by sliding periodic trajectories of type ρ_i, $i = 1, \ldots, 4$.*

equilibrium bifurcation takes place at Σ_1. If $\frac{16}{9} < \mu < \frac{17}{9}$, then E_1 is located on the first quadrant and it is real. For $\mu = \frac{17}{9}$, E_1 is located at $(0,1)$, that is, another boundary equilibrium bifurcation occurs at Σ_2. If $\mu > \frac{17}{9}$, then E_1 is on the second quadrant and it is virtual.

Part 2 - Tangency points and sliding regions: The tangency point $T_1 = \left(\frac{4}{9}, 0\right)$ does not depends on μ. However, it is visible if $\mu > \frac{16}{9}$ and invisible if $\mu \leq \frac{16}{9}$. For $\mu = \frac{16}{9}$, T_1 coincides with the equilibrium point E_1. Moreover, the segment $\left[0, \frac{4}{9}\right) \subset \Sigma_1$ is a sliding region.

The tangency point $T_4 = (0,2)$ is also fixed and it is a visible one. On the other hand, the tangency point $T_2 = \left(0, \frac{9\mu}{17}\right)$ only exist for $\mu \geq 0$. Moreover, it is visible if $0 \leq \mu < \frac{17}{9}$ and invisible if $\mu > \frac{17}{9}$. When $\mu = \frac{17}{9}$, T_2 collides with the equilibrium point E_1. Now, the segment $\overline{T_2T_4}$ is formed either by sliding points if $\mu < \frac{34}{9}$, or escaping ones for $\mu > \frac{34}{9}$. At $\mu = \frac{34}{9}$ we get $T_2 = T_4$.

Part 3 - Pseudo-equilibrium points: To find pseudo equilibria on Σ_1, it is sufficient to find a value x such that $X(x,0)$ and $Y(x,0)$ in (3-1) are linearly dependent, that is, x must satisfy

$$det \begin{bmatrix} 2-x & 2x+2\sqrt{2} \\ \mu-4x & 9x-4 \end{bmatrix} = 0.$$

From the last equation we obtain

$$x_{\pm} = 4\sqrt{2}+11-\mu \pm \left(\mu\left(\mu-10\sqrt{2}-22\right)+88\sqrt{2}+145\right)^{1/2},$$

so one get that $x_+ \in [0, \frac{4}{9}]$, the escaping region on Σ_1, provided that $-2\sqrt{2} \leq \mu < \frac{16}{9}$. Moreover, x_- does not belongs to the domain of the Filippov vector field regardless of μ. Similarly, a pseudo equilibrium point takes place in Σ_2 for $-2\sqrt{2} < \mu < \frac{17}{9}$.

Notice that up to this moment we have exhibited the configurations of the phase portrait of all lines in Table 3.1 except by the last column. Figures 3.1, 3.2, 3.3, and 3.4 illustrate the phase portrait which are $\Sigma-$topological equivalent to the phase portrait of all lines in Table 3.1 except by the last column.

Part 4 - Periodic trajectories: This part is split into 4 sub-parts. In the Sub-part 4.1 we argue about internally center type periodic trajectories. In the Sub-part 4.2 we address the limit cycles. In the Sub-part 4.3 we study the sliding and tangential periodic trajectories

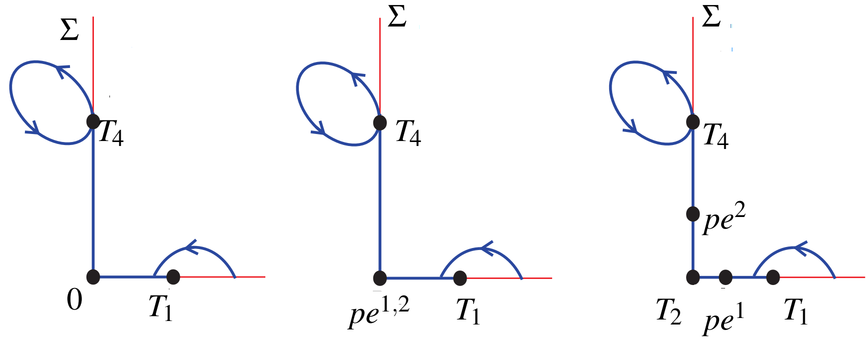

Figure 3.1: *T_i, $i =$ 1, 2, 4 is tangency point and $pe^{1,2}$ is pseudo-equilibrium points.*

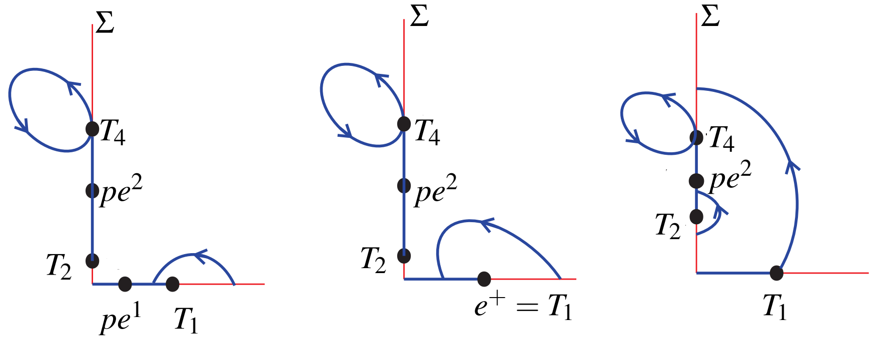

Figure 3.2: *T_i, $i =$ 1, 2, 4 is tangency points, $pe^{1,2}$ is pseudo-equilibrium points, e^+ is equilibrium point.*

and how the sliding periodic trajectories bifurcate into a limit cycle. Finally, in Sub-part 4.4 we argue about the semi-stable limit cycle and how the limit cycles disappear after a saddle-node bifurcation of limit cycles. Once these four parts are proven, the analysis of the phase portrait corresponding to the last column of Table 3.1 is also completed.

Sub-part 4.1 - Internally center type periodic trajectory: From the previous parts, T_4 is a visible tangency and the vector fields we are considering have centers equilibria, so an internally center type periodic trajectory takes place Γ_t when a center is real. Now we have three situations.

When $\mu < \frac{34}{9}$ there exists a sliding region connecting with the internally center type periodic trajectory. Let V be a small external neighborhood of Γ_t. If there exists no pseudo-equilibrium point in the sliding region, all trajectories in V reach Γ_t through the sliding, so Γ_t is an attractor. On the other hand, if a pseudo-equilibrium point does exist in this sliding region, then Γ_t is still attracting all trajectories in V. Moreover, it is enough to take V sufficiently small such that this pseudo-equilibrium is not in V, thus the

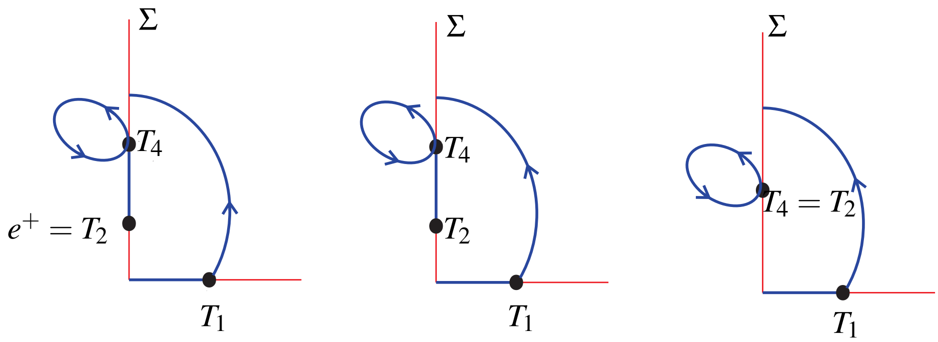

Figure 3.3: T_i, $i =$ 1, 2, 4 *is tangency point and* e^+ *is equilibrium point.*

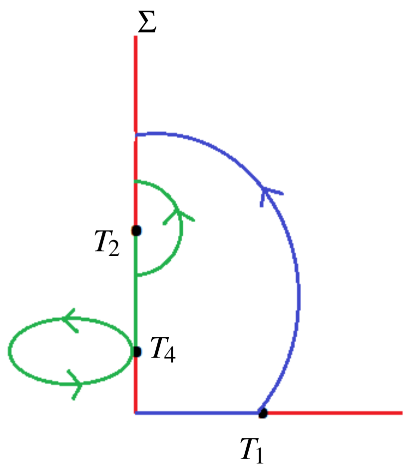

Figure 3.4: T_i, $i =$ 1, 2, 4 *is tangency points and green line is the escaping region.*

trajectories in V also reach Γ_t. In both cases, Γ_t attracts trajectories externally, i.e., we have the existence of a stable internally center type periodic trajectory.

When $\mu = \frac{34}{9}$ there exists neither a sliding nor an escaping region and $T_2 = (0,2)$ is an invisible tangency point for $X(x,y)$. Then, for some external neighborhood of Γ_t the trajectories move outward Γ_t, so Γ_t is an unstable internally center type periodic trajectory.

Finally, when $\mu > \frac{34}{9}$ there exists an escaping region connected with Γ_t. Moreover, all trajectories in a neighborhood move outward Γ_t. In fact, since the escaping region is connected with Γ_t the only possibility for trajectories near to Γ_t is cross Σ_2 at a point bigger that the point limit of this sliding region. Therefore Γ_t is also an unstable external internally center type periodic trajectory. The previous analysis describes all the internally center type periodic trajectories of X_μ.

Sub-part 4.2 - Limit cycles: Proceeding as in the proof of Theorems 25 and 26, we obtain the following pair of conics associated with X_μ

$$2x\left(x+2\sqrt{2}\right) = (y-4)y,$$
$$18\mu y + 9x(9x-8) = 17y^2.$$

The first equation corresponds to two concurrent straight lines and the second one to a hyperbola. They intersect each other at the point $P_1 = (0,0)$ and the points

$$P_2 = \left(\tfrac{18}{47}\left(\sqrt{2}\mu+4, -\tfrac{36}{47}\left(\mu+2\sqrt{2}\right)\right)\right),$$
$$P_3 = \left(\tfrac{1}{47}\left(-9\sqrt{2}\mu+68\sqrt{2}+36-3\sqrt{\mathcal{M}}\right), \tfrac{6}{47}\left(-3\mu+6\sqrt{2}+54-\sqrt{\mathcal{N}}\right)\right) \text{ and}$$
$$P_4 = \left(\tfrac{1}{47}\left(-9\sqrt{2}\mu+68\sqrt{2}+36+3\sqrt{\mathcal{M}}\right), \tfrac{6}{47}\left(-3\mu+6\sqrt{2}+54+\sqrt{\mathcal{N}}\right)\right),$$

where $\mathcal{M} = 18\mu\left(\mu-4\left(\sqrt{2}+9\right)\right)+32\left(17\sqrt{2}+81\right)$ and $\mathcal{N} = 9\mu\left(\mu-4\left(\sqrt{2}+9\right)\right)+16\left(17\sqrt{2}+81\right)$. As before, we are only interested in the intersections occurring on the first quadrant, i.e., we need to study under which conditions the coordinates x and y of P_i, $i=2,3,4$ are both positive. Assuming that this happens, we obtain the following conditions in relation to the parameter μ :

$[C_1]$ For $\mu \leq \mu_8 = 2\left(\sqrt{2}+9\right) - \frac{2}{3}\left(94\sqrt{2}+423\right)^{1/2}$ we have one intersection in the first quadrant corresponding to point P_4. Notice that μ_8 is obtained doing the coordinates x and y of P_4 positive.

$[C_2]$ For $\frac{34}{9} = \mu_5 < \mu \leq \mu_8$ we have two intersections in the first quadrant corresponding to points P_3 and P_4. This interval of μ is obtained by setting positive coordinates x and y of both P_3 and P_4.

Point P_2 cannot be in the first quadrant because the $x-$coordinate is positive if $\mu > -2\sqrt{2}$ and the $y-$coordinate is positive if $\mu < -2\sqrt{2}$, which cannot simultaneously happen. Besides that, for $\mu > \mu_8$ there is no value of μ such that P_i is located on the first quadrant, so no limit cycles take place for $\mu > \mu_8$. Therefore, up to now, we can obtain at most two limit cycles that may exist or not because those intersections of the first quadrant are necessary but not sufficient conditions for the existence of limit cycles.

In order to determine which of these intersections on the first quadrant actually correspond to limit cycles, we employ the displacement function defined in Lemma 28. Indeed, the displacement function considering X_μ is obtained through the replacements $a=9$, $b=4$, $c=-4$, $d=\mu\in\mathbb{R}$, $w=2$, $A=2$, $B=1$, $C=2\sqrt{2}$, $D=2$ and $W=2$ in (2-5), leading to

$$d_\mu(r) \;=\; -\frac{3}{17}\left(9\mu^2+17r(9r-8)\right)^{1/2}-\frac{9\mu}{17}+\sqrt{2}\left(r+\sqrt{2}\right)+2. \tag{3-2}$$

The roots of d_μ are $r_{3,4}=\frac{1}{47}\sqrt{2}\left(-9\mu+18\sqrt{2}+68\mp3\sqrt{\mathcal{N}}\right)$, $r_1=0$, and $r_2=\frac{18}{47}\left(\sqrt{2}\mu+4\right)$ being $\mathcal{N}$ as defined before. Notice that r_i, $i=1,\ldots,4$ corresponds to the $x-$coordinates of the intersections of the considered conics.

In order to have a limit cycle, we must assume $r>\frac{4}{9}$ to get crossing intersections to Σ_1. Moreover, the trajectory starting at $(r,0)$ through the vector field X must find the positive $y-$axis also at a crossing point. From that point, the trajectory should find the initial condition $(r,0)$ again.

The $y-$coordinate of that intersection for both vector fields is provided by the equations of $y^+_{1,2}$ and $y^-_{1,2}$ in Lemma 28, so we replace again the values $a=9$, $b=4$, $c=-4$, $d=\mu\in\mathbb{R}$, $w=2$, $A=2$, $B=1$, $C=2\sqrt{2}$, $D=2$ and $W=2$. Now, to obtain crossing intersections with $\Sigma_{1,2}$ one of the following conditions should occur.

$[C_3]$ $\quad\frac{4}{9}<r<\frac{8}{9}$ and $\mu\geq\frac{1}{3}\sqrt{17}\sqrt{8r-9r^2}$

or

$[C_4]$ $\quad r>\frac{8}{9}$.

From $[C_i]$, $i=1,\ldots,4$ we conclude that there is a limit cycle for $\mu\leq\mu_8$ corresponding to the zero r_4 of the displacement function d_μ. Moreover, one can verify that the derivative of d_μ with respects to μ at r_4 is positive so the corresponding limit cycle is unstable.

Now, a second limit cycle can take place, according to $[C_2]$, for $\mu_5<\mu<\mu_8$ and if this is the case, the second limit cycle corresponds to the zero r_3 of the displacement function d_μ. Nevertheless, next, we prove that condition $[C_3]$ cannot occur because assuming $\frac{4}{9} < r < \frac{8}{9}$ the intersection point P_3 associated with r_3 corresponds to a trajectory reaching the sliding region on Σ_1 for $\mu_5 < \mu < \mu_7$. The conclusion is, as we will see, that a second limit cycle associated with r_3 only takes place for $\mu_7 < \mu < \mu_8$ and it emerges from a sliding periodic trajectory bifurcating at a tangency point. Moreover, in this case, it can be seen that the limit cycle is stable.

Sub-part 4.3 - Sliding and tangential periodic trajectories: Let us set again $a = 9$, $b = 4$, $c = -4$, $d = \mu \in \mathbb{R}$, $w = 2$, $A = 2$, $B = 1$, $C = 2\sqrt{2}$, $D = 2$ and $W = 2$. We obtain from Lemma 28 the following:

$$y_{1,2}^{+} = \frac{1}{34}\left(18\mu \pm 3\left(36\mu^2 + 612r^2 - 544r\right)^{1/2}\right),$$
$$y_{1,2}^{-} = \frac{1}{4}\left(8 \pm \sqrt{2}\left(16r^2 + 32\sqrt{2}r + 32\right)^{1/2}\right).$$

We start noticing that for $\mu = \mu_5$ there is neither sliding nor escaping points on Σ_2 and the internally center type periodic trajectory Γ_t is unstable. On the other hand, for this value of μ there exist an unstable limit cycle Γ_u containing Γ_t on its interior. Then from Theorem 1 in [25] there must exist some attracting set contained between Γ_u and Γ_t. We will show that this set is a sliding periodic trajectory.

(1) Consider $\mu_5 \leq \mu < \mu_6$. In this case, the trajectory from T_1 reaches Σ_2 at a crossing point y_1 then reaches Σ again at a crossing point y_2 with $y_2 < y_1$ and finally, it goes towards Σ_1 arriving at a sliding point. From these points, because there exists no pseudo-equilibrium point the trajectory slides to T_1 forming a sliding periodic trajectory that we refer to be of type 1 and denote Γ_{ρ_1}.

(2) Consider $\mu = \mu_6$. In this case, the second return to Σ_2 occurs at the corner $(0,0) = \Sigma_1 \cap \Sigma_2$ and then it slides to T_1 forming a sliding periodic trajectory that we refer to be of type 2 and denote Γ_{ρ_2}.

(3) Consider $\mu_6 < \mu < \mu_7$. In this case, the trajectory from T_1 crosses Σ_1 at a crossing point and then meets Σ again in the interior of Σ_1 at a sliding point. Then, as before

the trajectory slides to T_1 forming a sliding periodic trajectory that we refer to be of type 3 and denote Γ_{ρ_3}.

(4) Consider $\mu = \mu_7$. In this case, the trajectory behaves like in Case 3 before but the arriving point on Σ_1 occurs at T_1 forming a tangential periodic trajectory that we refer to be of type 4 and denote Γ_{ρ_4}.

(5) For $\mu_7 < \mu < \mu_8$ we have unstable periodic trajectories Γ_u and Γ_t, where Γ_t is contained on the interior of the limited region delimited by Γ_u. Therefore the intersection between the exterior of Γ_t and the interior of Γ_s contains and positive invariant compact region K. This region contains neither equilibria nor sliding nor tangential points so we can apply Poincaré-Bendixson theorem for crossing regions (see [4]) to assure the existence of at least one crossing periodic trajectory contained on K. However, from condition $[C_2]$ we can guarantee that at most one periodic trajectory Γ_s takes place, corresponding to the root r_3 of d_μ. From the construction of K (or equivalently, from verifying that $d'_\mu(r_3) < 0$), Γ_s is stable.

Therefore, for $\mu_5 \leq \mu \leq \mu_7$ we have a sliding periodic trajectory and for $\mu_7 < \mu < \mu_8$ we have two limit cycles.

Sub-part 4.4 - Semistable limit cycles: Setting $\mu = \mu_8$ we have a non-hyperbolic limit cycle Γ_{su}. It corresponds to a multiplicity two root of d_μ which writes $r_1 = 6\left(\frac{2}{47}\left(2\sqrt{2}+9\right)\right)^{1/2} - 2\sqrt{2}$ and it satisfies $d'_\mu(r_1) = 0$, so Γ_{us} is a semi-stable limit cycle because for $\mu = \mu_8$ there exists at most one intersection point $P_3 = P_4$ occurring on the first quadrant. For $\mu > \mu_8$ there are no such intersections so limit cycles cannot take place.

The proof is finished by noticing that every phase portrait of (3-1) for $u \neq \mu_i$, $i = 1, \ldots, 8$ is topologically equivalent because they are simple translations depending on μ for which neither changes of stability of critical elements nor collisions take place. This finishes the proof of Theorem 29.

Figure on left of 3.5 exhibit one phase portraits that are $\Sigma-$topologically equivalent to the periodic trajectories happening for $\mu < \mu_5$, while the figure on right of 3.5

exhibit the phase portraits for $\mu = \mu_5$. Figure 3.6 exhibit one phase portraits that are $\Sigma-$topologically equivalent to the periodic trajectories happening for $\mu_5 < \mu < \mu_6$. Figure on left of 3.7 exhibit the phase portraits for $\mu = \mu_6$, while the figure on right of 3.7 exhibit one phase portraits that are $\Sigma-$topologically equivalent to the periodic trajectories happening for $\mu_6 < \mu < \mu_7$. Figure on left of 3.8 exhibit the phase portraits for $\mu = \mu_7$, while the figure on right of 3.8 exhibit one phase portraits that are $\Sigma-$topologically equivalent to the periodic trajectories happening for $\mu_7 < \mu < \mu_8$. Figure on left of 3.9 exhibit the phase portraits for $\mu = \mu_8$, while the figure on right of 3.9 exhibit one phase portraits that are $\Sigma-$topologically equivalent to the periodic trajectories happening for $\mu > \mu_8$.

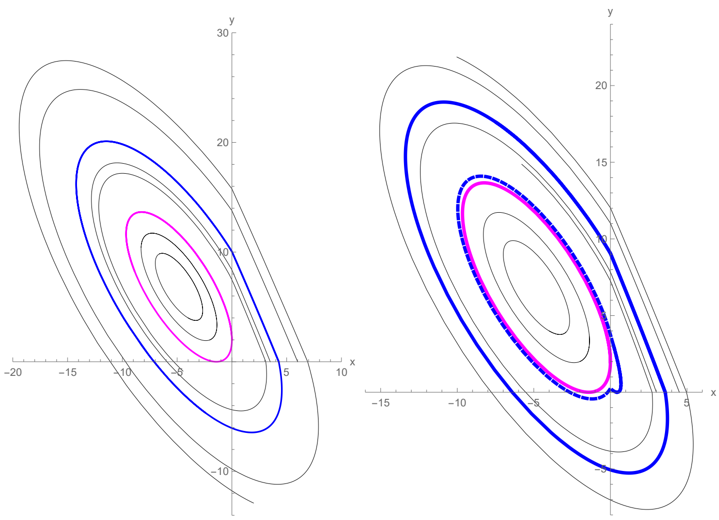

Figure 3.5: *On left, periodic trajectories of system* (3-1) *for* $\mu < \mu_5$ *and, on right, periodic trajectories of system* (3-1) *for* $\mu = \mu_5$.

Remark 30 *The realization provided in Theorem 25 is included in the bifurcation analysis of Theorem 26. More precisely, they occur, respectively, in the cases presented in lines **12** and **15** of Table 3.1.*

3.3 Coexistence of Periodic Trajectories

Through the statements of the main results of the chapter and their proofs of Theorems 25, 26, and 29 we have obtained several situations presenting the coexistence

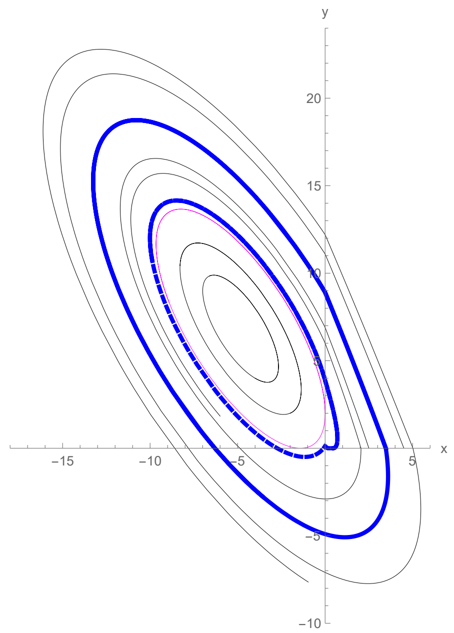

Figure 3.6: *Periodic trajectories of system (3-1) for $\mu_5 < \mu < \mu_6$.*

of periodic trajectories of a different types. Next, we present some straightforward results in this direction.

Corollary 31 *Under the hypotheses of Theorem 25 there exist at least two closed isolated periodic trajectories for system (2-2), being at most one of them a limit cycle.*

It is enough to consider the example provided in the proof of Theorem 25. Indeed, by taking a point $p \in Int(\Gamma_u)$, there is a time t^* such that the flow $\varphi(p,t^*) \bigcap \Sigma^s \neq \varnothing$, let q be the first point for which that happens. Since there exists no pseudo equilibrium, the trajectory passing through q slides to the visible tangency point T_1, i.e., to the internally center type periodic trajectory Γ_i passing through T_1. Therefore, the $\omega-$limit set of any trajectory starting in a point inside Γ_u is Γ_i, see Figure 2.2. Therefore, system (2-2) has one limit cycle Γ_u and an internally center type periodic trajectory Γ_i. It could have more periodic trajectories but we have obtained a lower bound for the number of such objects.

Corollary 32 *Under the hypotheses of Theorem 26 there exist at least three closed isolated periodic trajectories for system (2-2), being at most two of them limit cycles.*

Now we consider the examples provided in the proof of Theorem 26 and the many examples provided in Theorem 29. For instance, in the second example of Theorem 26 we

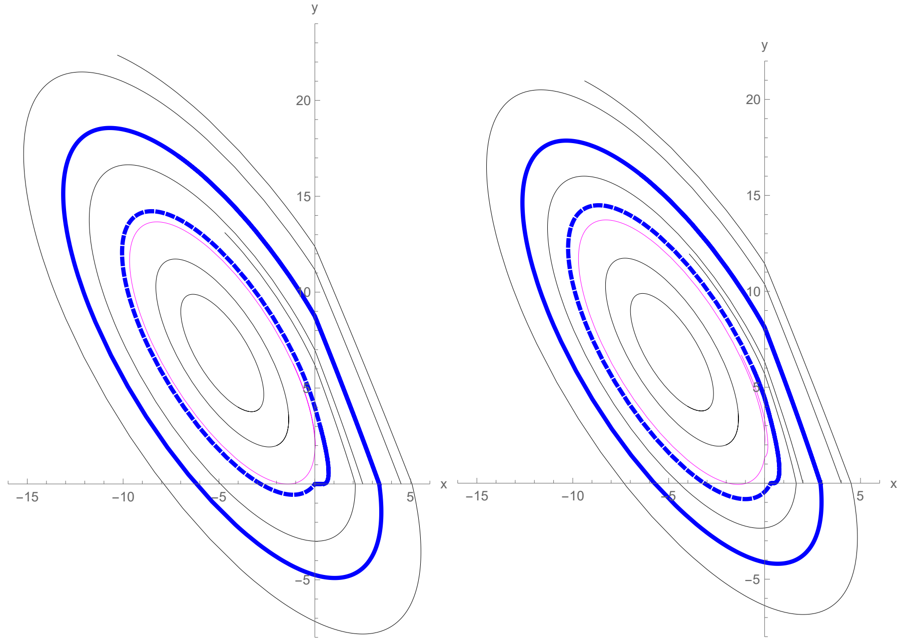

Figure 3.7: *On left, Periodic trajectories of system (3-1) for $\mu = \mu_6$ and, on right, Periodic trajectories of system (3-1) for $\mu_6 < \mu < \mu_7$.*

have two limit cycles and one internally center type periodic trajectory. In fact, let Γ_s the stable limit cycle, Γ_u the unstable limit cycle, and Γ_i the internally center type periodic trajectory. Since Γ_u is an unstable limit cycle, for all trajectory $\Gamma \subset Int\,(\Gamma_u)$, the $\omega-$ limit set of Γ is Γ_i. For all trajectory Γ outer Γ_u and $\Gamma \subset Int\,(\Gamma_s)$, the $\omega-$limit set of Γ is Γ_s. Thus, Γ_u is the $\alpha-$limit of all trajectories $\Gamma \subset Int\,(\Gamma_s)$, see Figure 2.8.

Besides, Theorem 29 gives us several examples of having three periodic trajectories simultaneously. For instance, one can have two limit cycles and one tangential limit cycle for $\mu = \mu_7$ or even three distinct periodic trajectories, namely, one limit cycle, one sliding periodic trajectory, and one internally center type periodic trajectory for $\mu_5 \leq \mu < \mu_7$.

We can also have a coexistence of tangential periodic trajectories, see the next result.

Proposition 33 *The non-smooth vector field $Z(X,Y)$ defined in equation (2-2) has at most two internally center type limit cycles if, and only if, $Z(X,Y)$ has two real centers equilibrium.*

Notice that if $Z(X,Y)$ has real equilibria (of center type) then $Z(X,Y)$ has two tangency

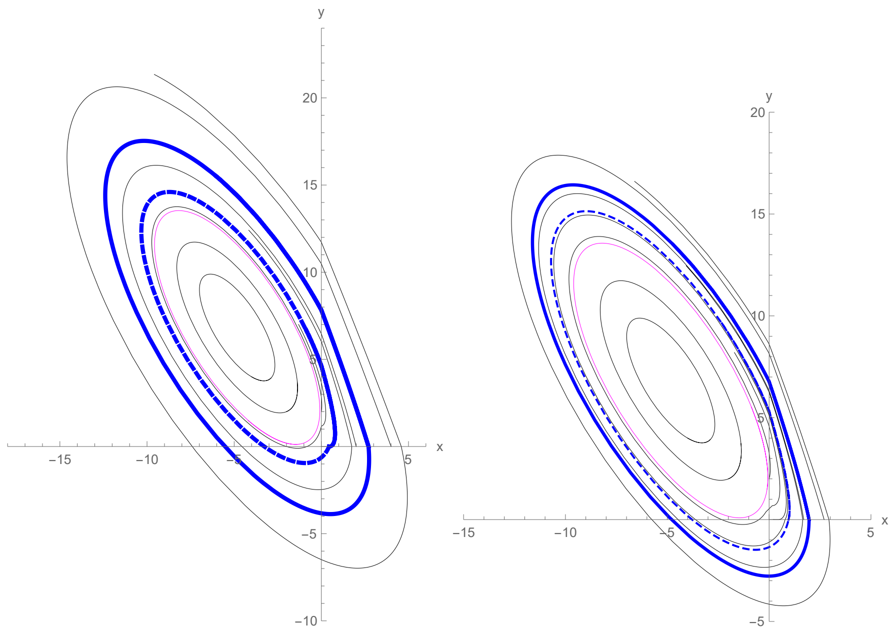

Figure 3.8: *On left, Periodic trajectories of system* (3-1) *for* $\mu = \mu_7$ *and, on right, Periodic trajectories of system* (3-1) *for* $\mu_7 < \mu < \mu_8$.

points T_1 and T_2, call Γ_{T_1} and Γ_{T_2} the tangential trajectories corresponding to T_1 and T_2, respectively. Since the equilibrium point is of center type, Γ_{T_1} and Γ_{T_2} are filled by periodic trajectories, then an internally center type periodic trajectory occurs for each equilibria. The contra-positive is straightforward. This concludes the proof.

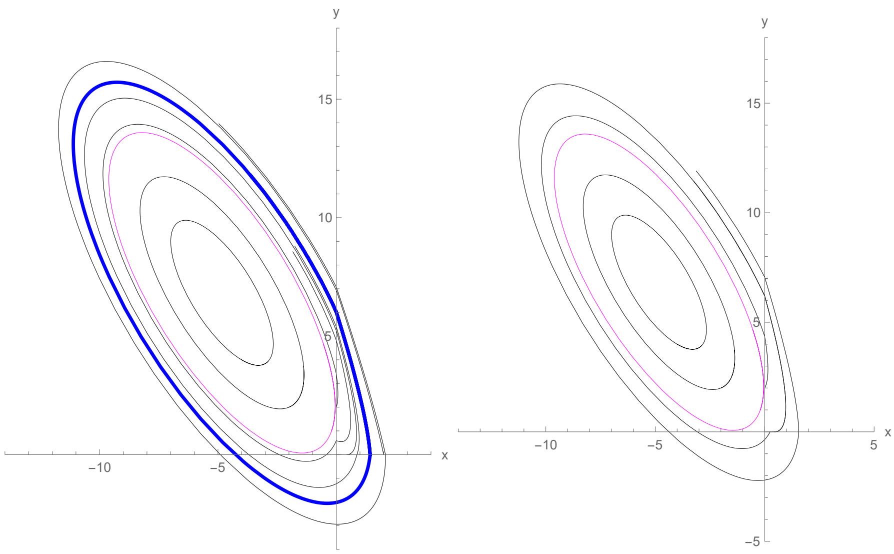

Figure 3.9: *On left, Periodic trajectories of system (3-1) for $\mu = \mu_8$ and, on right, Periodic trajectories of system (3-1) for $\mu > \mu_8$.*

CHAPTER 4

Fast-Slow Systems with Nonregular Discontinuity

Cardin at all [9], extended the Fenichel theory developed by Fenichel [27] for singularly perturbed Filippov systems. Roughly speaking, they proved that any phenomenon that persists under regular perturbations also persists under singular perturbations.

On Cardin at all [8] are studied the effects of singular perturbation when the phase portrait of the reduced problem has periodic orbits with sliding or sewing points. For this, the authors applied the Sotomayor-Teixeira regularization and Slow-Fast systems to allow the study of singular perturbations. This approach transforms a singular point into a regular one and provides a connection between discontinuous systems and singularly perturbed smooth systems. The authors also provide conditions that guarantee the persistence of periodic orbits with sliding or sewing by singular perturbation. Also in this context in [45] the authors describe some qualitative and geometric aspects of non-smooth dynamical systems theory around typical singularities and also establish an interaction between non-smooth systems and geometric singular perturbation theory. Still in this context in [20] the authors, by using transition functions without imposing the monotonicity condition, study minimal sets of regularized systems. They also analyzed the persistence of the sliding region of piecewise smooth slow-fast systems by singular perturbations.

In this chapter, we proposed something different. We did not apply the

Sotomayor-Teixeira regularization on our discontinuous piecewise linear systems. Instead, we propose to apply two blow-ups – see more about blow-ups in [24] –, one for each vector field of the discontinuous piecewise linear systems. Thereafter we obtain discontinuous piecewise smooth linear systems where each vector field is a slow-fast vector field.

The goal of this chapter is to study the non-regular point of a discontinuity set to understand better what happens at this point. For that, we will be fixing the same discontinuity set and the same piecewise vector fields of Chapter 2, i.e, Σ is given by $\Sigma = \Sigma_1 \cup \Sigma_2$ where $\Sigma_1 = \{f_1^{-1}(0); x \geq 0\}$ being $f_1(x,y) = y$ and $\Sigma_2 = \{f_2^{-1}(0); y \geq 0\}$ being $f_2(x,y) = x$. We define the sets $\Sigma^+ = Q_1 \cup \Sigma$ and $\Sigma^- = Q_2 \cup Q_3 \cup Q_4 \cup \Sigma$, where Q_n, $n = 1, 2, 3, 4$ is the $n-$th quadrant of the plane $\mathbb{R}^2$.

$$Z(X,Y) = \begin{cases} X(x,y), (x,y) \in \Sigma^+; \\ Y(x,y), (x,y) \in \Sigma^-, \end{cases} \tag{4-1}$$

where $X = (X_1, X_2)$, $Y = (Y_1, Y_2) \in \mathcal{X}$. Throughout this chapter we assume that X and Y have linear centers as equilibrium points oriented counter-clockwise on the normal form given on Lemma 23, i.e., $X(x,y)$ and $Y(x,y)$ are given by:

$$\begin{aligned} X(x,y) &= \left(-bx - \frac{4b^2+w^2}{4a}y + d,\ ax + by + c\right), \\ Y(x,y) &= \left(-Bx - \frac{4B^2+W^2}{4A}y + D,\ Ax + By + C\right), \end{aligned} \tag{4-2}$$

with a, A, b, B, w, $W > 0$.

4.1 Discontinuous Systems and Fast-Slow Systems

In this section, we explain the approach used in this chapter. The first step is to perform a polar blow-up in booth vector fields of the system (4-1), in other words we apply two blow-ups, one for each vector field of Z. After doing the blow-ups we obtain a discontinuous system where each vector field is a fast-slow system. The next step is studying the case $r = 0$ and applying Fenichel's theory for each fast-slow system and verifying which property is preserved at the non-regular point of Σ. Besides, we used Filippov's Convention to understand better the dynamics of the non-regular point of Σ.

4.2 General Case

The goal of this section, is to establish and prove a result about the origin point for the discontinuous fast-slow generated by applied two blow-ups, one for each vector field of $Z(X,Y)$ given in equation (4-2). By doing the blow-ups we obtain two independently fast-slow system of a discontinuous system $Z(X,Y)$.

We start applying the following blow-up $\phi : S^1 \times \mathbb{R} \to \mathbb{R}^2$ given by:

$$\phi(r,\theta) = (r\cos(\theta), r\sin(\theta))$$

in $X(x,y)$ defined in (4-2). We obtain:

$$\begin{aligned}
\dot{r}(r,\theta) = & \left(\frac{\cos(\theta)\left(r\sin(\theta)\left(4a^2-4b^2-w^2\right)+4ad\right)}{4a}+\frac{-4abr\cos(2\theta)+4ac\sin(\theta)}{4a}\right),\\
r\dot{\theta}(r,\theta) = & \quad ar\cos(\theta)+\cos(\theta)\left(c-2br\sin(\theta)\right)+\frac{\sin(\theta)\left(-4ad+r(4b^2+w^2)\sin(\theta)\right)}{4a}.
\end{aligned}$$

The reduce and layer problem associated with the system above are, respectively:

$$\begin{aligned}
\dot{r_1}(0,\theta) = c\sin(\theta_1)+d\cos(\theta_1) \text{ and}\\
c\cos(\theta_1)-d\sin(\theta_1) = 0.
\end{aligned} \tag{4-3}$$

$$\begin{aligned}
\dot{r_1}(0,\theta_1) &= 0,\\
\dot{\theta_1}(0,\theta_1) &= c\cos(\theta_1)-d\sin(\theta_1).
\end{aligned} \tag{4-4}$$

Analogously, we obtain the reduced and layer problems associated with the vector field $Y(x,y)$ defined in (4-2) is given by:

$$\begin{aligned} \dot{r_2}(0,\theta 2) &= C\sin(\theta_2) + D\cos(\theta_2) \text{ and} \\ C\cos(\theta_2) - D\sin(\theta_2) &= 0. \end{aligned} \tag{4-5}$$

$$\begin{aligned} \dot{r_2}(0,\theta_2) &= 0 \text{ and} \\ \dot{\theta_2}(0,\theta_2) &= C\cos(\theta_2) - D\sin(\theta_2). \end{aligned} \tag{4-6}$$

We remark that in the blow-ups above we replace θ, r by θ_1, r_1 for the vector field $X(x,y)$ and θ, r by θ_2, r_2 for the vector field $Y(x,y)$.

Theorem 34 *Consider the discontinuous fast-slow system $Z(r_1,\theta_1) = (X(r_1,\theta_1), Y(r_1,\theta_1))$. Also, consider $d, D, c, C \neq 0$. The following statements hold.*

i) If d, $D > 0$ then the origin is a sliding point for the discontinuous fast-slow system $Z(r_1,\theta_1)$.

ii) If $d > 0, D < 0$ or $d < 0, D > 0$ then the origin is a crossing point for the discontinuous fast-slow system $Z(r_1,\theta_1)$.

iii) If d, $D < 0$ then the origin is an escaping point for the discontinuous fast-slow system $Z(r_1,\theta_1)$.

Proof: The proof of Theorem 34 is carried out by doing the study of the discontinuous fast-slow system $Z(r_1,\theta_1)$. Since the calculation is similar for both vector fields $X(r_1,\theta_1)$ and $Y(r_2,\theta_2)$ we study the reduce problem of $X(r_1,\theta_1)$ and let the calculation for $Y(r_1,\theta_1)$ in charge of the reader. The reduced problem of $X(r_1,\theta_1)$ is given by equation (4-3). The critical set is given by:

$$C_0 = \{(\theta_1) \in \mathbb{R} : c\cos(\theta_1) - d\sin(\theta_1) = 0.\} \tag{4-7}$$

The equilibrium points of the critical set C_0 is the set E_0 of the points θ_1 such that

$$\theta_1 = \arctan\left(\frac{c}{d}\right); \; d \neq 0 \text{ with } 0 < \theta_1 < \frac{\pi}{2} \text{ or } \pi < \theta_1 < \frac{3\pi}{2}.$$

We notice that since the system is defined in $\mathbb{R}^2$, the critical set is a straight line with projections points on the θ_1 axis of the plane (r_1, θ_1), in other words, we have to project the trajectories within the critical set because the critical parameter is also a variable of the slow-fast system produced after employing the blow-up.

Replacing $\theta_1 = \arctan\left(\frac{c}{d}\right)$ on $\dot{r}_1(0,\theta_1) = c\sin(\theta_1) + d\cos(\theta_1)$ of equation (4-3) we get

$$\dot{r}_1(0,\theta_1) = d\sqrt{\frac{c^2}{d^2} + 1}.$$

Studying the Jacobian Matrix associated to $X(0,\theta_1)$ we obtain:

$$M_{\theta_1} = \begin{pmatrix} 0 & 0 \\ 0 & -c\sin(\theta_1) - d\cos(\theta_1) \end{pmatrix}, \tag{4-8}$$

and replacing $\theta_1 = \arctan\left(\frac{c}{d}\right)$ we get that Jacobian Determinant is:

$$J_{M_{\theta_1}} = -d\sqrt{\tfrac{c^2}{d^2} + 1}, \tag{4-9}$$

which implies that $\dot{r}_1(0,\theta_1)$ is the attractor if $d < 0$ and repelling if $d > 0$ if, and only if, c is not null. In other words, the critical manifold is given in (4-7) is normally hyperbolic if $d \neq 0$.

Figure 4.1 exhibit the critical plane for $d > 0$ on the left and the blow-up of the origin on right for $d,\ D > 0$. To prove item i) of Theorem 34, based on the calculation above it is enough to see the critical manifold is an attractor for booth vector fields $X(r_1,\theta_1)$ and $Y(r_2,\theta_2)$ if d and D are both positive.

To prove item ii) of Theorem 34, based on the calculation above it is enough to see the critical manifold associated with $X(r_1,\theta_1)$ is an attractor if d is positive and the critical manifold associated with $Y(r_2,\theta_2)$ is repelling if D is negative and vice-versa.

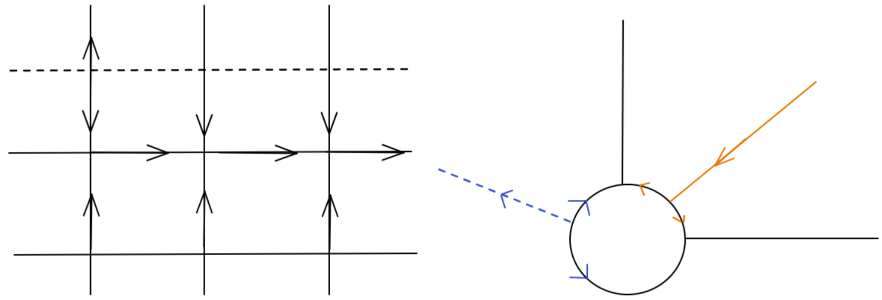

Figure 4.1: *The critical plane for $d > 0$ on left and the blow-up of the origin on right for $d, D > 0$.*

To prove item iii) of Theorem 34, it is enough to see the critical manifold is repelling for both vector fields $X(r_1, \theta_1)$ and $Y(r_2, \theta_2)$ if d and D are booth positive. □

Corollary 35 *Consider the same hypotheses of Theorem 34. If $d = 0$ or $D = 0$ then nothing can be said about the dynamic of the origin point with this approach.*

Proof: To prove Corollary 35 is enough to see that if $d = 0$ or $D = 0$ the equilibria point of the critical set belongs to the discontinuity set Σ_2. □

4.3 A Particular Case Studied

In this section, we present a particular case to study the trajectories through the origin for fixed parameter values. This particular case is the same as presented in Chapter 3. The reason why we choose to study the system for these particular values of parameters is due to the many kinds of periodic trajectories this system has. There are also many situations involving the non-regular point of Σ. Accordingly, fixing $a = 9, b = 4, c = -4, d = \mu \in \mathbb{R}^2, w = 2, A = 2. B = 1, C = 2\sqrt{2}, D = 2$ and $W = 2$ we obtain the system:

$$\begin{aligned} X(x,y) &= \left(-4x - \frac{17}{9}y + \mu,\, 9x + 4y - 4\right) \text{ and} \\ Y(x,y) &= \left(-x - y + 2,\, 2x + y + 2\sqrt{2}\right). \end{aligned} \tag{4-10}$$

The goal of this section is to prove the following theorem.

Theorem 36 *Consider the system (4-10) and fix $\mu = 4$. Then, there is a bifurcation of a homoclinic orbit into two sliding limit cycles for $\mu < 4$ and $\mu > 4$ with the homoclic periodic orbit passing through to the origin point for $\mu = 4$. Besides that, the sliding limit cycles are not topological equivalent.*

Proof: The first step to prove Theorem 36 is to prove the following lemma. The Lemma gives us statements about the origin point for all values of $\mu \neq 0$.

Lemma 37 *Consider the system (4-10) and $\mu \neq 0$. The following statements hold.*

i) If $\mu > 0$ then the origin is an equilibria point of the system (4-10). Besides, it is a sliding one.

ii) If $\mu < 0$ then the origin is an equilibria point of the system (4-10). Besides, it is a crossing one.

Proof: Notice that in the system (4-10) the value of D is fixed as $D = 2$ and both c and C are not null. Also note that we are assuming the same hypotheses of Theorem 34 proved in the previous section, so the statements of Theorem 34 are held in this case. To prove the statement i) of Lemma 37 it is enough to see that if $\mu > 0$ the statement i) of Theorem 34 holds. Similarly, if $\mu < 0$ statement ii) of Theorem 34 held. This concludes the proof.

$\square$

Corollary 38 *Consider the system (4-10). For $\mu < 0$ there exist a sliding connection passing by the origin point, i.e., there is a sliding region on Σ_2 arriving at the origin and following the sliding region through the Filippov vector field on Σ_1.*

The proof of Corollary follows from item ii) of Lemma 37 above and from the analysis of the phase portrait of the system (4-10) provided in the proof of Theorem 29, with for $\mu < 0$ having two sliding regions passing through the origin point.

To conclude the proof of Theorem 36 remember that in Theorem 29 we describe all the possible phase portraits of the system (4-10). in this description, we showed that for $\mu = 4$ there is a sliding periodic trajectory passing by the origin point and the tangential point $T_2 = (\frac{4}{9}, 0)$. Since in Lemma 37 we proved that the origin is a sliding equilibria then we have a homoclinic orbit passing through the origin. Besides, as shown, this homoclinic orbit bifurcates into two sliding periodic trajectories for $\frac{34}{9} < \mu < \frac{4(631\sqrt{2}+6408)}{6399}$ with μ small enough and these trajectories are not topological equivalents because they contain different trajectories of vector fields $X(x,y)$ and $Y(x,y)$. Figures 4.2, 4.3, and 4.4 exhibit the phase portraits of the periodic trajectories happening for $\mu = \frac{34}{9}$, $\mu = 4$ and $4 < \mu < \frac{4(631\sqrt{2}+6408)}{6399}$, which explicit that the sliding limit cycles are not topologically equivalent.

□

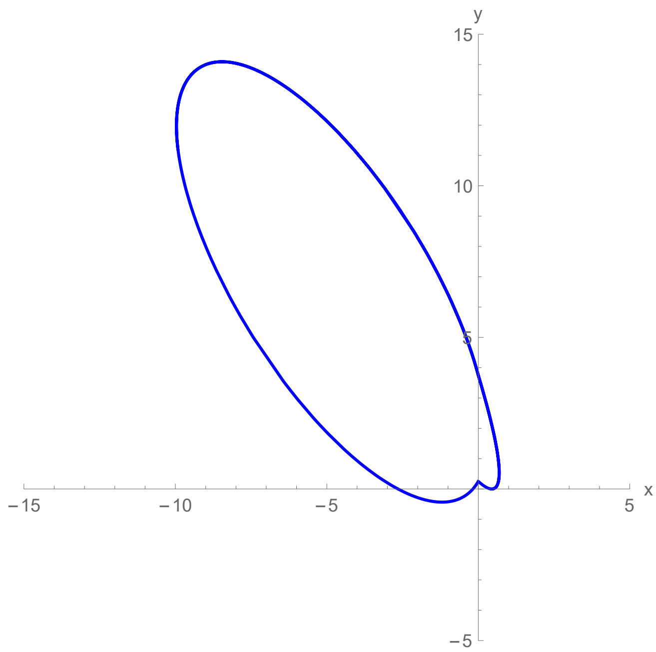

Figure 4.2: *The position 1 of the sliding limit cycle happening for* $\mu = \frac{34}{9}$.

The theory presented in this chapter allowed us to study the system (4-10) from a different perspective in the sense the we carried a more specific study of the origin and consequently the sliding periodic trajectory passing by the origin and the tangential point $T_2 = (\frac{4}{9}, 0)$.

We remark that some aspects of the theory present in this chapter are in development although it does not compromise the results presented in this chapter. The results present provides some important conclusions about a non-regular point of a non-regular

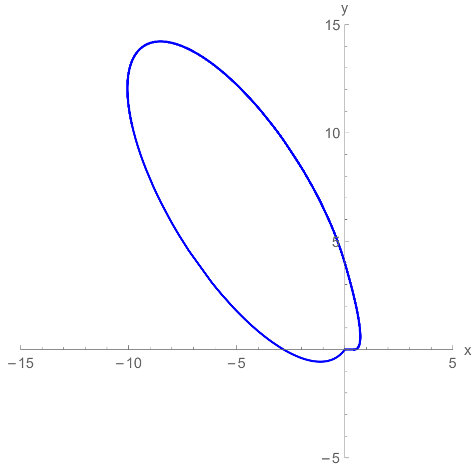

Figure 4.3: *The homoclinic orbit happening for* $\mu = 4$.

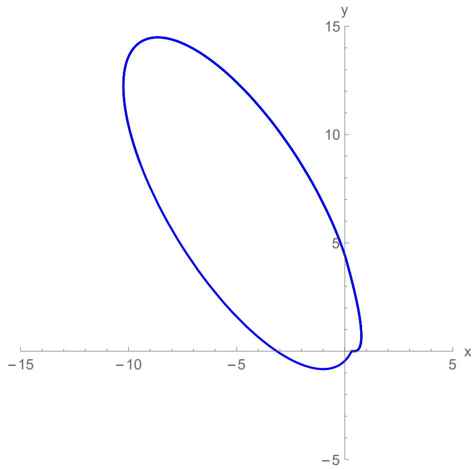

Figure 4.4: *The position 2 of the sliding limit cycle happening for* $4 < \mu < \frac{4\left(631\sqrt{2}+6408\right)}{6399}$.

discontinuity set.

CHAPTER 5

Piecewise Smooth Rotated Vector Fields

This chapter is addresses rotated piecewise smooth vector fields in order to understand the effects that discontinuities imply in the rotation of distinct vector fields. As far as we know this is the first time that such a framework is considered, so we present a preliminary theory to understand this class of piecewise smooth vector fields. Rotated vector fields proved to be an immensely useful tool in research and bifurcation of limit cycles as also provide important insights into studying the global behavior of one-parameter families of limit cycles. Perko [57] show that any global family of limit cycles of a planar analytic family of vector fields is the union of a finite number of one-parameter families of limit cycles that are either cyclic or satisfy the same type of termination principle as Duff's families. He also showed how a one-parameter family of limit cycles can be continued through a complex bifurcation in a unique way. In what follows we present some particular applications of classical rotated vector fields.

Zhang [68] studied limit cycle bifurcations either from homoclinic loops or from families of periodic orbits in slow-fast systems being the theory of rotated vector fields the main tool for proving the results. In [69] the authors applied this theory to establish conditions for the existence of limit cycles and homoclinic bifurcations in a plant-herbivore model with the toxin-determined functional response. The authors of [17] studied a general Kolmogorov system where they use the rotated vector fields theory to provide sufficient conditions for the existence and uniqueness of limit cycles for that system. The same is done in [19] where the authors studied a general predator-prey model and prove the existence of heteroclinic cycles and positive periodic solutions of order 1. Caubergh [13] used properties of uniqueness associated to rotated vector fields to study some problems related to the bifurcation of polycycles and limit cycles in an one-parameter family of planar vector fields. In [55], it was proved using the non-intersection theorem that a specific system has no limit cycle by proving that the system is one-parameter family of rotated vector fields.

Concerning rotated piecewise smooth vector fields, in [36] the authors present a family of scalar periodic equations with a parameter and establish the theory of rotated equations and as application, they studied a piecewise smooth population model verifying the existence of saddle-node bifurcation. The case that we present in this chapter is more general that the case presented by Han at al in [36] because they studied rotated vector fields with time discontinuity and we studied piecewise vector fields such that each of the vector fields is rotated. We show in Section 5.1 that the rotated vector fields with time discontinuity is a particular case of our problem.

The goals of this chapter concern the comprehension of how the trajectories of two families of rotated vector fields behave as the same parameter is varied. The extension of the results from the classical theory of dynamical systems to the discontinuous framework is not clear since the last one involves the existence of tangency points, sliding and escaping points besides the fact that the vector fields can be rotated in different ways even in the case they depend on the same parameter which is the case considered in this chapter. The first goal of the chapter is to present some general results on rotated vector fields. First, we state sufficient conditions for which the regularization of a rotated piecewise smooth vector fields is still rotated, see Theorem 42. After, we study how the rotation of a family of rotated vector fields affects the contact of fold points with a co-dimension one manifold, see Theorem 44. We also study the robustness of certain closed trajectories when the small parameter defining the rotation of the vector fields varies, see Theorem 45.

Another goal of the chapter is concentrated on stating results related to non-intersections of closed trajectories of rotated piecewise smooth vector fields. We recall that a central result concerning classical rotated vector fields is the Non-intersection Theorem which states that limit cycles associated with distinct parameter values of one-parameter family of rotated vector fields does not intersect each other, see for instance [56]. Under suitable results, we are able to generalize that important result to the discontinuous scenario, although we can not avoid intersections occurring on sliding or escaping segments of periodic trajectories, although we are able to control how those intersections occur, see Theorems 46, 47 and 48.

Notice that over this chapter, we do not fix a discontinuity set, i.e., for this chapter Σ could be any fixed smooth function. When is the case, we make it explicit the change of the discontinuity set. This chapter is organized as follows. In Section 39 we introduce rotated piecewise smooth vector fields along with some examples. In section 5.2 we state some general results on rotated piecewise smooth vector fields and in section 5.3 we present some non-intersection theorems for different types of closed trajectories of those vector fields.

5.1 Rotated Piecewise Smooth Vector Fields

We start defining a rotated piecewise smooth vector fields as follows.

Definition 39 *We say that a piecewise smooth vector fields $Z = (X,Y) \in \Omega^r$ defines a family of rotated vector fields if X and Y are one-parameter families of rotated vector fields. We say that Z defines a family of positively (respec. negatively) oriented rotated vector fields if X and Y are a positively (respect. negatively) rotated vector fields.*

Let $Z_\mu = (X_\mu, Y_\mu)$ be a family of oriented rotated vector fields where $X_\mu = (p_\mu, q_\mu)$ and $Y_\mu = (P_\mu, Q_\mu)$. We fix the notation for the determinant (1-4) associated to X_μ and Y_μ as Δ_X and Δ_Y, respectively.

In what follows we present two examples. In the first one, we show how to relay systems can be rotated with respect to one of the parameters present in these systems. In the second one, we analyze the model present in Han et al [36] and how we can transform this model into an autonomous system. This autonomous system is rotated in a classical way. We also present the definition of rotated vector fields introduced by them.

Example 40 *An important class of piecewise vector fields are the so called relay systems which are systems of the form $\dot{x} = Ax + Bu$ with $y = C^T x$ and $u = -sgn(y)$. Relay systems are widely used in applications as control systems, see [21]. A particular class of relay systems in $\mathbb{R}^n$ is presented in [65], which in $\mathbb{R}^2$ have the form*

$$\dot{X} = AX + k\, sgn(z) \tag{5-1}$$

where $z = (x, y)$, $A \in M_2(\mathbb{R})$, $k = (k_1, k_2)$, and $sgn(z)$ is 1 if $x \geq 0$ and -1 otherwise. Let us call

$$A = \begin{pmatrix} a & b \\ c & d \end{pmatrix},$$

so the relay system writes as

$$\begin{cases} \dot{x} = ax + by + k_1, \\ \dot{y} = cx + dy + k_2, \end{cases} \quad if\, x \geq 0 \qquad and \qquad \begin{cases} \dot{x} = ax + by - k_1, \\ \dot{y} = cx + dy - k_2, \end{cases} \quad if\, x \leq 0.$$

If we take $c = k_2 = 0$ and $b \neq 0$ so the relay systems of the form (5-1) is rotated with respect to the parameter a. In fact, the equilibrium points are $e^+ = \left(0, \frac{-k_1}{b}\right)$ for $x \leq 0$ and $e^- = \left(0, \frac{k_1}{b}\right)$ for $x \geq 0$. Also, in both cases, the determinant (1-4) associated with these systems is equal to $-dx^2$ which is always positive for $d < 0$ and negative for $d > 0$.

Example 41 *In Han et all [36], it is presented a not autonomous system defined by the differential equation:*

$$\dot{x} \;=\; f(t, x, \lambda), \tag{5-2}$$

where $t \in \mathbb{R}$, $x \in I \subset \mathbb{R}$, $\lambda \in J \subset \mathbb{R}$ with I and J intervals. They suppose that $f(t, x, \lambda)$ satisfies the following hypotheses:

- *H1: The function $f(t, x, \lambda)$ is $T-$periodic in $t \in \mathbb{R}$, where t is a constant.*

- *H2: There are $n+1$ constants such that t_0, t_1, $\cdots$ t_{n-1}, t_n satisfying $t_0 = 0 < t_1 < \cdots < t_{n-1} < t_n = T$ independent of x and λ and C^1 functions $f_1(t,x,\lambda), \cdots, f_n(t,x,\lambda)$ defined on $\mathbb{R} \times I \times J$ such that $f(t,x,\lambda) = f_j(t,x,\lambda)$ for $(t,x,\lambda) \in I_j \times I \times J$, where $I_j = \left[t_{j_1}, t_j\right), j = 1, \cdots, n$.*

Notice the function f is piecewise smooth on $\mathbb{R} \times I \times J$ and the partial derivatives $\frac{\partial f}{\partial x}$ and $\frac{\partial f}{\partial \lambda}$ exists for all $(t,x,\lambda) \in \mathbb{R} \times I \times J$ and are piecewise continuous on $\mathbb{R} \times I \times J$ and $T-$periodic in t. Thus, they defined rotated vector fields as follows: if

$$\frac{\partial f}{\partial \lambda}(x,t,\lambda) \geq 0 \; (resp. \leq 0) \quad for \quad (t,x,\lambda) \in [0,T] \times I \times J \tag{5-3}$$

and

$$\frac{\partial f}{\partial \lambda} \neq 0 \quad on\, [0,T]$$

along any solution $x(t,\lambda)$ of (5-2) for each $\lambda \in J$, we say that the system (5-2) defines a family of rotated equations with respect to λ.

Notice that we can transform the non-autonomous equation (5-2) in an autonomous system doing the changing of variables $t = y$. Therefore, it follows:

$$\begin{cases} \dot{x} = f(x,y,\lambda), \\ \dot{y} = 1. \end{cases} \tag{5-4}$$

In this way, the system (5-4) has a discontinuity in the variable y. Now, suppose the system (5-2) is rotated as defined in (5-3), then the autonomous system (5-4) is rotated with respect to the parameter λ according to Definition 12. In fact, the determinant (1-4) equals $\frac{\partial f}{\partial \lambda}$ which is nonzero by hypothesis.

5.2 General Aspects of Rotated Piecewise Smooth Vector Fields

In this section, the goal is to prove that with some hypotheses, families of rotated piecewise smooth vector fields can be preserved under regularizations. The local aspect of the regularization is not a problem here, because, outside the strip where the regularization does not act, the piecewise smooth vector fields are already rotated, so we concentrate in proving this property inside the strip. This result will be a tool for the proof of the main results of this chapter. We also present some auxiliary results that will be used throughout this chapter. In what follows, we fix Z_μ^δ as a regularization of a piecewise smooth rotated vector fields Z_μ. Before we enunciate and demonstrate these results, we will fix some notation.

Consider $S(x,y,\mu) = X(x,y,\mu) + Y(x,y,\mu)$ and $M(x,y,\mu) = X(x,y,\mu) - Y(x,y,\mu)$. Although the vector fields S and M are not necessarily rotated with respect to the parameter μ we can prove that they preserve orientation, in the way that if X and Y are positively (negatively) oriented then S and M also are positively (negatively) oriented. To prove this fact it is enough to consider the parallelogram law. That means that the determinants (1-4) associated with S and M are not null, consequently, S and M are always positively (respect. negatively) oriented if X and Y are positively (respect. negatively) oriented. We will fix the notation for these determinants as Δ_S and Δ_M, respectively.

Theorem 42 *Let Z_μ be a rotated piecewise smooth vector fields and Z_μ^δ its corresponding regularization. Assume that Z_μ^δ has no equilibrium point depending on μ, ie, the equilibrium points of Z_μ^δ do not change when μ changes. The following statements hold:*

i) If Z_μ is positively oriented and $\Delta_S < \Delta_M$ then Z_μ^δ is one-parameter positively orientated family of rotated vector fields with respect to the parameter μ.

ii) If Z_μ is negatively oriented and $\Delta_S > \Delta_M$ then Z_μ^δ is one-parameter negatively orientated family of rotated vector fields with respect to the parameter μ.

We remark that, if either Z_μ is positively oriented with $\Delta_S > \Delta_M$ or negatively oriented with $\Delta_S < \Delta_M$ then nothing can be established about the orientation of Z_μ without extra hypotheses, these cases will not be studied in this thesis.

Proof: Notice that the equilibrium points of Z_μ^δ are isolated. Thus we have to prove that the equation (1-4) associated with the vector fields Z_μ^δ is satisfied. Since we have two cases to prove and the proof is similar we present only the proof of bullet (i).

We know by the hypothesis that Δ_X and Δ_Y are positive because $Z_\mu = (X_\mu, Y_\mu)$ is positively oriented. We also notice that the vector fields $S(x,y,\mu)$ and $M(x,y,\mu)$ write $S(x,y,\mu) = \big(p_\mu(x,y,\mu) + P_\mu(x,y,\mu), q_\mu(x,y,\mu) + Q_\mu(x,y,\mu)\big)$ and $M(x,y,\mu) = \big(p_\mu(x,y,\mu) - P_\mu(x,y,\mu), q_\mu(x,y,\mu) - Q_\mu(x,y,\mu)\big)$. Consequently, the determinant Δ_S associated with S is given by

$$-(q(x,y,\mu)+Q(x,y,\mu))\frac{\partial(p+P)}{\partial\mu}(x,y,\mu)+(p(x,y,\mu)+P(x,y,\mu))\frac{\partial(q+Q)}{\partial\mu}(x,y,\mu),$$

the determinant Δ_M associated with M is

$$(-q(x,y,\mu)+Q(x,y,\mu))\frac{\partial(p-P)}{\partial\mu}(x,y,\mu)+(p(x,y,\mu)-P(x,y,\mu))\frac{\partial(q-Q)}{\partial\mu}(x,y,\mu).$$

From hypotheses $\Delta_S < \Delta_M$. We are going to use that fact for the regularization Z_μ^δ. Nevertheless, the expression of Z_μ^δ according to the previous discussion is

$$Z_\mu^\delta(x,y,\mu,\delta) = \left(\frac{1}{2}\left(p+P+(p-P)\,\varphi\left(\frac{h(x,y)}{\delta}\right)\right), \frac{1}{2}\left(q+Q+(q-Q)\,\varphi\left(\frac{h(x,y)}{\delta}\right)\right)\right)$$

where we avoid the point (x,y,μ) for simplicity. The expression of the determinant (1-4) associated with the vector fields $Z_\mu^\delta(x,y,\mu,\delta)$ is given by

$$\begin{aligned}\det\left(Z_\mu^\delta\right) &= \tfrac{1}{4}\varphi\left(\tfrac{h(x,y)}{\delta}\right)^2((q_\mu-Q_\mu)(p-P)-(p_\mu-P_\mu)(q-Q))+\\ &\quad \tfrac{1}{2}\varphi\left(\tfrac{h(x,y)}{\delta}\right)(-p_\mu q+P_\mu Q+q_\mu p-Q_\mu P)+\\ &\quad \tfrac{1}{4}((q_\mu+Q_\mu)(p+P)-(p_\mu+P_\mu)(q+Q)).\end{aligned}$$

which can be rewritten as

$$\begin{aligned}\det\left(Z_\mu^\delta\right) &= \frac{1}{8}\left(\Delta_S\left(\varphi\left(\frac{h(x,y)}{\delta}\right)^2-1\right)+\Delta_M\left(1-\varphi\left(\frac{h(x,y)}{\delta}\right)^2\right)\right.\\ &\left.+2\left(\Delta_X\left(\varphi\left(\frac{h(x,y)}{\delta}\right)+1\right)^2+\Delta_Y\left(\varphi\left(\frac{h(x,y)}{\delta}\right)-1\right)^2\right)\right).\end{aligned}$$

Therefore, equation above can be rewrite as:

$$\det\left(Z_\mu^\delta\right)=\frac{1}{8}\left(\Delta_S\left(z^2-1\right)+\Delta_M(1-z^2)+2\left(\Delta_X(z+1)^2+\Delta_Y(z-1)^2\right)\right),$$

where $z=\varphi\left(\frac{h(x,y)}{\delta}\right)$. We notice that $\Delta_X>0$ and $\Delta_Y>0$, so $\Delta_X(z+1)^2+\Delta_Y(z-1)^2>0$ since $(z+1)^2,(z-1)^2>0$.

Now, because $|\varphi(t)|<1$ inside the strip for all $t\in\mathbb{R}$ we have $|z|<1$ since φ is a transition function. Moreover, the expression $\Delta_S\left(z^2-1\right)+\Delta_M(1-z^2)$ is positive because:

$$\begin{aligned}\Delta_S\left(z^2-1\right)+\Delta_M(1-z^2) &= \Delta_S\left(z^2-1\right)-\Delta_M(z^2+1)\\ &= (\Delta_S-\Delta_M)\,(z^2+1).\end{aligned}$$

The factor $\Delta_S-\Delta_M$ is negative since, by hypothesis, $\Delta_S<\Delta_M$. Moreover, as $-1<z<1$, we have $z^2-1<0$, so indeed $(\Delta_S-\Delta_M)\,(z^2+1)$ is positive.

We have proved that (5-5) is a sum of two positive factors, so the expression (5-5) is positive. In particular, we notice that $\det Z_\mu^\delta(x,y,\mu,\delta)$ does not depend on φ. Therefore, $Z_\mu\delta$ is a one-parameter positively orientated family of rotated vector fields with respect to the parameter μ. □

The following example shows that the set of rotated piecewise smooth vector fields satisfying the hypotheses of Theorem 42 are not empty.

Example 43 *Consider the piecewise smooth vector fields $Z(x,y,\mu)=(X_\mu(x,y),Y_\mu(x,y))$ with $X(x,y,\mu)=(\mu x+y+1,2x)$, $Y(x,y,\mu)=(\mu x-1,2x)$ and Σ an arbitrary discontinuity set. We claim that $Z(x,y)$ is a family of one-parameter rotated vector fields with respect to the parameter μ. In fact is straightforward that the equilibrium point of the vector* *fields $X(x,y,\mu)$ and $Y(x,y,\mu)$ does not depend on μ, besides that, for both vector fields, the determinant (1-4) is equal to $-2x^2$ for all regular points. The regularization is given by*

$$Z_\mu^\delta(x,y) = \left(\frac{1}{2}\left(2\mu x + (y+2)\varphi_\delta(x) + y\right), 2x\right).$$

The equilibrium points of Z_δ^μ is the point $\left(0, -\frac{2\varphi_\delta(x)}{\varphi_\delta(x)+1}\right)$ which does not depends on μ. The determinant $\det Z_\mu^\delta$ is equal to $-2x^2$. Therefore, Z_μ^δ is one-parameter negatively orientated family of rotated vector fields with respect to the parameter μ.

The following propositions provide some properties about fold points for piecewise smooth vector fields and hyperbolic poly-trajectory of kind 3.

Theorem 44 *Assume that Z_μ is a family of rotated vector fields and Σ do not depend on μ. If $p = p_{\mu_0} \in \Sigma$ is a fold point for some $\mu = \mu_0$, then there exists $\delta > 0$ such that the following statements hold:*

(i) p_μ is a fold point for every $p_\mu \in \mathcal{N}_\delta^1(\mu_0) \cap \Sigma$ where $\mathcal{N}_\delta^1(\mu_0)$ is a small neighborhood of p_{μ_0};

(ii) the map $\mu \mapsto p_\mu$ from $\mathcal{N}_{\mu_0}$ a small neighborhood of p_{μ_0} to Σ is a strictly monotone function. In other words, when μ varies on $\mathcal{N}_{\mu_0}$, the tangency point p_μ moves on some open subset of Σ containing p_{μ_0} in such way that $p_{\mu_1} \neq p_{\mu_2}$ for every $\mu_1 \neq \mu_2$ of $\mathcal{N}_{\mu_0}$.

Proof: From Theorem 3.5 in [33] there exists $\delta_1 > 0$ such that bullet (i) holds for every $\mu \in (\mu_0 - \delta_1, \mu_0 + \delta_1)$, so it is enough to set $\delta = \delta_1$ and $N_{\delta_1}^1(\mu_0) = N_\delta^1(\mu_0)$.

To prove bullet (ii) let us consider $Z_\mu = (X_\mu, Y_\mu)$ and assume without loss of generality that p_μ is a tangency point for X_μ with $X_\mu = (P_\mu, Q_\mu)$. Since $\Sigma = h^{-1}(0)$ does not depend on μ, we get $\nabla h_\mu(x,y) \equiv 0$ and then

$$\frac{\partial Z_\mu h}{\partial \mu}(p_\mu) = \left\langle \nabla h(p_\mu), \left(\frac{\partial P_\mu}{\partial \mu}, \frac{\partial Q_\mu}{\partial \mu}\right)\right\rangle.$$

The vector $\nabla h(p_{\mu_0}) \neq 0$ because $p_{\mu_0} \in h^{-1}(0)$ is a regular value of h. Moreover, $X_\mu(p_{\mu_0}) \neq 0$ because otherwise the second line in (1-4) is zero so Z_μ is not rotated, which is absurd.

Finally, because the determinant of Z_μ is nonzero the lines of it are linearly independent and then the vectors $\nabla h(p_{\mu_0})$ and $\left(\frac{\partial P_\mu}{\partial \mu}(p_{\mu_0}), \frac{\partial Q_\mu}{\partial \mu}(p_{\mu_0})\right)$ are not orthogonal because we are considering it in the fold point p_{μ_0} with $p_{\mu_0} \in \mathcal{N}_{\mu_0}$. Thus by Thom 's Transversality Theorem present in [32] there is a δ_2 such that all folds points p_μ in the neighborhood $\mathcal{N}^2_{\delta_2}(\mu_0) \cap \Sigma$, $\left(\frac{\partial P_\mu}{\partial \mu}(p_{\mu_0}), \frac{\partial Q_\mu}{\partial \mu}(p_{\mu_0})\right)$ is transversal to Σ and $\frac{\partial Z_\mu h}{\partial \mu}(p_\mu)$ has the same signal of $\frac{\partial Z_\mu h}{\partial \mu}(p_{\mu_0})$. Therefore, the map $\mu \mapsto p_\mu$ from $\mathcal{N}_{\mu_0}$ to Σ is a strictly monotone function. To complete the proof of Theorem 44, it is enough to take $\delta = \min\{\delta_1, \delta_2\}$. $\square$

Theorem 45 *Let $Z_\mu = (X_\mu, Y_\mu)$ be a rotated piecewise smooth vector fields having a hyperbolic poly-trajectory Γ_{μ_0} of kind 3 for $\mu = \mu_0$ and V_r a small neighborhood of Γ_{μ_0}. If $|\mu_1 - \mu_0|$ is small enough, then Z_{μ_1} has a hyperbolic poly-trajectory of kind 3 Γ_{μ_1} contained in $\subset V_r$.*

Proof: We prove the result for poly-trajectories of kind 3 having only one tangency point and one sliding segment. The proof assuming more than one tangency point is completely analogous. Figure 5.1 illustrated the construction that we do in what follows on the proof.

Let P_1^0 be the regular fold point of Γ_{μ_0} and V_{r_1} a neighborhood of P_1^0 of diameter $r_1 > 0$. Then, from Theorem 44 if μ_1 satisfies that $|\mu_0 - \mu_1|$ is small enough, there is a regular fold point P_1^1 for Z_{μ_1} in V_{r_1}. Moreover, Theorem 44 assures that tangency points do not intercept each other for different values of μ in V_{r_1}. Let P_2^0 be the sewing point corresponding to the first intersection between the trajectory arc Γ_{μ_0} starting at P_1^0 and Σ^c. Consider the trajectory arc $\gamma^1_{\mu_1}(t)$ of Z_{μ_1} starting at P_1^1. There exists a time $\tau_1 > 0$ such that $\gamma^1_{\mu_1}(\tau_1) \cap \Sigma = P_2^1$. By continuous dependence on initial conditions outside Σ, there exists a neighborhood V_{r_2}, $r_2 > 0$ of P_2^0 such that $P_2^1 \in V_{r_2}$ and it is a sewing point.

Let P_3^0 be the sliding point corresponding to the first intersection between Γ_{μ_0} starting at P_2^0 and Σ^s. Consider the arc of trajectory $\gamma^2_{\mu_1}(t)$ of Z_{μ_1} starting at P_2^1, then there exists a time τ_2 such that $\gamma^2_{\mu_1}(\tau_2) \cap \Sigma^s = P_3^1$. Moreover, shrinking $r_2 > 0$ if necessary and employing again continuous dependence on initial conditions, there exists $r_3 > 0$ small and a neighborhood V_{r_3} of P_3^0 such that $P_3^1 \in V_{r_3}$. Now, shrinking r_1 and r_2 if necessary, we can assume that the segment $[P_3^1, P_1^1]$ is formed by sliding points having the sliding vector fields the same direction as the one defined on $[P_3^0, P_1^0]$. Accordingly, take now the arc of trajectory $\gamma_{\mu_1}^3(t)$ of Z_{μ_1} starting at P_3^1. Again, there exists a time τ_3 such that $\gamma_{\mu_1}^3(\tau_3) = P_1^1$.

Finally, set the trajectory Γ_{μ_1} as the concatenation $\gamma_{\mu_1}^1 \cup \gamma_{\mu_1}^2 \cup \gamma_{\mu_1}^3$ which is a closed positive trajectory of Z_1, and repeat this concatenation in such a way that Γ_{μ_1} is well defined all $t \in \mathbb{R}$. By the construction, Γ_{μ_1} is a poly-trajectory of kind 3. It is contained in V_r since we can make r_1 as small as necessary and so employ continuous dependence on initial conditions. We notice that the previous constructions hold on compact arcs of trajectories for Γ_{μ_0}. The hyperbolicity follows from the fact that for every μ_1 in V_{r_1}, Γ_{μ_1} satisfies the condition of Definition 9. □

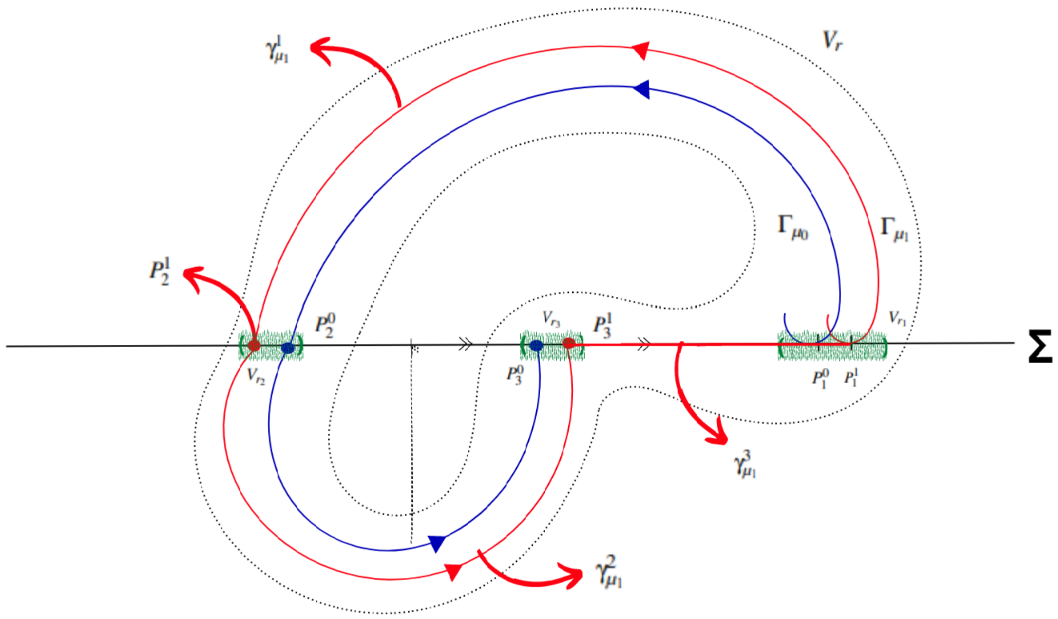

Figure 5.1: *Illustration of Poly-trajectories of kind 3 in a small neighborhood of* Γ_{μ_0}.

5.3 Non-intersection of Poly-trajectories

One of the main results of rotated C^1 vector fields is the so called *Non-intersection Theorem*. Roughly speaking, it states that limit cycles with different values parameters does not intersect with each other and this is the problem we address in this chapter.

Theorem 46 *(The Non-intersection Theorem for piecewise smooth rotated vector fields for poly-trajectories of kind1.) Let Z_μ be a piecewise smooth rotated vector fields and assume that Z_μ satisfies the hypotheses of Theorem 42. Then distinct hyperbolic poly-trajectories of kind 1 do not intersect each other.*

Proof: Let $Z_\mu = (X,Y)$ be a piecewise smooth rotated vector fields and assume that Z_{μ_1} has a hyperbolic poly-trajectory Γ_{μ_1} of kind 1 for some $\mu = \mu_1$. Without loss of generality we assume that Z_μ is positively oriented. Let $V \subset \mathbb{R}^2$ be a small neighborhood of Γ_{μ_1} and μ_2 sufficiently close to μ_1. Because Γ_{μ_1} is a hyperbolic poly-trajectory of kind 1 it is locally structurally stable so employing the continuity respect to the parameters on Σ^+ and Σ^- one can assure the existence of Γ_{μ_2} poly-trajectory of kind 1 in V for $|\mu_1 - \mu_2|$ sufficiently small. That Γ_{μ_1} is locally structural stable follows from the hyperbolicity of the fixed point associated to the first return map of Γ_{μ_1} which is a C^r diffeomorphism.

We are going to prove that $\Gamma_1, \Gamma_2 \subset V$ do not intercept each other. For that, set $\delta_0 > 0$ small and let $Z^\delta_{\mu_1}$ and $Z^\delta_{\mu_2}$ be the regularizations of Z_{μ_1} and Z_{μ_2}, respectively. By Proposition 16, choosing $\delta_1 < \delta_0$ sufficiently small there exists periodic orbits $\Gamma^\delta_{\mu_1}$ of $Z^\delta_{\mu_1}$ and $\Gamma^\delta_{\mu_2}$ of $Z^\delta_{\mu_2}$ entirely contained in V for $\delta < \delta_1$ (shrinking V if necessary). Consider V_1^δ and V_2^δ tubular neighborhoods of $\Gamma^\delta_{\mu_1}$ and $\Gamma^\delta_{\mu_2}$, respectively, having radius $\delta < \delta_2$ with $\delta_2 < \delta_1$. We claim that there exists $\delta^* < \delta_2$ sufficiently small such that, for all $0 < \delta < \delta^*$, $V_1^\delta \cap V_2^\delta = \emptyset$. The proof of the claim goes as follows: if for all $\delta > 0$, $\delta < \delta_2$, we have $V_1^\delta \cap V_2^\delta \neq \emptyset$, then we can take $p \in V_1^\delta \cap V_2^\delta$. Now, since V_1^δ and V_2^δ are tubular neighborhoods containing p, then taking $\delta \to 0$ we get $p \in \Gamma^\delta_{\mu_1} \cap \Gamma^\delta_{\mu_2}$ because $V_i^\delta = \{\Gamma^\delta_{\mu_i}\}$ when $\delta \to 0$, $i = 1,2$. Making $|\mu_1 - \mu_2|$ smaller if necessary, by hypothesis Z^δ_μ is a one-parameter positively orientated family of rotated vector fields and therefore $\Gamma^{\delta}_{\mu_1}$ and $\Gamma^{\delta}_{\mu_2}$ cannot intercept in a point p. Therefore the claim is proved.

From Theorem 17, we get that $\Gamma^{\delta}_{\mu_i} \to \Gamma_{\mu_i}$ when $\delta \to 0$ for $i = 1,2$. Thus, from the claim above, $V_1^{\delta} \cap V_2^{\delta} = \emptyset$ and consequently $\Gamma_{\mu_1} \cap \Gamma_{\mu_2} = \emptyset$. □

Let Γ_{μ} be a hyperbolic poly-trajectory of kind 3. Assume that Γ_{μ} contains k sliding segments $I^1_{\mu}, \dots, I^k_{\mu}$ writing $I^j_{\mu} = [s^j_{\mu}, P^j_{\mu}]$, where s^j_{μ} are sliding points and P^j_{μ} are fold points, $j = 1, \dots, k$. Following that notation, we have the following result.

Theorem 47 *(The Non-intersection Theorem for piecewise smooth rotated vector fields for poly-trajectories of kind3.) Let Z_{μ} be a piecewise smooth rotated vector fields and assume that Z_{μ} satisfies the hypotheses of Theorem 42. Then the following statements hold:*

- *(i) distinct hyperbolic poly-trajectories of kind 3 do not intersect each other either in crossing points or outside Σ.*
- *(ii) If $|\mu_1 - \mu_2|$ is sufficiently small and $\Gamma_{\mu_1}, \Gamma_{\mu_2}$ are two hyperbolic poly-trajectories of kind 3 then they intercept each other on $I^j_{\mu_1} \cap I^j_{\mu_2}$ in the following way: if for some j, $P^j_{\mu_1} > P^j_{\mu_2}$ (respect. "$<$") then $s^j_{\mu_1} > s^j_{\mu_2}$ (respect. "$<$").*

Bullet (ii) states that tangency and sliding points of distinct hyperbolic poly-trajectories of kind 3 move in the same direction when μ is varied, in either positive or negative sense.

Proof: Let $Z_{\mu} = (X,Y)$ be a piecewise smooth rotated vector fields and assume that Z_{μ_1} has a hyperbolic poly-trajectory Γ_{μ_1} of kind 3 for some $\mu = \mu_1$. Again we assume that Z_{μ} is positively oriented and we take $V \subset \mathbb{R}^2$ a small neighborhood of Γ_{μ_1}. Let μ_2 be sufficiently close to μ_1 so that Z_{μ_1} has a hyperbolic poly-trajectory Γ_{μ_2} of kind 3 in V, from Theorem 45. As in the proof of Theorem 46, we can take regularizations of Z_{μ_1} and Z_{μ_2} and suitable tubular neighborhoods (as in [5]) such that Γ_{μ_1} and Γ_{μ_2} intercept each other neither in crossing points nor outside Σ so we prove bullet (i).

In order to prove bullet (ii), we first notice that, from Theorem 44, distinct fold points of Z_{μ_1} do not intercept the respective fold points of Z_{μ_2} for distinct (but close enough) μ_1 and μ_2. Let us assume that Z_{μ_1} has k tangency points $P^1_{\mu_1},\dots,P^k_{\mu_1}$ and let $s^1_{\mu_1},\dots,s^k_{\mu_1}$ the sliding points of Γ_{μ_1} such that every point of the segment $I^j_{\mu_1}=[s^j_{\mu_1},P^j_{\mu_1}]$ is formed by regular points of the sliding vector fields. From Theorem 45, as $|\mu_1-\mu_2|$ is sufficiently small, Z_{μ_2} has the same number k of fold and respective sliding points as intervals bounded by those points. We call those objects $P^j_{\mu_2}$, $s^j_{\mu_2}$ and $I^j_{\mu_2}$, $j=1,\dots,k$.

Now let us assume that, for some j, say j^*, we have $I^{j^*}_{\mu_1}\subset I^{j^*}_{\mu_2}$, the opposite inclusion can be considered in an analogous way. Assume also that $s^{j^*}_{\mu_i}<P^{j^*}_{\mu_i}$, $i=1,2$. Since Σ is co-dimension one manifold of class C^r, we can assume that the portion of Σ for which $\Gamma_{\mu_{1,2}}\cap\Sigma\neq\emptyset$ is diffeomorphic to an open interval of $\mathbb{R}$ so we can naturally order Σ. Once Σ has a natural order and because $I^{j^*}_{\mu_1}\subset I^{j^*}_{\mu_2}$, we get $s^{j^*}_{\mu_2}<s^{j^*}_{\mu_1}<P^{j^*}_{\mu_1}<P^{j^*}_{\mu_2}$. Now, choosing $\delta>0$ sufficiently small, we can proceed as in the Proof of Theorem 46 to assure that the regularizations $Z^\delta_{\mu_1}$ of Z_{μ_1} and $Z^\delta_{\mu_2}$ of Z_{μ_2} have periodic orbits $\Gamma^\delta_{\mu_i}$ completely contained in V in such way that any tubular neighborhood of those periodic orbits tends to the sets $\{\Gamma_{\mu_i}\}$ when $\delta\to 0$, $i=1,2$. Therefore, by Theorem 17, the periodic orbits associated to the C^r-vector fields $Z^\delta_{\mu_1}$ satisfy the following:

- there exist two sequences of points of $\Gamma^\delta_{\mu_2}$, say $\{u^s_i\}_i$ and $\{u^P_i\}_i$ with $i\to\infty$ when $\delta\to 0$ such that u^s_i converges to $s^{j^*}_{\mu_2}$ and u^P_i converges to $P^{j^*}_{\mu_2}$.
- Analogously, there exist two sequences of points of $\Gamma^\delta_{\mu_1}$, say $\{v^s_\ell\}_\ell$ and $\{v^P_\ell\}_\ell$ with $\ell\to\infty$ when $\delta\to 0$ such that v^s_ℓ converges to $s^{j^*}_{\mu_1}$ and u^P_ℓ converges to $P^{j^*}_{\mu_1}$.

Then, $s^{j^*}_{\mu_2}<s^{j^*}_{\mu_1}<P^{j^*}_{\mu_1}<P^{j^*}_{\mu_2}$, there exists some $\delta^*>0$ small such that, for every $\delta<\delta^*$, there exists an arc of the trajectory of $\Gamma^\delta_{\mu_2}$ entirely contained in the interior of the Jordan curve $\Gamma^\delta_{\mu_1}$. That is a contradiction to the fact that $Z^\delta_{\mu_1}$ is a one-parameter positively orientated family of rotated vector fields by hypothesis so $\Gamma^\delta_{\mu_1}$ cannot intercept $\Gamma^\delta_{\mu_2}$. The conclusion is that, for every $j\in\{1,\dots,k\}$ the interval $I^j_{\mu_2}$ cannot contain $I^j_{\mu_1}$. Analogous statements can be proved either assuming that $I^{j^*}_{\mu_2}\subset I^{j^*}_{\mu_1}$ or considering $P^{j^*}_{\mu_i}<s^{j^*}_{\mu_i}$, so the bullet (ii) of Theorem 47 is proved. $\square$

Theorem 48 *(The Non-intersection Theorem for piecewise smooth rotated vector fields* *for poly-trajectories of kind 2.) Let Z_μ be a piecewise smooth rotated vector fields and assume that Z_μ satisfies the hypotheses of Theorem 42. If Σ depends on μ then distinct hyperbolic poly-trajectories of kind 2 do not intersect each other.*

Proof: If Z_{μ_1} has hyperbolic poly-trajectories of kind 2 for a certain μ_1 then for every μ_2 satisfying that $|\mu_1 - \mu_2|$ is sufficiently small, Z_{μ_2} also has hyperbolic poly-trajectories of kind 2. That is true because of the transversality theorem which assures that sliding and escaping points are maintained under small perturbations of the vector fields. The proof is done after applying the same approach as Theorem 46 using regularizations, tubular neighborhoods, and Proposition 16 and Theorem 17. $\square$

Conclusion

In the first part of this thesis, we contribute to the theory of piecewise linear systems with a complete study of periodic trajectories in planar piecewise linear systems with a nonregular switching line for a proposed model. In each linear zone, a vector field having an equilibrium point of center type is defined. Under certain conditions, we state that at most one or two hyperbolic limit cycles can exist. Within the proof of these results we provide a novel and useful incrementation to other results on the maximum number of possible limit cycles for certain planar piecewise linear differential systems. We also show the importance of the discontinuity set in the existence and number of limit cycles. It is known that a discontinuous piecewise linear differential system separated by one straight line formed by two linear centers has no limit cycles, and if the switching set is formed by two parallel straight lines, a discontinuous piecewise linear differential system formed by three linear centers can have at most one limit cycle. Wherefore with the nonregular switching line studied in this thesis, we obtain two more limit cycles.

In the second part of this thesis, we studied Fast-Slow Systems with nonregular discontinuity with a new approach and we identify a bifurcation of a homoclinic orbit passing through the nonregular point of the discontinuity set. Finally, we propose a theory of piecewise rotated vector fields. As far as we know this is the first time that such a framework is considered.

APPENDIX A

Future Works

In this appendix, we present some problems to be studied in the future. We start propose to study the existence of periodic orbits associated with the two differential systems in (A-5) as we did in the chapter for the particular case of centers. If those periodic orbits exist, they could be associated to the existence of a canard point at the origin of the system (A-3). The attempt of considering the discontinuity region as normally hyperbolic manifolds has not been developed yet. Still, that potential relation has been already noticed before in papers dealing with climate discontinuous models, we mention the papers [1] and [67].

Problem 1: Further Discussions and Generalizations of the Model Studied in Chapter 2

Nonlinear Oscillations

We briefly discuss some aspects of the considered vector fields X and Y related to nonlinear oscillations. In practical terms, we shall verify that those vector fields are mathematical models of a pair of undamped, undriven harmonic oscillators. Separately, each vector field X and Y can be modeled by a second order ODE with discontinuous coefficients of the form

$$\ddot{x} + m(x, \dot{x})\dot{x} + n(x, \dot{x})x = 0, \tag{A-1}$$

where m and n are bi-valuated constants depending on x and $\dot{x}$. It can be seen by performing the change of variables for X setting $(x,y) = \varphi(u,v) = ((-b+\frac{\beta c}{\gamma})u+v,(a-\frac{\alpha c}{\gamma})u+\frac{c}{\gamma}v)$ and then the translation $(u,v) = \psi(\widetilde{u},\widetilde{v}) = (\widetilde{u}-\frac{\gamma}{\beta a-\alpha b},\widetilde{v})$ which yields $\widetilde{X}(\widetilde{u},\widetilde{v}) = (\widetilde{v},(\beta a-\alpha b)\widetilde{u}+(\alpha+b)\widetilde{v})$. This vector field corresponds to the planar system of first order differential equations $\dot{x} = y$, $\dot{y} = (\beta a-\alpha b)x+(\alpha+b)y)$ or, equivalently, to the second order differential equation

$$\ddot{x}+(-\alpha-b)\dot{x}+(\beta a-\alpha b)x = 0.$$

Imposing the condition $\alpha = -b$ from equation (2-2) we obtain

$$\ddot{x}+\delta x = 0, \tag{A-2}$$

where $\delta = \beta a-\alpha b$ is a negative value corresponding to the determinant of the homogeneous part of vector field X. Proceeding analogously we get that the vector field Y can be associated to the equation $\ddot{x}+\widetilde{\delta}x = 0$, that is, X and Y indeed correspond to the classical equations of the undamped undriven harmonic oscillator. Hence, coming back to equation (A-1), $m(x,\dot{x})$ vanishes while $n(x,\dot{x})$ writes either δ or $\widetilde{\delta}$ depending on the signs of x and $y = \dot{x}$. Each one of the second order differential equations models a harmonic oscillator. However, when they are put together by means of the piecewise linear system $Z = (X,Y)$, the switching manifold Σ previously defined induces a nonlinear behavior. Indeed, Z can have not one but two limit cycles as we stated in Theorem 26 in Section 2.1. Thus, the combination of the two models should be better investigated for a precise physical meaning in a future work because the previous change of variables does not preserves the switching manifold. A preliminary analysis shows that a nontrivial transition between the two harmonic oscillator takes place generating not only periodic trajectories but also the so called sliding motion.

We exemplify the last comments considering system (3-1) with $\mu = 4$ for which it presents a sliding periodic trajectory, see Figures A.1 and A.2. In Figure A.1 we observe

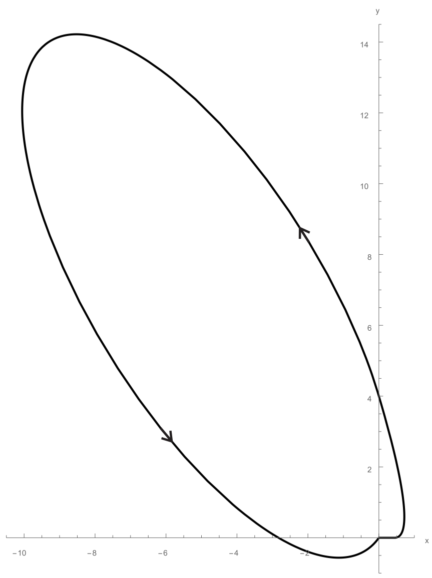

Figure A.1: *A sliding periodic trajectory for system* (3-1) *with* $\mu = 4$ *and initial condition* $(x_0, y_0) = (\frac{1}{100}, 0)$.

the sliding motion for which the trajectory slides during a finite time maintaining $y = 0$ while x increases. In some sense it corresponding to a indecision of the model that could switch to $y < 0$ or $y > 0$ eventually. This situation can be observed in Figure A.2 corresponding to the graphics of $x(t)$ and $y(t)$ between the dashed lines. These indecisions are frequently associated to impacts or friction experienced by the system, see [22]. We also notice that the model also experiences an abrupt motion when reaching the switching manifold, see in Figure A.1 and the doted lines in Figure A.2. This abrupt changes are related to jumps or discontinuities associated to instantaneous changes in the velocity of acceleration of the system, we also refer to [22] for more details.

Slow fast models for membrane potential of neurons

Several dynamical systems associated to the behavior of neurons are modeled in terms of two or more time scales, we mention for instance the Hodgkin-Huxley [37] and Fitzhugh-Nagumo [29, 53] models. Although those models can be natively non-smooth

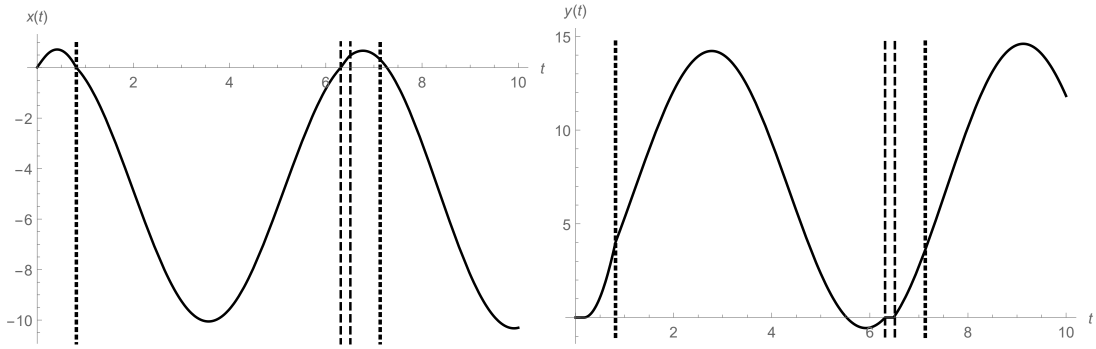

Figure A.2: *Periodic solutions of system (3-1) with $\mu = 4$ and initial condition $(x_0, y_0) = (\frac{1}{100}, 0)$. The trace of $x(t)$ and $y(t)$ between the dashed lines corresponds to the sliding motion. The doted lines correspond to crossing points on the switching manifold.*

[26], the existence of normally hyperbolic manifolds in smooth systems can bring together nonlinear behavior as complex as those observed in non-smooth dynamics; we mention the relation between the slow manifold associated to slow-fast systems and the sliding motion, see [7]. A nice reference for slow-fast systems can be found in [44].

According to the previous discussion it is expected that some discontinuous system may approximate the dynamics of some slow-fast systems. Next we show that some planar neuron models can be studied through equations (2-1) for general values of parameters, that is, piecewise linear discontinuous systems having centers or not.

Following [41], consider the class of slow-fast models of neurons of the form

$$\begin{aligned} \varepsilon \dot{x} &= y - x^2, \\ \dot{y} &= h(x,y). \end{aligned} \tag{A-3}$$

where $\varepsilon \neq 0$ is an arbitrarily small parameter and h is some arbitrary linear function. The dot "$\cdot$" denotes derivative with respect to time t which we call *slow* time. By performing an time rescaling of the form $\tau = \frac{t}{\varepsilon}$ we obtain the equivalent differential system

$$\begin{aligned} x' &= y - x^2, \\ y' &= \varepsilon h(x,y). \end{aligned} \tag{A-4}$$

where now "$\,'\,$" denotes the derivative with respect to the time τ, the *fast* time. There are some ways the approximate a discontinuous differential system by a smooth one as the so-called *pinching*, see [41]. Nevertheless, due to the symmetric critical manifold $y = x^2$ associated to the slow system (A-3) (setting $\varepsilon = 0$), a more crude way consists in replacing the x^2-term of the fast system (A-4) by $|x|$. That have been done, for instance, in the Michelson three-dimensional system in [11] and [12]. The obtained slow and fast discontinuous systems are then given by

$$\begin{array}{rcl} \varepsilon\dot{x} & = & y - |x|, \\ \dot{y} & = & h(x,y), \end{array} \quad \text{and} \quad \begin{array}{rcl} x' & = & y - |x|, \\ y' & = & \varepsilon h(x,y), \end{array} \tag{A-5}$$

respectively, where we assume that h writes $h(x,y) = mx + ny + p$.

There is no general theory so far addressing discontinuous slow-fast systems. However, here we can adapt the linear systems considered in the paper to study the full discontinuous system (fast and slow) on compact regions as does Fenichel, see for instance [44]. To see that, we notice that the critical manifold of the previous slow system coincides with the discontinuity region Σ considered in the paper. Indeed, that critical manifold writes $y = |x|$ which has a corner at the origin and coincides with Σ after a suitable rotation of it (and the respective vector fields X and Y). Moreover, the fast system of equation (A-5) is a discontinuous linear system that can be modeled by considering suitable parameters a, b, c, α, β, γ, $\widetilde{a}$, $\widetilde{b}$, $\widetilde{c}$, $\widetilde{\alpha}$, $\widetilde{\beta}$, $\widetilde{\gamma}$ associated to equation (2-1). Nevertheless, the choice of parameters to reproduce the fast discontinuous system resembling that considered in this paper is $\alpha = -1$, $\beta = \widetilde{\alpha} = \widetilde{\beta} = 1$ and all other constant vanishing.

Next, we propose some problems to be studied in other contexts.

Problem 2: What Happens to the Trajectories of the System Studied in Chapter 3 at Infinity?

Consider the one-parameter family of piecewise vector fields studied on Chapter 3, i.e., the family given by:

$$X_{\mu}(x,y)=\begin{cases} X(x,y)=\left(-4x-\frac{17}{9}y+\mu, 9x+4y-4\right), & (x,y)\in\Sigma^{+}, \\ Y(x,y)=\left(-x-y+2, 2x+y+2\sqrt{2}\right), & (x,y)\in\Sigma^{-}. \end{cases}, \tag{A-6}$$

whit $\Sigma=\Sigma_1\cup\Sigma_2$ where $\Sigma_1=\{f_1^{-1}(0); x\geq 0\}$ and $\Sigma_2=\{f_2^{-1}(0); y\geq 0\}$ being $f_1(x,y)=y$ and $f_2(x,y)=x$. Furthermore, we define the sets $\Sigma^{+}=Q_1\cup\Sigma$ and $\Sigma^{-}=Q_2\cup Q_3\cup Q_4\cup\Sigma$, where $Q_n,\ n=1, 2, 3, 4$, is the $n-$th quadrant of the plane $\mathbb{R}^2$.

In Chapter 3 we studied the phase portrait of X_{μ} for all values of μ. A natural question to do is what happens to the trajectories of system (A-6) at infinity? An attempt to answer this question is to apply the Poincaré Compactification, see [24] for more details. Accordingly, the expression of $Y(x,y)=\left(-x-y+2, 2x+y+2\sqrt{2}\right)$ on the local chart U_1 is given by:

$$\begin{aligned} \dot{u}(u,v) &= 2+u(2+u-2v)+2\sqrt{2}v, \\ \dot{v}(u,v) &= (1+u-2v)v, \end{aligned}$$

which implies that at the point $P=(u,0)$ we get:

$$\begin{aligned} \dot{u}(u,0) &= 2+u(2+u), \\ \dot{v} &= 0. \end{aligned} \tag{A-7}$$

The equilibrium points of $\dot{u}(u,0)$ are $u_{1,2}=-1\pm i$, which are not real. The expression of

$Y(x,y) = \left(-x-y+2, 2x+y+2\sqrt{2}\right)$ on the local chart U_2 is given by:

$$
\begin{aligned}
\dot{u}(u,v) &= -1+2u(1+u+\sqrt{2}v), \\
\dot{v}(u,v) &= -v(1+2u+2\sqrt{2}v).
\end{aligned}
$$

At the point $P = (u,0)$ we get:

$$
\begin{aligned}
\dot{u}(u,0) &= -1-2u(1+u), \\
\dot{v} &= 0,
\end{aligned} \tag{A-8}
$$

whose equilibrium points are $u_{1,2} = -\frac{1}{2} \pm \frac{i}{2}$, again not real.

Analogously we obtain what follows for the vector field $X(x,y)$ of the system $X_\mu(x,y)$ for the local charts U_1 and U_2 on the point $P = (u,0)$:

$$
\begin{aligned}
\dot{u}(u,0) &= 9+8u+\frac{17u^2}{9}, \\
\dot{v} &= 0,
\end{aligned} \tag{A-9}
$$

and

$$
\begin{aligned}
\dot{u}(u,0) &= -\frac{17}{9}-u(8+9u), \\
\dot{v} &= 0,
\end{aligned} \tag{A-10}
$$

respectively. Notice that both equations do not have real equilibrium points. Therefore we can enunciate the following result:

Proposition 49 *The infinity is an attractor periodic trajectory for the system $X_\mu(x,y)$.*

Proof: Notice that by the previous equations there is no equilibrium points for the vector fields $X(x,y)$ and $Y(x,y)$ in the local charts U_1 and U_2. This means that there is no equilibrium points on infinity for the vector fields $X(x,y)$ and $Y(x,y)$. Therefore, infinity is a periodic trajectory for the system $X_\mu(x,y)$.

Remember that on Theorem 29 we prove that for $\mu < \mu_8 = \frac{4(631\sqrt{2}+6408)}{6399}$ always there is a repelling periodic trajectory for $X_\mu(x,y)$. For $\mu = \mu_8$ we have a semi-stable periodic trajectory that is externally repelling. For $\mu > \mu_8$ we do not have a periodic trajectory but we have a tangential repelling trajectory. In all cases, the infinity is an attractor for the trajectories if $X_\mu(x,y)$. □

We remark that this is a previous discussion that needs to be studied in more detail.

Problem 3: What can State Linear Rotated Piecewise Vector Field?

A way of trying to better understand Piecewise Rotated Vector Fields is to study the linear case. How would be the case where booth vector fields of $Z_\mu = (X_\mu, Y_\mu)$ are linear? In the next Proposition, we establish conditions for a piecewise linear vector field to be to one-parameter family of rotated vector fields.

Proposition 50 *Consider a linear vector field $L(x,y) = (ax+by+c, dx+ey+f)$. Then L defines one-parameter family of rotated vector fields according to the following cases:*

(i) L is rotated respect to the parameter a if $e = f = 0$ and $d \neq 0$. More specifically, two families can occur, $L_a^1(x,y) = (ax+by+c, dx)$ if $b \neq 0$ and $L_a^2(x,y) = (ax+c, dx)$ if $b = 0$ and $c \neq 0$;

(ii) L is rotated respect to the parameter b if, and only if, $d = f = 0$ and $e \neq 0$. More specifically, two families can occur, $L_b^1(x,y) = (ax+by+c, ey)$ if $a \neq 0$ and $L_b^2(x,y) = (by+c, ey)$ if $a = 0$ and $c \neq 0$;

(iii) L is rotated respect to the parameter c if, and only if, $d = e = 0$ and $f \neq 0$. More specifically, one family can occur, $L_c(x,y) = (ax+by+c, f)$;

(iv) L is rotated respect to the parameter d if, and only if, $b = c = 0$ and $a \neq 0$. More specifically, two families can occur, $L_d^1(x,y) = (ax, dx+ey+f)$ if $e \neq 0$ and $L_d^2(x,y) = (ax, dx+f)$ if $e = 0$ and $f \neq 0$;

(v) *L is rotated respect to the parameter e if, and only if,* $a = c = 0$ *and* $b \neq 0$. *More specifically, two families can occur,* $L_e^2(x,y) = (by, dx+ey+f)$ *if* $d \neq 0$ *and* $L_e^2(x,y) = (by, ey+f)$ *if* $d = 0$ *and* $f \neq 0$;

(vi) *L is rotated respect to the parameter f if, and only if,* $a = b = 0$ *and* $c \neq 0$. *More specifically, one family can occur,* $L_f(x,y) = (c, dx+ey+f)$;

The proof of the last result is direct but we insert it here for completeness.

Proof: We prove bullets (i) and (iii) of Proposition 50, the proof of other bullets are similar. To prove bullet (i) notice that L is rotated with respect to the parameter a if

$$\begin{vmatrix} ax+by+c & de+ey+f \\ x & 0 \end{vmatrix} = -dx^2 - exy - fx$$

is positive or negative. Since the last inequality must hold for every regular point of L we prove the first part of the proof. Assuming $e = f = 0$ and $d \neq 0$, the linear vector field L has a equilibrium point (x_0, y_0) if $b \neq 0$ which is located at $(x_0, y_0) = \left(0, -\frac{c}{b}\right)$, so we get the family L_a^1. If $b = 0$ and $c \neq 0$ then L has no equilibria and in this case, we obtain the family L_a^2. Notice that when $b = c = 0$ there exists a continuum of equilibria so L cannot be rotated in this case.

The proof of bullet (iii) follows noticing that L is rotated if $-dx - ey - f$ is always positive or negative, which occurs when $d = e = 0$ and $f \neq 0$, obtaining the one-parameter linear vector field L_c given in (iii). □

A direct consequence of Proposition 50 is the vector field $Z(X,Y)$ studied in Chapters 2 and 4 given by:

$$\begin{aligned} X(x,y) &= \left(-bx - \frac{4b^2+w^2}{4a}y + d,\ ax+by+c\right), \\ Y(x,y) &= \left(-Bx - \frac{4B^2+W^2}{4A}y + D,\ Ax+By+C\right), \end{aligned} \tag{A-11}$$

can not be one-parameter family of rotated vector fields. The same is true for the one-parameter family of rotated piecewise vector fields $X_\mu(X,Y)$ studied in Chapter 5. Moreover, Proposition 50 allowed the building a variety examples of Piecewise Rotated Vector Fields.

To improve this discussion it would be necessary a more careful study in order to get more results about the properties of the Linear Rotated Piecewise Vector Field.

Problem 4: Is it Possible to Generalize the Classical Expansion and Contraction Theorem of Rotated Vector Fields for Piecewise Rotated Vector Fields?

A natural question to do about piecewise rotated vector field would be to try to generalize the Classical Expansion and Contraction Theorem of Rotated Vector Field for Piecewise Rotated Vector Fields, i.e., would be to prove something like the following result:

Result 51 *Let Z_μ be a piecewise rotated vector field. Assume that Z_μ satisfies the hypotheses of Fundamental Lemma 42. Then, stable and unstable poly-trajectories of kind 1 of $Z_\mu = (X_\mu, Y_\mu)$ expand or contract monotonically as the parameter μ varies in a fixed sense and the motion covers an annular neighborhood of the initial position.*

So far as we studied this problem, we cannot get enough tools to prove this result. We leave this study open for the future.

Bibliography

[1] Barry, A.M., Widiasih, E., McGehee, R.: Nonsmooth frameworks for an extended Budyko model, DCDS-B, 22, 2447–2463, 2017.

[2] Braga, D.C., Mello, L.F.: Limit cycles in a family of discontinuous piecewise linear differential system with two zones in the plane, Nonlin. Dyn., 73, 1283–1288, 2013.

[3] Broucke, M.E., Pugh, C.C., Simić, S.N.: Structural stability of piecewise smooth systems, Comput. Appl. Math., 20, 51–89, 2001.

[4] Buzzi, C.A., Carvalho, T., Euzébio, R.D.: On Poincaré-Bendixson Theorem and non-trivial minimal sets in planar non-smooth vector fields, Publ. Mat., 62, no. 1, 113–131. 34A36 (34A12 34D30), 2018.

[5] Buzzi, C.A., Carvalho, T.: da Silva P.R.: Closed poly-trajectories and Poncaré index of non-smooth vector fields. Journal of Dynamical and Control Systems, Vol. 19, No. 2, April 2013, 173 -193.

[6] Buzzi, C.A., Pessoa, C., Torregrosa, J.: Piecewise linear perturbations of a linear center, Discrete Contin. Dyn. Syst., 9, 3915–3936, 2013.

[7] Buzzi, C.A, da Silva, P.R., Teixeira, M.A.: A singular approach to discontinuous vector fields on the plane, J. Differ. Equ., 231, 633–655, 2006.

[8] Cardin, P.T., de Moraes, J.R., da Silva, P. R.: Persistence of periodic orbits with sliding or sewing by singular perturbation. Journal of Mathematical Analysis and Applications, v. 423, n. 2, p. 1166–1182, 2015.

[9] Cardin, P.T.; da Silva, P.R.; Teixeira, M. A.: On singularly perturbed Filippov systems. European Journal Of Applied Mathematics. New York: Cambridge Univ Press, v. 24, p. 835-856, 2013.

[10] Cardin, P., Torregrosa, J.: Limit cycles in planar piecewise linear differential systems with nonregular separation line, Physica D., 337, 67–82, 2016.

[11] Carmona, F., Fernández-Garcia, S., Fernández-Sanches, F., García-Medina, E., Teruel, E.: Noose bifurcation and crossing tangency in reversible piecewise linear systems, Nonlinearity, 27, 585–606, 2014.

[12] Carmona, F., Fernández-Sanches, F., García-Medina, E., Teruel, E.: Noose Structure and Bifurcations of Periodic Orbits in Reversible Three-Dimensional Piecewise Linear Differential Systems, J. Nonlinear Sci, 25, 1209–1224, 2015.

[13] Caubergh, M.: Bifurcation of the separatrix skeleton in some 1-parameter families of planar vector fields, J. Differential Equations 259 989-1013, 2015.

[14] Chen, X.: Applications of rotated vector fields, I, J. Nanjing University 1, 19–25, 1963.

[15] Chen, X.: Applications of rotated vector fields, II, J. Nanjing University 2, 43–50, 1963.

[16] Chen, X.: Generalized rotated vector fields, J. Nanjing University 1, 100–108, 1975.

[17] Chen, H., Du, C., Youn, Y., Yuon, Y.: The limit cycles of a general Kolmogorov system, J. Math. Anal. Appl. 392 225–237, 2012.

[18] Chillingworth, D. R. J.: Discontinuity geometry for an impact oscillator, Dyn. Syst., 17, 389–420, 2002.

[19] Dai, B., Xiao, Q.: Heteroclinic bifurcation for a general predator-prey model with allee effect and state feedback impulsive control strategy, Mathematical Biosciences and Engineering, 12, 5, 2015.

[20] da Silva, P.R., de Moraes, J.R.: Piecewise-Smooth Slow-Fast Systems. J Dyn Control Syst 27, 67–85, 2021. https://doi.org/10.1007/s10883-020-09480-8

[21] Davydov, A.A.: Qualitative theory of control systems (English summary) Translated from the Russian manuscript by V. M. Volosov. Translations of Mathematical Monographs, 141. American Mathematical Society, Providence, RI, 1994. viii + 147 pp.

[22] Di Bernardo, M., Budd, C. J.: Champneys, A. R., Kowalczyk, P.: Piecewise smooth Dynamical Systems Theory and Applications, Springer - Verlag, 2008.

[23] Duff, G.F.D.: Limit cycles and rotated vector fields, Ann. of Math. 67, 15–31, 1953.

[24] Dumortier, F., Llibre, J., Artés, J.C.: Qualitative theory of planar differential systems, 1 ed., 2006. https://doi.org/10.1007/978-3-540-32902-2

[25] Euzébio, R. D., Jucá, J. S.: Limit sets of discontinuous vector fields on two-dimensional manifolds, 2020, submitted.

[26] Euzébio, R.D., Pazim, R., Ponce, E.: Jump bifurcations in some degenerate planar piecewise linear differential systems with three zones, Physica D, vol. 325, pp. 74–85, 2016.

[27] Fenichel, N.: Geometric Singular Perturbation Theory for Ordinary Differential Equations. Journal of Differential Equations, v. 31, n. 1, 53–98, 1979.

[28] Filippov, A.F.: Differential Equations with Discontinuous Righthand Sides, Mathematics and its Applications (Soviet Series), Kluwer Academic Publishers-Dordrecht, 1988.

[29] Fitzhugh, R.: Impulses and physiological states in theoretical models of nerve membrane, Biophys. J., 1, 445, 1961.

[30] Freire, E., Ponce, E., Rodrigo, F., Torres, F.: Bifurcation sets of continuous piecewise linear systems with two zones, International J. Bifur. Chaos Appl. Sci. Engrg., 8, 2073–2097, 1998.

[31] Freire, E., Ponce, E., Torres, F.: Canonical discontinuous planar piecewise linear systems. SIAM J. Appl. Dyn. Syst., 11, 181–211, 2012.

[32] Gibson, C.G.: Singular Points os smooth maps, Pitman Publish - London, 1979.

[33] Guardia, M., Seara, T.M., Teixeira M.A.: Generic bifurcations of low codimension of planar Filippov Systems, J. Diff. Eq. 250, 1967–2023, 2011.

[34] Han, M.: Global Behavior of Limit Cycles in Rotated Vector Fields, Journal of Differential Equations 151, 20–35, 1999.

[35] Han, M., Zhang, W.: On Hopf bifurcation in non-smooth planar systems, J. Differential Equations, 248, 2399–2416 2009.

[36] Han, M., Hou, X., Sheng, L., Wang C.: Theory of Rotated Equations and Applications to a Population Model, Discrete and Continuous Dynamical Systems, vol 38, No. 4, 2171–2185, 2018.

[37] Hodgkin, A.L., Huxley, A.F.: A quantitative description of membrane current and its application to conduction and excitation in nerves, J. Physiol., 117, 500, 1952.

[38] Huan, S.M., Yang, X.S.: On the number of limit cycles in general planar piecewise linear systems, Discr. Contin. Dyn. Syst., 32, 2147–2164, 2012.

[39] Huan, S.M., Yang, X.S.: Limit Cycles in a Family of Planar Piecewise Linear Differential Systems with a Nonregular Separation Line, International Journal of Bifurcation and Chaos, 29, No. 8, 1950109, 2019.

[40] Jacquemard, A., Teixeira, M.A., Tonon D.J.: Piecewise smooth reversible dynamical systems at a two-fold singularity, International Journal of Bifurcation and Chaos, 22, 1250192-1–250192-13, 2012.

[41] Jeffrey, M.: Hidden Dynamics, Springer, 2018.

[42] Jimenez, J., Llibre, J., Medrado, J.: Crossing limit cycles for a class of piecewise linear differential centers separated by a conic. Electronic Journal of Differential Equations, v. 2020, p. 1–36, 2020.

[43] Kozlova, V. S.: Roughness of a discontinuous system, Vestnik Moskovskogo Universiteta Seriya 1 Matematika Mekhanika, 5, 16–20, 1984.

[44] Kuehn, C., Multiple time scale dynamics, Springer, 2015.

[45] Llibre, J., da Silva, P.R., Teixeira, M.A.: Study of singularities in nonsmooth dynamical systems via singular perturbation. SIAM Journal on Applied Dynamical Systems 8.1, 508–526, 2009.

[46] Llibre, J., Ordóñez, M., Ponce, E.: On the existence and uniqueness of limit cycles in a planar piecewise linear systems without symmetry. Nonlinear Anal. Ser. B RealWorld Appl., 14, 2002–2012, 2013.

[47] Llibre, J., Ponce, E.: Three nested limit cycles in discontinuous piecewise linear differential systems with two zones, Dyn. Contin. Discrete Impuls. Syst. Ser. B Appl. Algorithms, 19 no. 3, 325–335, 34C05 (34A36), 2012.

[48] Llibre, J., Teixeira, M.A.: Piecewise linear differential systems with only centers can create limit cycles?, Nonlinear Dynamics, 91, 249–256, 2018.

[49] Llibre, J., Zhang, X.: Limit cycles created by piecewise linear centers, Chaos, 29(5):053116, 2016.

[50] Luo, C.J.: Singularity and dynamics on discontinuous vector fields, Monograph Series on Nonlinear Science and Complexity, Elsevier Sc., 2006.

[51] Lum, R., Chua, L.O.: Global properties of continuous piecewise-linear vector fields. Part I: Simplest case in $\mathbb{R}^2$, Memorandum UCB/ERL M90/22, University of California at Berkeley, 1991.

[52] Lum, R., Chua, L.O.: Global properties of continuous piecewise-linear vector fields. Part II: simplest symmetric in $\mathbb{R}^2$. Int. J. Circuit Theory Appl., 20, 9–46, 1992.

[53] Nagumo, J.S. Arimoto, S., Yoskizawa S.: An active pulse transmission line stimulating nerve axon, Proc. IRE, 50, 2061, 1962.

[54] Novaes, D.D., Torregrosa, J.: On extended Chebyshev systems with positive accuracy, J. Math. Anal. Appl., 448, 171–186, 2017.

[55] Pereira, W.F, Pessoa C.: A class of reversible quadratic polynomial vector fields on $\mathbb{S}^2$, J. Math. Anal. Appl. 371 203–209, 2010.

[56] Perko, L.M.: Differential Equations and Dynamical Systems, 3rd. ed., Springer, New York, 2001.

[57] Perko, L.M.: Global families of limit cycles of planar analytic systems, Trans. Amer. Math. Soc. 322, 627–656, 1990.

[58] Perko, L.M.: Rotated vector fields and the global behavior of limit cycles for a class of quadratic systems in the plane, J. Differential Equations 18, 63–86, 1975.

[59] Perko, L.M.: Rotated vector fields, J. Differential Equations 103, 127–145, 1993.

[60] Poincaré, H.: Sur les courbes définies une équation différentielle, Oeuvres 1, page 1.

[61] Ponce, E., Torres, F.: A general mechanism to generate three limit cycles in planar Filippov systems with two zones, Nonlinear Dyn., 78, 251–263, 2014.

[62] Sotomayor, J., Machado, A.L.: Structurally stable discontinuous vector fields on the plane., Qual. Theory of Dynamical Systems 3, 227–250, 2002.

[63] Sotomayor, J. Teixeira, M.A.: Regularization of discontinuous vector fields., International Conference on Differential Equations, Lisboa, 207–223, 1996.

[64] Simpson, D.J.W., Kuske, R.: Stochastic Perturbations of Periodic Orbits with Sliding. J Nonlinear Sci., 25, 967–1014, 2015.

[65] Teixeira, M.A.: Perturbation Theory for Non-smooth Systems, Meyers: Encyclopedia of Complexity and Systems Science, 152, 2008.

[66] Teixeira, M.A.: Stability conditions for discontinuous vector fields, J. Differential Equations, 88, 15–29, 1990.

[67] Walsh, J., Widiasih, E., Hahn, J., McGehee, R.: Periodic orbits for a discontinuous vector field arising from a conceptual model of glacial cycles, Nonlinearity, 29, 1843–1864, 2016.

[68] Zhang, X.: Homoclinic, heteroclinic and periodic orbits of singularly perturbed systems. Sci. China Math. 62, 1687–1704, 2009.

[69] Zhao, Y., Feng, Z., Zheng, Y., Cen, X.: Existence of limit cycles and homoclinic bifurcation in a plant-herbivore model with toxin-determined functional response, Journal of Differential Equations, 258, 8, 2847–2872, 2015.

[70] Zhao, Q., Yu, J.: Poincaré Maps of "$<$"-Shape Planar Piecewise Linear Dynamical Systems with a Saddle, International Journal of Bifurcation and Chaos, 29, no 12, 1950165, 2019.